# Late Cretaceous Paleoceanographic Evolution and the Onset of Cooling in the Santonian at Southern High Latitudes (IODP Site U1513, SE Indian Ocean)

Maria Rose Petrizzo

Kenneth G. MacLeod

David K. Watkins

Erik Wolfgring

Brian T. Huber

**AGU** ADVANCING EARTH AND SPACE SCIENCE

# Late Cretaceous Paleoceanographic Evolution and the Onset of Cooling in the Santonian at Southern High Latitudes (IODP Site U1513, SE Indian Ocean)

**Maria Rose Petrizzo[1]** , **Kenneth G. MacLeod[2]** , **David K. Watkins[3]** , **Erik Wolfgring[1,4]**, and **Brian T. Huber[5]**

[1]Department of Earth Sciences "Ardito Desio", University of Milan, Milan, Italy, [2]Department of Geological Sciences, University of Missouri-Columbia, Columbia, MO, USA, [3]Department of Earth and Atmospheric Sciences, University of Nebraska, Lincoln, NE, USA, [4]Department of Geology, University of Vienna, Vienna, Austria, [5]National Museum of Natural History, Smithsonian Institution, Washington, DC, USA

**Abstract** The latest Cenomanian to Santonian sedimentary record recovered at IODP Expedition 369 Site U1513 in the Mentelle Basin (SE Indian Ocean, paleolatitude 60°S at 85 Ma) is studied to interpret the paleoceanographic evolution in the Southern Hemisphere. The planktonic foraminiferal assemblage changes, the depth ecology preferences of different species, and the surface and seafloor temperature inferred from the stable isotopic values measured on foraminiferal tests provide meaningful information to the understanding of the Late Cretaceous climate. The hothouse climate during the Turonian-Santonian, characterized by weak latitudinal temperature gradients and high atmospheric $CO_2$ concentrations, is followed by a progressive cooling during the Campanian. At Site U1513 the beginning of this climatic transition is nicely recorded within the Santonian, as indicated by an ~1‰ increase in $\delta^{18}O$ values of planktonic foraminifera suggesting a decline in surface water paleotemperatures of 4°C. The onset of cooling is mirrored by changes in the planktonic foraminiferal assemblages including extinctions among surface and deep dwellers, appearances and diversification of newly evolving taxa, and changes from predominantly epifaunal oxic to infaunal dysoxic/suboxic taxa among co-occurring benthic foraminifera. Overall, the data presented here document an interval in the Santonian during which the rate of southern high latitude cooling increased. Both surface and bottom waters were affected, although the cooling signal is more evident in the data for surface waters. This pattern of cooling ascribes the deterioration of the Late Cretaceous climate to decreased $CO_2$ in the atmosphere and changes in the oceanic circulation correlated with enhanced meridional circulation.

## 1. Introduction

The evolution of Cretaceous climate has been extensively studied through paleontological records, proxy-based reconstructions, and model simulations of sea-surface temperatures (e.g., Barron et al., 1995; Craggs et al., 2012; Donnadieu et al., 2006; Hallam, 1985; Hay, 2008; Huber et al., 1995; Otto-Bliesner et al., 2002; Poulsen et al., 2001; Pucéat et al., 2003). The Cretaceous Period was characterized by a climate with much warmer tropical and polar temperatures than today and weak latitudinal temperature gradients (e.g., Barron, 1983; Huber et al., 1995; Littler et al., 2011; O'Brien et al., 2017) as well as high atmospheric $CO_2$ concentrations (e.g., Barclay et al., 2010; Bice et al., 2006; Bice & Norris, 2002; Sinninghe Damsté et al., 2008; Wang et al., 2014). The latter is considered responsible for triggering and maintaining the globally warm climate (e.g., Barron et al., 1995; Crowley & Berner, 2001; Fletcher et al., 2008; Foster et al., 2017; Hay & Floegel, 2012; Royer et al., 2007; Wang et al., 2014). Eustatic sea level during the Cretaceous was higher than present-day (Haq, 2014; Miller et al., 2005) and permanent ice sheets were absent (e.g., Barron, 1983; Huber et al., 2002; Jenkyns et al., 2004; MacLeod et al., 2013), although small-scale glaciation events have been proposed (e.g., Bornemann et al., 2008; Ladant & Donnadieu, 2016; Price, 1999; Price & Nunn, 2010). The Cretaceous was also marked by oceanographic changes, such as the opening of the Equatorial Atlantic Gateway (Friedrich & Erbacher, 2006; Wagner & Pletsch, 1999), the enlargement and deepening of the North and South Atlantic basins (Frank & Arthur, 1999), and progressive narrowing of the Tethyan Ocean (Cramer et al., 2009; Friedrich et al., 2012; Jones et al., 1995; Sewall et al., 2007) and Caribbean Gateway (Ladant et al., 2020; MacLeod et al., 2011).

Low to high latitude paleotemperature estimates for the Late Cretaceous, mainly based on global stable oxygen isotopes ($\delta^{18}O$) and $TEX_{86}$ compilations, reveal a similar trend that highlights extreme warmth during the

Cenomanian-Turonian, some amelioration but continued warmth through the Coniacian-Santonian, and progressive cooling extending through the Campanian and into the Maastrichtian (e.g., Ando et al., 2013; Bornemann et al., 2008; Clarke & Jenkyns, 1999; Cramer et al., 2011, 2009; Douglas & Savin, 1975; Friedrich et al., 2012; Huber et al., 2002, 1995, 2018; Jarvis et al., 2011; Jenkyns et al., 1994; Linnert et al., 2018, 2014; MacLeod et al., 2013; Moriya, 2011; Norris & Wilson, 1998; O'Brien et al., 2017; Pucéat et al., 2005; Savin, 1977; Schouten et al., 2003; Scotese et al., 2021; Steuber et al., 2005; Takashima et al., 2006; van Helmond et al., 2014; Voigt et al., 2004). Specifically, the transition from the hothouse of the latest Cenomanian and Turonian into the coolhouse of the late Campanian and Maastrichtian is reported to occur in concert with a number of global changes that affected the ocean-climate system and Earth's biota. These include: (a) large-scale tectonic changes including the expansion of the Atlantic and Southern Ocean (e.g., Sewall et al., 2007); (b) decreasing atmospheric $CO_2$ levels (e.g., Barron et al., 1995; Fletcher et al., 2008; Tabor et al., 2016; Wang et al., 2014) probably associated with continental volcanism and/or with reduced $CO_2$ flux from mid-ocean ridge volcanism and arc magmatism (e.g., Berner, 2004; Berner et al., 1983; Cogné & Humler, 2006; Kent & Muttoni, 2013; McKenzie et al., 2016; van der Meer et al., 2014); (c) radiation of angiosperms (e.g., Boyce et al., 2009); (d) opening of the Equatorial Atlantic Gateway and northward intrusion of cooler Atlantic water masses from higher southern latitudes (Forster et al., 2007; Frank & Arthur, 1999; Friedrich & Erbacher, 2006; Friedrich et al., 2012; MacLeod & Huber, 1996); (e) formation of deep- and/or intermediate-water at high latitudes and reduction of warm and saline water masses in the subtropics (Barrera et al., 1997; Barrera & Savin, 1999; Friedrich et al., 2009, 2012; MacLeod, 1994; MacLeod et al., 2005, 2011; MacLeod & Huber, 2001) which coincide with a major reorganization of oceanic circulation during the Santonian-Campanian evidenced by neodymium isotopic data (Haynes et al., 2020; MacLeod et al., 2011; Murphy & Thomas, 2012; Robinson et al., 2010; Robinson & Vance, 2012); and (f) increasing continental weathering and erosion resulting from enhanced $CO_2$ consumption by silicate weathering (Chenot et al., 2018). The occurrence of ephemeral ice sheets (Stoll & Shrang, 2000) and glacio-eustasy (Miller et al., 2005) have been invoked as possible mechanisms responsible for sea level changes despite evidence for global warmth. The complex interaction of the mechanisms listed above make determining the ultimate cause of the long-term Late Cretaceous cooling uncertain.

Paleogeographic changes have been invoked as having a significant influence on global temperature evolution across the Late Cretaceous (Donnadieu et al., 2006; Fluteau et al., 2007; Frank & Arthur, 1999; Haynes et al., 2020; Ladant & Donnadieu, 2016; Poulsen et al., 2003). However, there is a lack of consensus among climate model results. Some model simulations indicate a minor impact of paleogeographic changes on the Late Cretaceous cooling suggesting that a decrease in $CO_2$ concentration was the main driver (Tabor et al., 2016) in agreement with paleotemperatures proxies (Haynes et al., 2020; Linnert et al., 2014; Pucéat et al., 2007) and $CO_2$ reconstructions (Fletcher et al., 2008; Wang et al., 2014). Some other models (Donnadieu et al., 2016; Ladant et al., 2020; Lunt et al., 2016) and proxy-based evidence (e.g., Friedrich et al., 2012; Huber et al., 2018; MacLeod et al., 2011; Martin et al., 2012; Murphy & Thomas, 2013; Robinson et al., 2010; Robinson & Vance, 2012) suggest an important role of paleogeographic reorganization. In these studies geometry and depth of oceanic basins and gateways coupled with decreased $CO_2$ are considered to be responsible for changes in oceanic circulation, particularly increasing importance of high latitude sources of intermediate and deep waters, that paced the long-term cooling in the Late Cretaceous.

In terms of planktonic foraminiferal evolution, the climatic transition from the hot to cool climate in the Santonian-early Campanian coincides with a remarkable compositional change characterized by taxonomic diversification followed by extinctions. A 3 My-long major foraminiferal turnover is documented in the Coniacian-Santonian interval during which pre-Campanian keeled taxa became extinct and were replaced by newly evolved late Santonian-early Campanian taxa. The assemblage changes (also known as the Santonian turnover: Petrizzo et al., 2017) is registered worldwide (e.g., Caron & Homewood, 1983; Hart, 1999; Hart & Bailey, 1979; Petrizzo, 2002; Premoli Silva & Sliter, 1999; Wonders, 1980), although it is better documented and resolved at low and mid-latitudes than at high latitudes at least in part because the low to mid-latitude assemblages have a higher diversity and more species changes compared to the record at high latitudes (Petrizzo et al., 2020). Thus, the potential signal is higher.

Hypotheses proposed to explain the Santonian foraminiferal turnover include: (a) tectonically forced changes in ocean circulation (Ando et al., 2013; Premoli Silva & Sliter, 1999); (b) the onset of the Late Cretaceous cooling trend during the late Santonian (Petrizzo, 2002) combined with species competition within particular depth

habitats (Falzoni et al., 2016); and (c) the development of regional anoxic events (i.e., Oceanic Anoxic Event 3; e.g., Arthur & Schlanger, 1979; Jenkyns, 1980; Ryan & Cita, 1977; Schlanger & Jenkyns, 1976; Wagreich, 2012) in the Atlantic and adjacent epicontinental sea resulting in the enlargement of ecological niches in the more oxygenated Tethys, Pacific and Indian oceans (Wagreich, 2009).

This study is focused on the latest Cenomanian to Santonian sedimentary sequence recovered at Site U1513 during International Ocean Discovery Program (IODP) Expedition 369. The site is located in the Mentelle Basin (eastern flank of the Naturaliste Plateau, SE Indian Ocean, SW Australia) and was at a paleolatitude calculated as ranging from 57°S to 62°S during the Late Cretaceous (Hay et al., 1999; Müller et al., 2016; Scotese, 2016; van Hinsbergen et al., 2015; Figure 1a). We investigate the foraminiferal record to interpret the paleoceanographic changes and the paleotemperature evolution from the thermal maximum across the Cenomanian-Turonian interval followed by progressive cooling through the Santonian. In the present study, quantitative foraminiferal assemblage data and depth habitat ecologies based on species-specific stable isotope analyses are used to interpret the paleoceanographic changes and the history of surface water circulation in the southern high latitudes. Paleotemperature estimates derived from foraminiferal and bulk carbonate stable isotopic measurements provide information on the pattern of the climatic transition from the hothouse to the coolhouse which are crucial to an accurate understanding of the evolution of the circum-Antarctic climate.

## 2. Materials and Methods

IODP Site U1513 (33°47.6084S, 112°29.1338E) lies at 2,800 m water depth on the western margin of the Mentelle Basin located on the eastern flank of the Naturaliste Plateau and off the south western margin of Australia (SE Indian Ocean; Figure 1a). This study focuses on the latest Cenomanian to Santonian sedimentary record recovered from Holes U1513A, U1513B, and U1513D whose overlapping portions together provide relatively continuous recovery of this interval (Figure 2). Site U1513 is located 1.1 km east-northeast of Deep Sea Drilling Project (DSDP) Leg 26 Site 258 (Figure 1b), which was spot-cored (20% recovery) in the Late Cretaceous interval (Luyendyk & Davies, 1974). The objectives at Site U1513 were to improve recovery within gaps of the record at Site 258, to recover a complete record of Oceanic Anoxic Event 2 (OAE 2), and to sample unaltered basalts from the basement of the Naturaliste Plateau.

The Late Cretaceous sedimentary record is separated from the overlying Miocene sediments by a 40 cm-thick complex of hardgrounds with at least two distinct mineralized surfaces that were recovered in the intervals U1513A-9H-1, 0–10 cm and U1513B-8H-2, 7–47 cm, although the features are best seen in the latter. A 182.93 m-thick Upper Cretaceous sedimentary record was recovered beneath the hardground complex (Figure 2). The stratigraphic succession is assigned to lithostratigraphic Unit II which is composed of white to greenish gray calcareous and nannofossil ooze and chalk, clayey nannofossil chalk, and silicified limestone that becomes generally more clay rich down core. The bottom of the studied stratigraphic succession (U1513A-43X and U1513D-17R) is about 3 m above a 2.3 m-thick bed of mottled grayish green claystone that has a sharp basal contact with a bed of black claystone assigned to lithostratigraphic Unit III. Investigating these grayish and black lithologies characterized by low carbonate content ($CaCO_3$ <0.5 wt%), that were interpreted as the sedimentary expression of Oceanic Anoxic Event 2 (OAE 2) by Huber et al. (2019a), is beyond the scope of this study and will be the subject of future publications.

Data from Holes U1513A, U1513B, and U1513D are plotted on the CCSF depth scale (Core Composite Depth below Sea Floor, equivalent to mcd, meters composite depth; Huber et al., 2019b; LIMS online report portal at http://web.iodp.tamu.edu/LORE/). The chronostratigraphy is according to Gradstein et al. (2020).

For micropaleontological analysis, 145 rock samples were dried, weighed, soaked in a solution of water and Hydrogen Peroxide ($H_2O_2$), washed over 250, 125, and 38 µm sieves, and dried. Radiolaria and foraminifera genera and species were counted in splits for each size fraction of these washed residues. The number of specimens for each category were calculated from the number of specimens counted and the fraction of the total counted split represented; the total number of specimens were obtained for each sample by adding the values of specimens/category for all the size fractions examined. Absolute abundances of microfossils were calculated as the number of specimens per gram of dry sediment. Planktonic foraminiferal taxonomy (Supporting Information S1) follows the pforams@mikrotax database at http://www.mikrotax.org/pforams (Huber et al., 2016). The planispiral species traditionally assigned to the genus *Globigerinelloides* are grouped together (=planispiral taxa) because this group
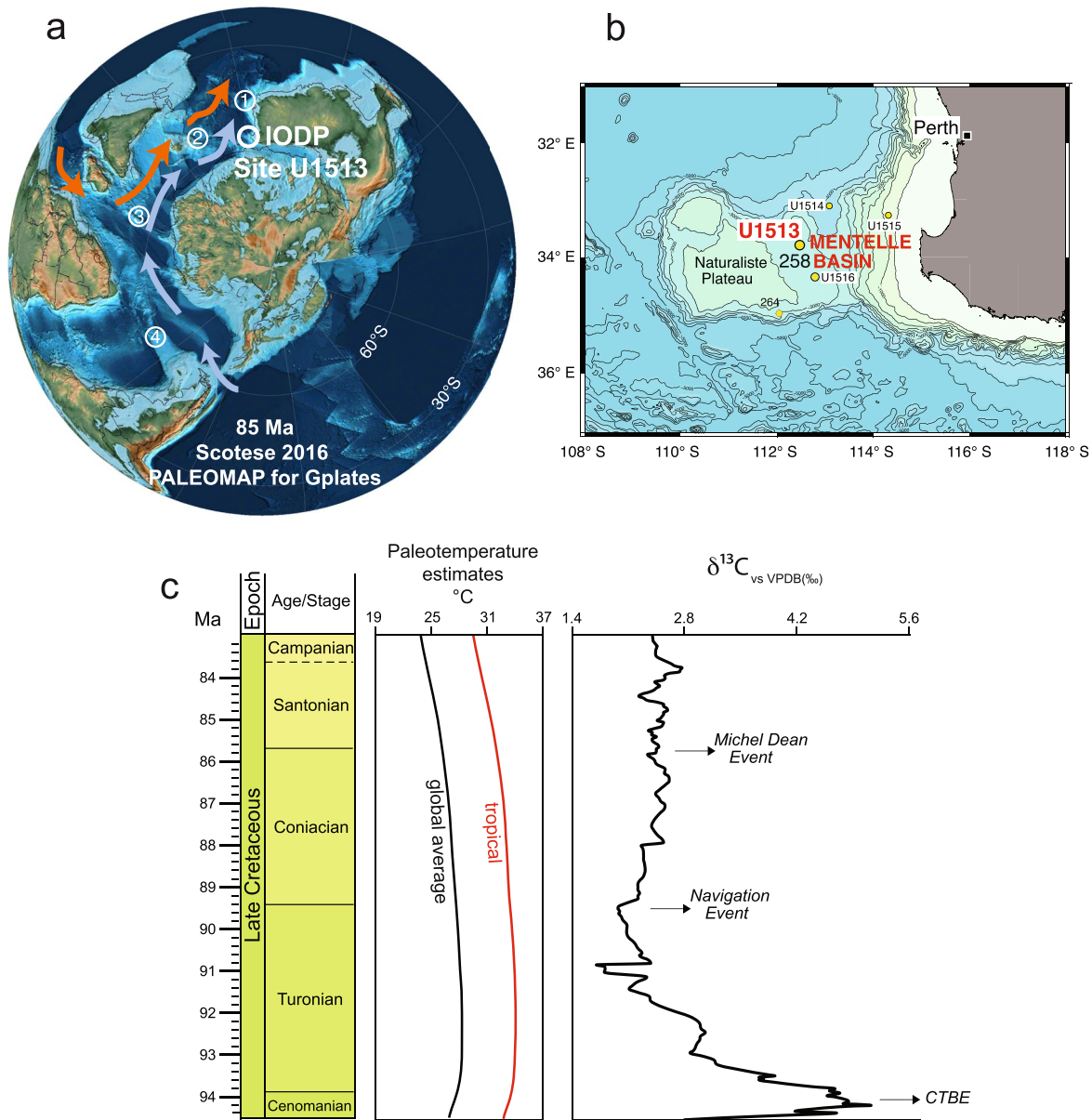
**Figure 1.** (a) Paleogeographic reconstruction (Scotese, 2016) for the Santonian (85 Ma), with location of International Ocean Discovery Program (IODP) Expedition 369 Site U1513 and of the other localities mentioned in the text: 1—Exmouth Plateau, 2—Kerguelen Plateau, 3—Northeast Georgia Rise, 4—Falkland Plateau. The paleolatitude of Site U1513 is calculated as 59.7°S at 85 Ma using paleolatitude.org (van Hinsbergen et al., 2015). The inferred subtropical gyre (orange arrows) and the subantarctic gyre (light blue arrows) are shown, see explanation in the text. (b) Location of the sites drilled during IODP Expedition 369 (U1513, U1514, U1515, and U1516) and nearby Deep Sea Drilling Project (DSDP) Sites 258 and 264 (modified after Huber et al., 2019a). (c) Paleotemperature estimates (Scotese et al., 2021) and carbon isotope references curve (Cramer & Jarvis, 2020) for the Turonian-Santonian interval; chronostratigraphy according to GTS 2020 (Gradstein et al., 2020). *Abbreviations*: CTBE, Cenomanian/Turonian Boundary Event.

is currently under taxonomic revision as the genus has been shown to be polyphyletic (see discussion in Petrizzo et al., 2017). The planktonic foraminiferal biozonation follows Robaszynski & Caron (1995), Premoli Silva & Sliter (1995), Petrizzo (2003), and Petrizzo et al. (2020).

Benthic foraminifera counts were made using the >125 μm size fraction; specimens present in size fractions between 125 and 38 μm were excluded because of the difficulty in confidently identifying juvenile individuals in these small size fractions. Benthic foraminiferal taxonomy follows the references listed in Supporting Information S1. Benthic foraminiferal taxa were tallied as either infaunal and epifaunal taxa, and also as oxic, dysoxic, or suboxic/anoxic taxa according to their environmental preferences following the classifications by Alegret et al.
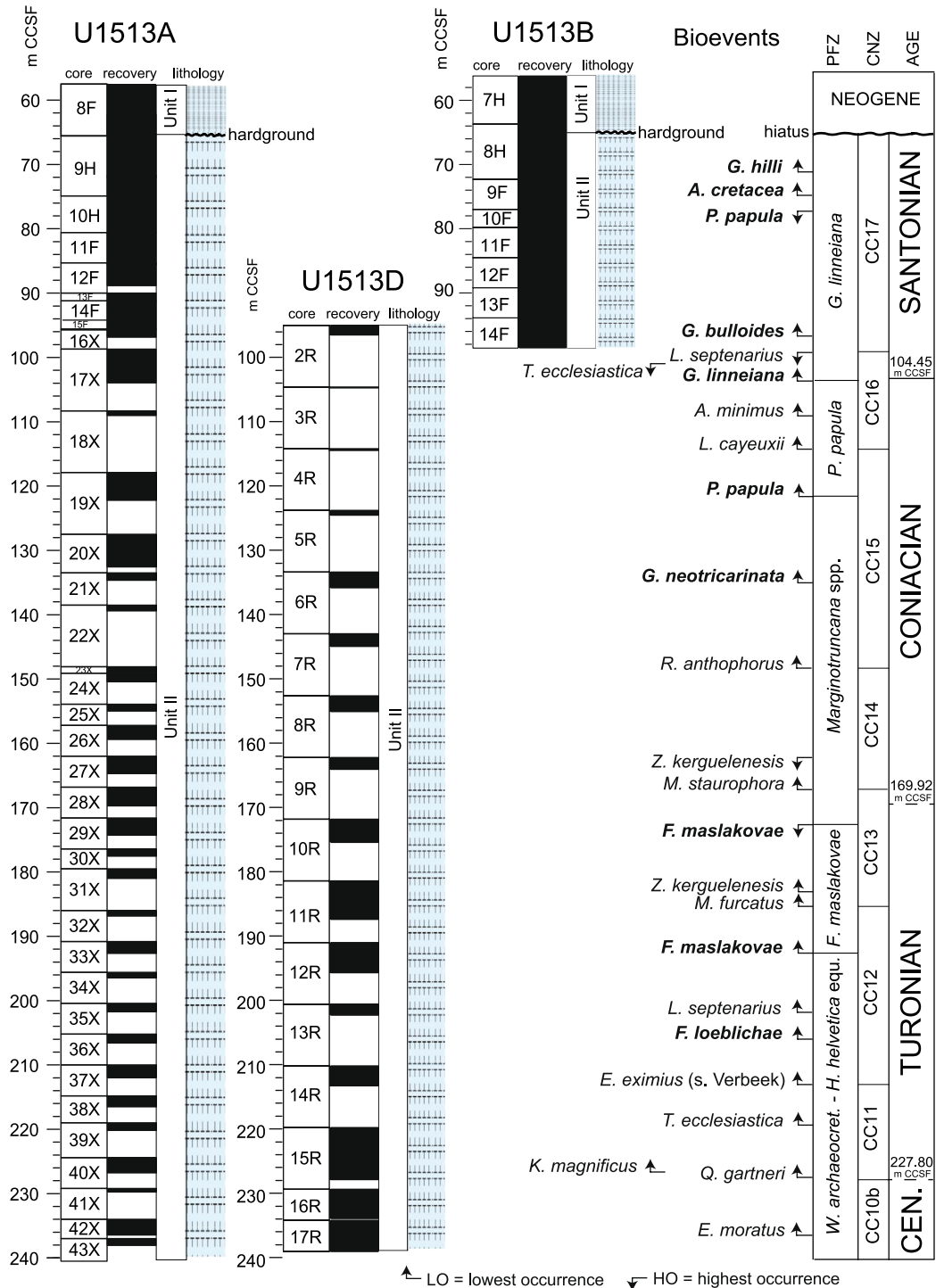
**Figure 2.** Holes U1513A, U1513B, and U1513D: planktonic foraminifera and calcareous nannofossil bioevents. Core recovery and lithologic units according to Huber et al. (2019a). Age: the Cenomanian/Turonian boundary is approximated at the lowest occurrence of *Quadrum gartneri* (dashed line); the Turonian/Coniacian boundary is tentatively placed at the midpoint between the highest occurrence of *Falsotruncana maslakovae* and the lowest occurrence of *Micula staurophora* (dashed line); and the Coniacian/Santonian boundary is identified at the lowest occurrence of *Globotruncana linneiana*, secondary criterion for the identification of the Santonian GSSP (solid line). Planktonic foraminiferal biozonation follows Robaszynski & Caron (1995) and Petrizzo et al. (2020). Calcareous nannofossil biozonation follows Perch-Nielsen (1985). Planktonic foraminiferal bioevents are in bold. *Abbreviations:* m CCSF, core composite depth below sea floor in meters; CNZ, calcareous nannofossils zones; PFZ, planktonic foraminifera zones. See text for further explanation.

(2003), Alegret & Thomas (2007), Murray (2006), Jorissen et al. (2007), and references therein. The changes in benthic foraminiferal assemblages for oxic, dysoxic, and suboxic groups of taxa were analyzed using the statistics package of R (R Core Team, 2021) to calculate a smoother LOWESS curve (span = 0.2) through the data.

Epifaunal benthic foraminifera are similar to recent analogs and mostly characterized by taxa having planispiral or trochospiral chamber arrangements such as *Notoplanulina, Nuttallinella, Cibicides, Gavelinella, Eponides*, and *Gyroidinoides*. The latter genus is also known as an opportunistic taxon with unclear habitat preference being either considered an infaunal or epifaunal taxon and even tolerant to anoxic environments (Alegret et al., 2003; Friedrich et al., 2006; Jorissen et al., 2007). Agglutinated benthic foraminifera (*Dorothia, Gaudryina*), calcareous elongated uniserial and flattened benthic foraminifera (*Dentalina, Nodosaria*, *Planularia*, *Pleurostomella*), len- ticulinid forms (*Lenticulina, Astacolus*), and polymorphinid foraminifera (*Ellipsoglandulina, Ellipsoidella*) are inferred to prefer an infaunal habitat. Most epifaunal benthic foraminiferal taxa recorded at Site U1513 share a preference for well oxygenated habitats. Taxa inferred as tolerant to anoxic conditions include agglutinated taxa (*Dorothia, Ammodiscus*) as well as polymorphinid foraminifera and pleurostomellids (e.g., *Ellipsoglandulina, Ellipsoidella, Glandulina*). Taxa considered tolerant of suboxic habitats include lagenids, vaginulinids, *Dentali- na*, and *Nodosaria*.

Biostratigraphic analysis of calcareous nannofossils was performed on 123 samples from Holes U1513A, U1513B, and U1513D using smear slides prepared following Watkins & Bergen (2003). Presence/absence data for taxa encountered for each sample is tabulated in data table at https://doi.pangaea.de/10.1594/PANGAEA.939392. Calcareous nannofossil biostratigraphy follows Perch-Nielsen (1985).

Foraminiferal isotope data ($\delta^{13}C$ and $\delta^{18}O$) were obtained from single species separates of well-preserved plank- tonic and benthic foraminifera picked from samples where sufficient number of such individuals were present. Species were selected according to their abundance and degree of preservation, and only specimens showing no visible diagenetic calcite and infilled sparry calcite in the chambers or minor test wall recrystallization were measured. Material for bulk analyses were milled from cleaned surfaces of sediment samples. All analyses were made at the University of Missouri using a Kiel III carbonate device and Delta Plus IRMS. External precision calculated as 1 standard deviation of the uncorrected repeated analyses of the standard NBS-19 run every seventh or eighth sample on average throughout the course of the study, and that value was ±0.03‰ and ±0.08‰, for $\delta^{13}C$ and $\delta^{18}O$, respectively. Internal standards (fine fraction separates of Cretaceous chalk) are used to monitor machine performance before each run is started and at the start of each set of 46 analyses. To reduce effects of day-to-day variation, analyses within each run were corrected by the difference between the average values meas- ured for the NBS-19 during the run (typically 6) and the nominal values of 1.95‰ ($\delta^{13}C$) and −2.20‰ ($\delta^{18}O$) for the standard. Results are reported on the Vienna-PDB scale. Paleotemperature estimates at Site U1513 are calculated from the foraminiferal $\delta^{18}O$ values, assume seawater $\delta^{18}O$ of $-1‰_{SMOW}$ and use the paleotemperature equation of Kim & O'Neil (1997) reformulated by Bemis et al. (1998) following the assumptions detailed in Huber et al. (2018).

## 3. Calcareous Plankton Bioevents and Integrated Biostratigraphy

The studied stratigraphic interval at Site U1513 spans from the uppermost Cenomanian to the upper Santonian according to planktonic foraminiferal and calcareous nannofossil biostratigraphy. The planktonic foraminiferal biozonation for southern mid- to high latitudes by Petrizzo et al. (2020) is applied and correlated with calcareous nannofossil CC zones of Perch-Nielsen (1985) to provide an integrated calcareous plankton biozonation scheme at about 60°S paleolatitude. Lowest and highest occurrences of calcareous plankton events, including those that mark zonal boundaries, are shown in Table 1 and Figure 2.

The lowest occurrence (LO) of *Quadrum gartneri* at 227.80 m CCSF defines the base of Zone CC11 and is a consistently reliable datum for approximating the base of the Turonian Stage as it occurs slightly above the stage criterion in the Global Stratotype Section and Point (GSSP) type section (Kennedy et al., 2000, 2005) and in many other localities worldwide (e.g., Corbett et al., 2014; Dickson et al., 2017; Gale et al., 2020, 2019; Gradstein et al., 2012; Linnert et al., 2011, 2010; Petrizzo et al., 2021; Tsikos et al., 2004; von Salis, 1998). Nannofossil as- semblages in the interval below are assigned to Zone CC10b, yield *Eprolithus moratus* at 236.65 m CCSF and are cosmopolitan in nature with only very rare specimens of species considered to be high latitude taxa. Nannofossil Zone CC11 contains two important biostratigraphic events: the LOs of *Kamptnerius magnificus* at 227.13 m

**Table 1**
*Planktonic Foraminifera and Calcareous Nannofossil Bioevents at Site U1513*

| Sample | Depth m CCSF | Bioevents |
|---|---|---|
| U1513B-8H-2, 7–47 cm | 64.98 | hardground |
| U1513B-8H-5, 98–100 cm | 70.43 | **LO** *Globotruncana hilli* |
| U1513B-9F-3, 30–32 cm | 75.29 | **LO** *Archaeoglobigerina cretacea* |
| U1513B-10F-1, 50–52 cm | 77.60 | **HO** *Planoheterohelix papula* |
| U1513A-15F-CC, 0–10 cm | 95.60 | LO *Calculites obscurus* |
| U1513A-16X-1, 30–33 cm | 97.26 | **LO** *Globotruncana bulloides* |
| U1513A-17X-1, 50–53 cm | 99.20 | HO *Lithastrinus septenarius* |
| U1513A-17X-2, 88–90 cm | 101.08 | HO *Thiersteinia ecclesiastica* |
| U1513A-17X-3, 80–83 cm | 104.45 | **LO** *Globotruncana linneiana* |
| U1513A-18X-CC, 0–5 cm | 108.64 | LO *Amphizygus minimus* |
| U1513A-18X-CC, 0–5 cm | 108.64 | LO *Lithastrinus grillii* |
| U1513D-4R-CC, 0–1 cm | 114.30 | LO *Lucianorhabdus cayeuxii* |
| U1513D-4R-CC, 0–1 cm | 114.30 | LO *Prediscosphaera desiderograndis* |
| U1513A-19X-3, 75–78 cm | 121.66 | **LO** *Planoheterohelix papula* |
| U1513D-6R-2, 60–63 cm | 135.42 | **LO** *Globotruncana neotricarinata* |
| U1513A-23X-1, 10–13 cm | 148.20 | LO *Reinhardtites anthophorus* |
| U1513A-27X-1, 8–11 cm | 162.08 | HO *Zeugrhabdotus kerguelensis* |
| U1513A-28X-1, 18–21 cm | 166.98 | LO *Micula staurophora* |
| U1513A-29X-1, 127–130 cm | 172.87 | **HO** *Falsotruncana maslakovae* |
| U1513D-11R-2, 40–43 cm | 183.06 | LO *Reinhardtites biperforatus* |
| U1513D-11R-2, 40–43 cm | 183.06 | LO *Zeugrhabdotus kerguelensis* |
| U1513D-11R-4, 45–48 cm | 185.61 | LO *Marthasterites furcatus* |
| U1513A-33X-1, 10–13 cm | 193.62 | **LO** *Falsotruncana maslakovae* |
| U1513D-13R-CC, 17–18 cm | 202.25 | LO *Lithastrinus septenarius* |
| U1513A-36X-1, 86–89 cm | 206.06 | **LO** *Falsotruncana loeblichae* |
| U1513A-37X-2, 111–114 | 211.72 | **LO** *Marginotruncana pseudolinneiana* |
| U1513D-14R-CC, 13–18 cm | 213.22 | LO *Eiffellitus eximius* (s. Verbeek) |
| U1513A-39X-1, 40–43 cm | 219.40 | LO *Thiersteinia ecclesiastica* |
| U1513A-40X-2, 80–83 cm | 227.13 | LO *Kamptnerius magnificus* |
| U1513D-15R-CC, 7–12 cm | 227.80 | LO *Quadrum gartneri* |
| U1513D-17R-2, 120–123 cm | 236.65 | LO *Eprolithus moratus* |
| U1513A-42X-2, 37–40 cm | 236.45 | **LO** *Dicarinella hagni* |
| U1513A-43X-1, 35–38 cm | 239.06 | **LO** *Whiteinella brittonensis* |

*Note.* Planktonic foraminiferal bioevents are in bold. m CCSF, core composite depth below sea floor in meters; HO, highest occurrence; LO, lowest occurrence.

CCSF and *Thiersteinia ecclesiastica* at 219.40 m CCSF. In addition to the austral species *T. ecclesiastica*, the high latitude species *Seribiscutum primitivum* and *Repagulum parvidentatum* become common elements of these assemblages at Site U1513 in this zone. The LO of *Eiffellithus eximius* (sensu Verbeek) at 213.22 m CCSF is used to determine the base of the overlying Zone CC12, following the criteria proposed in Gaer & Watkins (2020). At Site U1513, this zone contains the LO of *Lithastrinus septenarius* at 202.25 m CCSF using the criteria of Corbett & Watkins (2014) to differentiate this taxon from its ancestor *Eprolithus moratus*.

The planktonic foraminifera *Rotalipora cushmani* and *Helvetoglobotruncana helvetica* whose highest occurrence (HO) and LO, respectively, are used to constrain and approximate the position of the Cenomanian/Turonian

boundary at low to mid-latitudes (e.g., Caron et al., 2006; Desmares et al., 2007; Elderbak & Leckie, 2016; Eldrett et al., 2015; Falzoni et al., 2018, 2016; Falzoni & Petrizzo, 2020; Gradstein et al., 2012; Keller et al., 2001; Kennedy et al., 2005, 2000; Paul et al., 1999). These species are absent from the Mentelle Basin sediments both at Site U1513 and nearby Site U1516 (Petrizzo et al., 2021). The planktonic foraminifera assemblages from the base of the studied stratigraphic interval (U1513A-43X and U1513D-17R) to the LO of *Falsotruncana maslakovae* at 193.62 m CCSF are characterized by low diversity and are dominated by whiteinellids (*Whiteinella baltica* and *Whiteinella brittonensis*), muricohedbergellids, and a few keeled species of *Marginotruncana* and *Dicarinella*. For these reasons, and because no species with remarkable or short stratigraphic ranges have been found, this stratigraphic interval has been considered equivalent to the combined low latitude *Whiteinella archaeocretacea* and *H. helvetica* Zones (Premoli Silva & Sliter, 1995; Robaszynski & Caron, 1995) based on the composition of the assemblages (and despite the absence of the Tethyan biozonal species). *Falsotruncana loeblichae* is recorded at 206.06 m CCSF preceding the lowest occurrence of *F. maslakovae* in agreement with its stratigraphic distribution at low latitudes (Tunisia: Caron, 1981; Robaszynski et al., 1993) and mid-to high latitudes (Exmouth Plateau, NW Australia, 47°S paleolatitude: Petrizzo, 2000; Kerguelen Plateau, southern Indian Ocean, 50°S paleolatitude: Petrizzo, 2001).

The Turonian/Coniacian boundary, ratified in May 2021 by the International Union of Geological Sciences (IUGS), is defined by the first appearance of the inoceramid bivalve species *Cremnoceramus deformis erectus* and complemented by the Navigation Carbon Isotope Event (Walaszczyk et al., 2021). In the stratotype section (Salzgitter-Sadler, Germany) and in the auxiliary sections of the GSSP there are no reliable calcareous nannofossil biohorizons closely associated with the Turonian/Coniacian boundary, although the boundary lies within Zone CC13 (Jarvis et al., 2021; Lees, 2008; Sikora et al., 2004; Voigt et al., 2021; Walaszczyk et al., 2021). Accordingly, at Site U1513 the Turonian/Coniacian boundary is inferred to fall within Zone CC13 between the LO of *Marthasterites furcatus* at 185.61 m CCSF and the LO of *Micula staurophora* at 166.98 m CCSF. The LO of the austral species *Zeugrhabdotus kerguelenensis* coincides with that of *Reinhardtites biperforatus* (=*Zeugrhabdotus biperforatus* of some authors) which has its LO at 183.06 m CCSF. The close stratigraphic association of *M. furcatus*, *Z. kerguelenensis*, and *R. biperforatus* is consistent with the literature reports (e.g., Bergen & Sikora, 1999; Burnett, 1998).

The absence at Site U1513 of the planktonic foraminifera *Dicarinella concavata*, whose LO occurs slightly below the stage criterion in the auxiliary sections of the GSSP (Walaszczyk et al., 2021), prevents the precise identification of the base of the Coniacian Stage. Therefore, in this study the Turonian/Coniacian boundary is tentatively placed at the midpoint (169.92 m CCSF) between the HO of the planktonic foraminifera *F. maslakovae* (172.87 m CCSF) and the LO of the calcareous nannofossil *M. staurophora*, which defines the base of Zone CC14 Zone following correlations with the record from Tanzania and Exmouth Plateau (NW Australia, ODP Hole 762) where the two taxa are recorded in the same stratigraphic order (Huber et al., 2017). According to this correlation the *F. maslakovae* Total Range Zone is entirely comprised within the upper Turonian (Petrizzo et al., 2020).

The Coniacian at Site U1513 appears to be completely represented. Nannofossil Zone CC14 is defined by the LO of *M. staurophora* at 166.98 m CCSF and the LO of *Reinhardtites anthophorus* at 148.20 m CCSF. This zone includes the HO of *Z. kerguelenensis* at 162.08 m CCSF, a placement that agrees precisely with that of Burnett (1998). The appearance of austral taxa, such as *Biscutum notaculum* and *Biscutum dissimilis*, in addition to the consistent common abundance of *R. parvidentatum* and the persistent presence of *S. primitivum*, indicates the clearly austral nature of these assemblages. The overlying Coniacian calcareous nannofossils Zone CC15 extends from the LO of *R. anthophorus* to the LO of *Lucianorhabdus cayeuxi* at 114.30 m CSSF, the latter marking the base of Zone CC16.

The stratigraphic interval from the HO of *F. maslakovae* to the LO of *Planoheterohelix papula* (121.66 m CCSF) is assigned to the *Marginotruncana* spp. Zone (Petrizzo, 2000; Petrizzo et al., 2020). The planktonic foraminifera *Globotruncana neotricarinata*, first recorded at 135.42 m CCSF, is a cosmopolitan species with a diachronous range (Petrizzo et al., 2011) which is confirmed at Site U1513 where it precedes the appearance of *P. papula* whereas it first occurs near the top of the *P. papula* Zone in the Exmouth Plateau record at 47°S paleolatitude (Petrizzo, 2000; Petrizzo et al., 2020).

The Coniacian/Santonian boundary is placed at the LO of *Globotruncana linneiana* (104.45 m CCSF), the secondary criterion for the identification of the Santonian GSSP which falls 10 cm above the first occurrence of

the primary marker, the inoceramid *Cladoceramus undulatoplicatus* in the GSSP stratotype section at Olazagutia (Spain; Lamolda et al., 2014). This assignment is confirmed by correlation of the sequence of calcareous nanno-fossils bioevents documented in the stratotype section of the Coniacian/Santonian boundary where the boundary lies within Zone CC16 and between the LO *L. cayeuxii* and the LO of *G. linneiana*.

The interval from the LO of *G. linneiana* to the top of the Cretaceous sediments is assigned to the *G. linneiana* Zone (Petrizzo et al., 2020), and registers a sequence of appearances (*Globotruncana bulloides* at 97.26 m CCSF, *Archaeoglobigerina cretacea* at 75.29 m CCSF, and *Globotruncana hilli* at 70.43 m CCSF) and the disappearance of *P. papula* (77.60 m CCSF) that show similar stratigraphic distributions at low and mid-latitudes (e.g., Petrizzo, 2019; Petrizzo et al., 2017; Premoli Silva & Sliter, 1995).

In general, *Lithastrinus* specimens are rare within the austral Santonian record, although *L. septenarius*, which has its HO at 99.20 m CCSF, usually occur in sufficient abundance to have a biostratigraphic significance. This utility cannot be claimed for its sister species, *Lithastrinus grilli*, whose LO is stratigraphically higher at Site U1513 and is known to be sporadic and very rare in the southern high latitudes (Watkins, 1992; Watkins & Guerra, 2020; Wise, 1983), although this datum reliably identifies the upper Coniacian in temperate regions (Blair & Watkins, 2009; Burnett, 1998; Melinte & Lamolda, 2007). *Amphizygus minimus* and *Prediscophaera desiderograndis*, whose first appearances are closely associated with the Coniacian/Santonian boundary, are well represented at Site U1513. The LO of *A. minimus,* which consistently occurs just above the Coniacian/Santonian boundary (Bergen & Sikora, 1999; Burnett, 1998; Gale et al., 2007; Hampton et al., 2007; Howe et al., 2007), is first observed at 108.64 m CCSF at Site U1513. The HO of the high-latitude species *Thiersteinia ecclesiastica* at 101.08 m CCSF indicates direct correlation with the top of the *T. ecclesiastica* Zone, established by Wise (1983) for the Coniacian-Santonian in the Falkland Plateau record and evident throughout the Southern Ocean (Watkins et al., 1996; Wise, 1988). Burnett (1998) placed this biohorizon in Subzone UC11b, although evidence from Site U1513 indicates a later placement in what would correlate to Subzone UC11c.

Subdivision of the middle and upper Santonian is difficult in many areas, but especially so in austral paleolat-itudes. Holococcoliths, including the genus *Calculites*, are generally quite rare or absent in the Santonian and lower Campanian of the austral oceans (e.g., Watkins et al., 1996). As a result, Zone CC16 could not be differen-tiated at Site U1513 based on the appearance of *Calculites obscurus*. The applicability of this zonal biohorizon, though, is dubious, at best, as it is often absent from other settings (e.g., Western Interior Basin: Kita et al., 2017). In addition, *C. obscurus* has been shown conclusively to be affected by strong diachronism of its first appearance (Thibault et al., 2016). Thus, the HO of *L. septenarius* (99.20 m CCSF) is used as an alternate biohorizon for the base of Zone CC17. This zone continues to the top of the Cretaceous section at Site U1513, as no specimens of *Broinsonia parca parca*, or its ancestor *B. p. expansa* (s.s.) were observed in any sample. This age is corroborated by the presence throughout this interval and in the topmost sample at 62.70 m CCSF of *Eprolithus floralis*, which had a latest Santonian extinction.

Therefore, although the topmost sediments of the Cretaceous interval in Holes U1513A and U1513B were pre-viously dated Santonian-earliest Campanian by Huber et al. (2019a), re-examination of the calcareous plankton assemblages revealed the absence of the marker taxa used to identify the base of the Campanian (see discussion in Miniati et al., 2020). Thus, the Santonian-Campanian boundary interval is interpreted to be missing at Site U1513 and the hardground that overlies the Cretaceous sediments corresponds to a hiatus that spans from the upper Santonian to Miocene (Figure 2).

## 4. Composition of the Microfossil Assemblages

Apart from calcareous nannofossils, the microfossil assemblage throughout the studied stratigraphic section at Site U1513 is composed mainly of planktonic foraminifera that reach absolute abundance values of 50,000 to 60,000 specimens per gram of dry sediment in the upper Turonian-lower Coniacian and in the Santonian (Figure 3). Benthic foraminifera are subordinate in relative abundance and occur in high absolute abundance (600–700 specimens per gram of dry sediment) only in the Turonian to lower Coniacian sediments. Radiolaria are present from the upper Turonian to middle Coniacian and near the base of the Santonian reaching 700 spec-imens per gram of dry sediment. The carbonate content ($CaCO_3$) parallels the calcareous microfossil absolute abundance values and shows a progressive increase from the base to the top of the studied stratigraphic interval
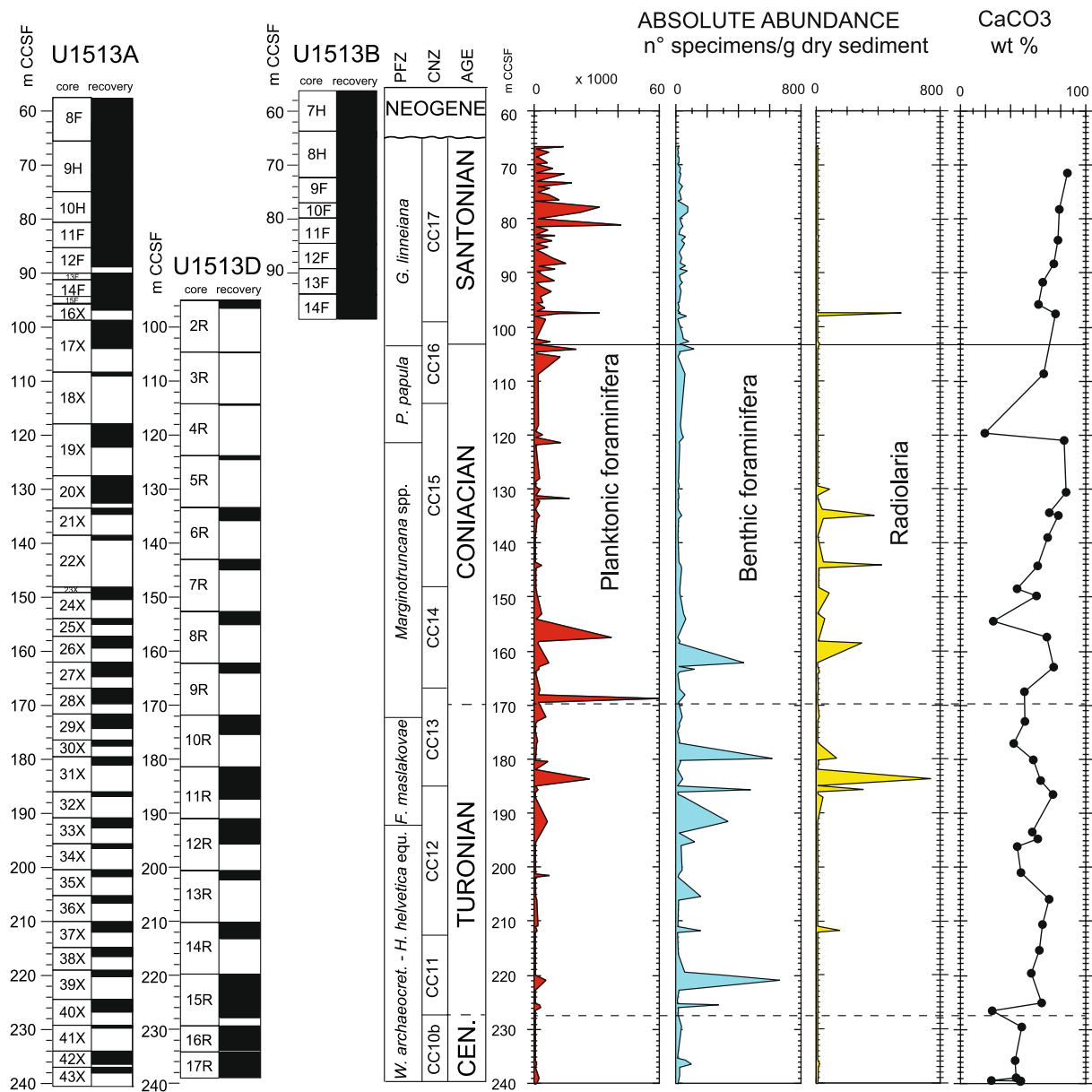
**Figure 3.** Holes U1513A, U1513B, and U1513D: absolute abundance in number of specimens per gram of dry sediments of planktonic foraminifera, benthic foraminifera, and radiolaria. CaCO₃ content according to Huber et al. (2019a). Core recovery, age, planktonic foraminiferal and calcareous nannofossils biozonations, and abbreviations as explained in the caption of Figure 2.

with episodic decreases related to the presence of more clay-rich intervals at 226.54, 196.09, 176.98, 154.32, and 119.59 m CCSF that contain a carbonate content ranging from 20 to 40wt% (Figure 3).

The diversity of planktonic foraminifera shows a gradual increase throughout the studied stratigraphic interval from 6–8 species in the upper Cenomanian-Turonian to 12–18 species in the Santonian (Figure 4). The Turonian-Coniacian interval is characterized by dominance of small-sized specimens (125–38 μm) belonging to the genera *Muricohedbergella*, *Whiteinella*, planispiral and biserial taxa, and by low absolute abundances of the large-sized (>125 μm) genera *Marginotruncana* and *Dicarinella*. The small-sized *Microhedbergella* are found in the upper Cenomanian and sporadically in the Turonian (Figure 4). The increase in species richness observed across the Coniacian and Santonian intervals is coincident with the diversification of species included in *Globotruncana* and the progressive decline in abundance and extinction of all species of *Marginotruncana* which last
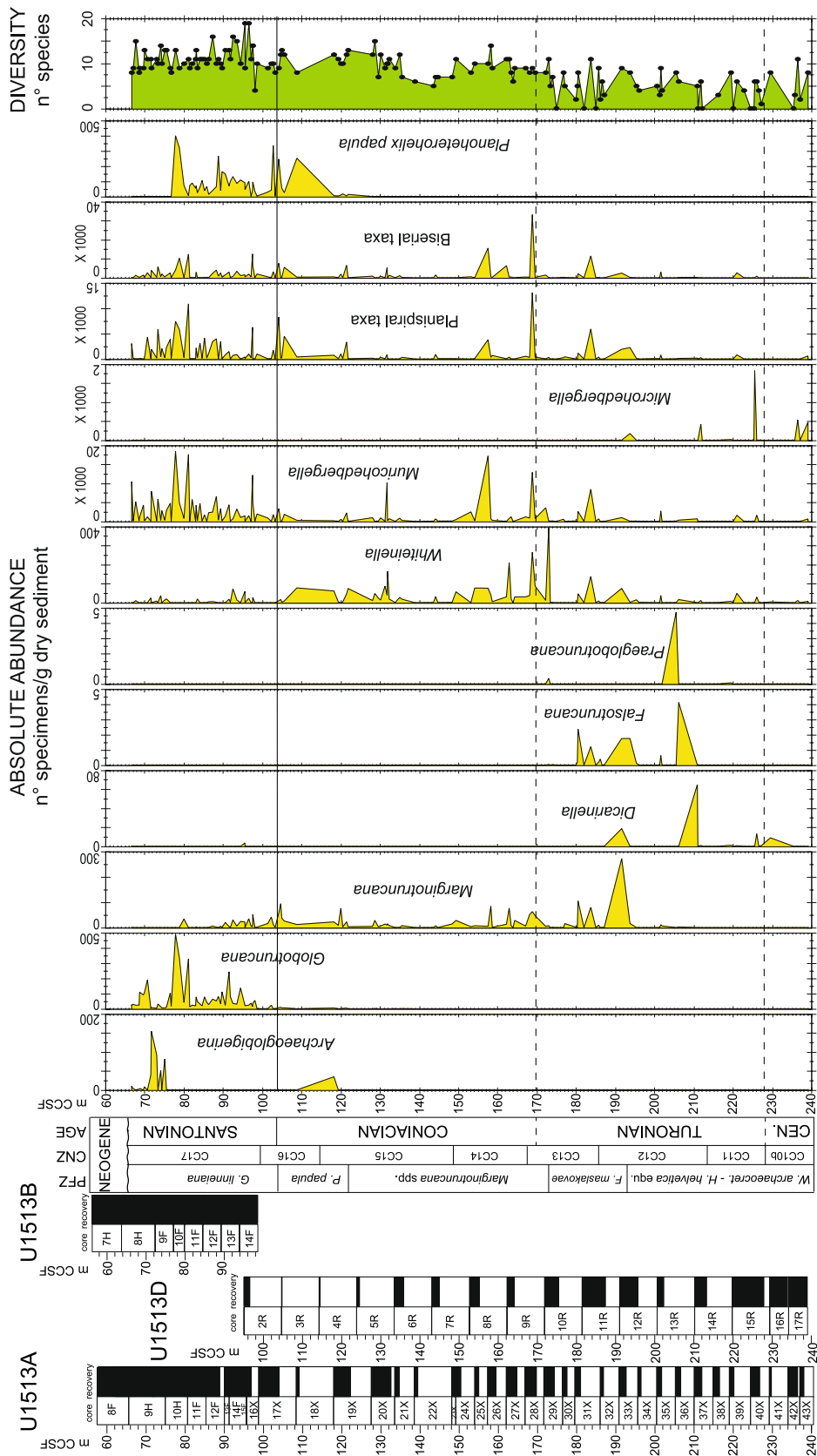
**Figure 4.** Holes U1513A, U1513B, and U1513D: absolute abundance in number of specimens per gram of dry sediments of planktonic foraminiferal genera, species and groups, and diversity of species. Core recovery, age, planktonic foraminiferal and calcareous nannofossils biozonations, and abbreviations as explained in the caption of Figure 2.

occur in the Santonian at 79.75 m CCSF. In the same interval, the biserial and large-sized *P. papula* shows a short stratigraphic distribution and disappears at about the same level of *Marginotruncana* (Figure 4).

Preservation is good to moderate in most of the latest Cenomanian-Santonian samples where tests exhibit slight to moderate recrystallization. Very rare specimens showing glassy preservation (=translucent tests lacking evidence of test wall recrystallization) were observed within the studied interval. Several samples in the Turonian and Coniacian intervals yield foraminifera that are strongly recrystallized and infilled with sparry calcite. Specimens showing this level of preservation were excluded from the isotopic analyses. Tests of the planktonic foraminifera *Planoheterohelix globulosa* were dissected and imaged in a scanning electron microscope (SEM) to show typical preservation of specimens analyzed for their stable isotopic composition. Test walls showing minor recrystallization (=good preservation) have wall pores that are still visible and calcite rhombs on the test interior are very small in size (Figures 5a and 5b, 5d). Test walls showing moderate recrystallization (=moderate preservation) have coarser calcite overgrowths that have infilled the original wall pores (Figure 5c).

The stratigraphic distribution of the planktonic foraminiferal species analyzed and the list of taxa occurring at Site U1513 are reported in Supporting Information S1 and at https://doi.pangaea.de/10.1594/PANGAEA.939392. The most important species are illustrated in Figures 6–8.

Calcareous benthic foraminifera commonly occur and show good preservation in the Turonian to Santonian sediments at Site U1513. The benthic foraminiferal assemblage is characterized by the common occurrence of *Notoplanulina* spp., *Gavelinella* spp., *Anomalinoides* spp., and various gyroidinids. *Nuttallides* and *Nuttallinella* are abundant and show a continuous occurrence in mid-Santonian sediments (91.26 and 76.50 m CCSF). Pleurostomellids occur frequently. The Polymorphinidae, the *Marginulina/Vaginulina* group, *Lenticulina* spp., and other nodosarids increase in abundance toward the top of the Cretaceous sediments. Agglutinated benthic foraminifera are present in some samples, and a slight increase in the abundance of these forms is recorded near the top of the Santonian succession (at about 75.00 m CCSF). Large gavelinellids, members of the *Notoplanulina* lineage, and *Nuttallinella* and *Nuttallides* decline in abundance up-section where they are partially replaced in relative abundance by specimens of *Gyroidinoides* spp. In general, the Turonian-Coniacian interval is characterized by bathyal benthic foraminiferal assemblages dominated by epifaunal taxa, whereas infaunal benthic foraminifera become more abundant toward the top of the Santonian. The list of taxa and the abundance of benthic foraminiferal groups throughout the Santonian at Site U1513 is reported in Supporting Information S1 and at https://doi.pangaea.de/10.1594/PANGAEA.939392.

## 5. Carbon Isotope Record

The carbon isotope record obtained from bulk carbonate and foraminiferal calcareous tests at Site U1513 (Figure 9; data at https://doi.pangaea.de/10.1594/PANGAEA.939392) shows generally parallel trends and consistent offsets among different foraminiferal species. These observations, combined with generally good preservation of foraminifera in the Santonian, good to moderate preservation in the Turonian-Coniacian, and high carbonate content in all samples, support that changes in $\delta^{13}C$ values record primary paleoceanographic signals. The relatively high carbon isotopic values observed at about 230 m CCSF (Figure 9) may be the local expression of the Cenomanian/Turonian Boundary Event (CTBE; Jarvis et al., 2006; Figure 1c), but high-resolution examination of the Cenomanian-Turonian boundary interval and OAE 2 at Site U1513 and correlation with Site U1516 (Petrizzo et al., 2021) have not been completed yet. Thus, these high $\delta^{13}C$ values are not discussed further here; the OAE 2 interval at Site U1513 will be the topic of future publications.

The carbon isotope trends of both bulk carbonate and foraminiferal values observed throughout the section at Site U1513 reveal positive and negative carbon isotope excursions and inflection points, but, with a couple of exceptions, the stratigraphic patterns of peaks and troughs cannot be confidently correlated with the bulk carbonate isotopic records of the European sections (e.g., English Chalk: Jarvis et al., 2006. Bottaccione section, Italy: Sprovieri et al., 2013. Lägerdorf: Voigt et al., 2010. North Sea Basin: Eldrett et al., 2021. See also Cramer & Jarvis, 2020; Figure 1c). The record at Site U1513 does register $\delta^{13}C$ minimum across the Turonian-Coniacian boundary interval at about 162–168 m CCSF (Figure 9) consistent with the Navigation Event (Jarvis et al., 2006), which has been interpreted as the inflection point in the long-term Late Cretaceous carbon isotope curve registered in several stratigraphic sections from Europe (e.g., Jarvis et al., 2006; Sprovieri et al., 2013; Voigt et al., 2021; Voigt & Hilbrecht, 1997) and Japan (Takashima et al., 2010, 2019). However, poor sediment
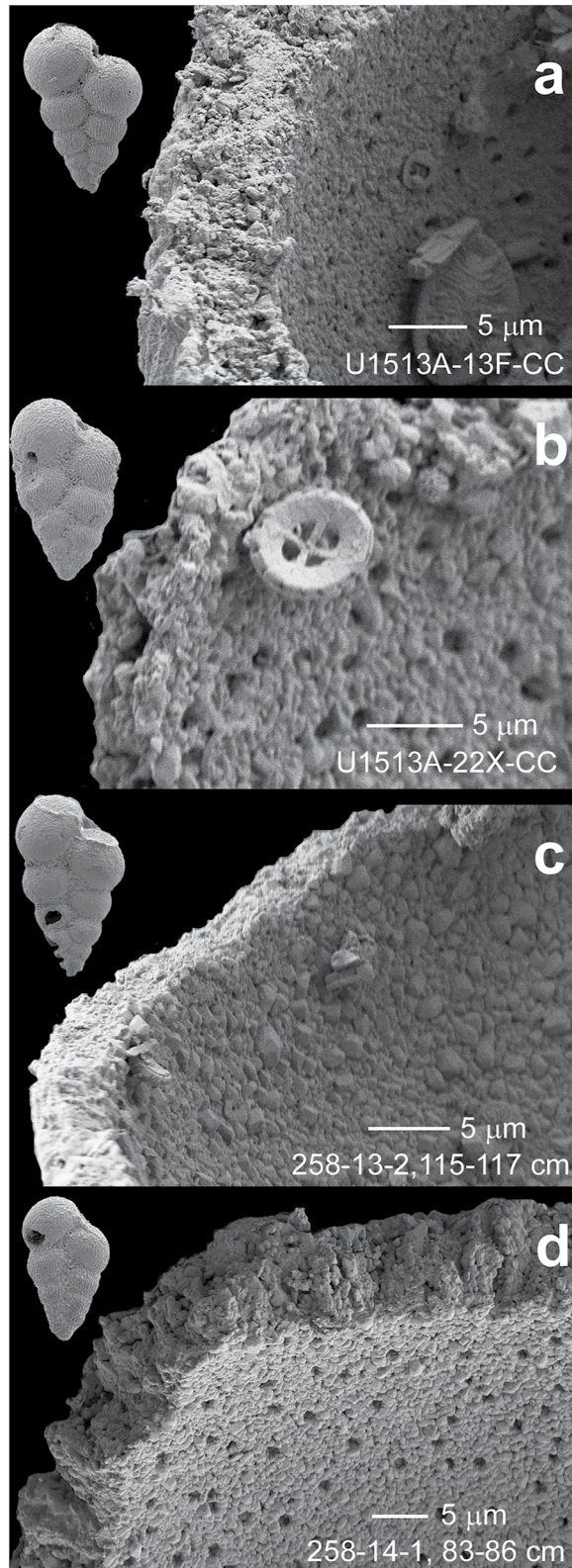
**Figure 5.** Comparison of test wall preservation among dissected specimens of *Planoheterohelix globulosa* showing interior of penultimate chamber and broken test wall surface for specimens from IODP Sites U1513 and nearby DSDP Site 258. (a) Sample U1513A-13F-CC, lower Santonian (*Globotruncana linneiana* Zone, Zone CC17). (b) Sample U1513A-22X-CC, lower Coniacian (*Marginotruncana* spp. Zone, Zone CC15). The calcareous nannofossil *Praedicosphaera columnata* (proximal view) is visible on the foraminiferal test. (c) Sample 258-13-2, 115–117 cm, lower Turonian (*Whiteinella baltica* Zone, Zone CC11; Huber et al., 2018). (d) Sample 258-14-1, 83–86 cm, upper Cenomanian (*Whiteinella baltica* Zone, Zone CC10a; Huber et al., 2018).
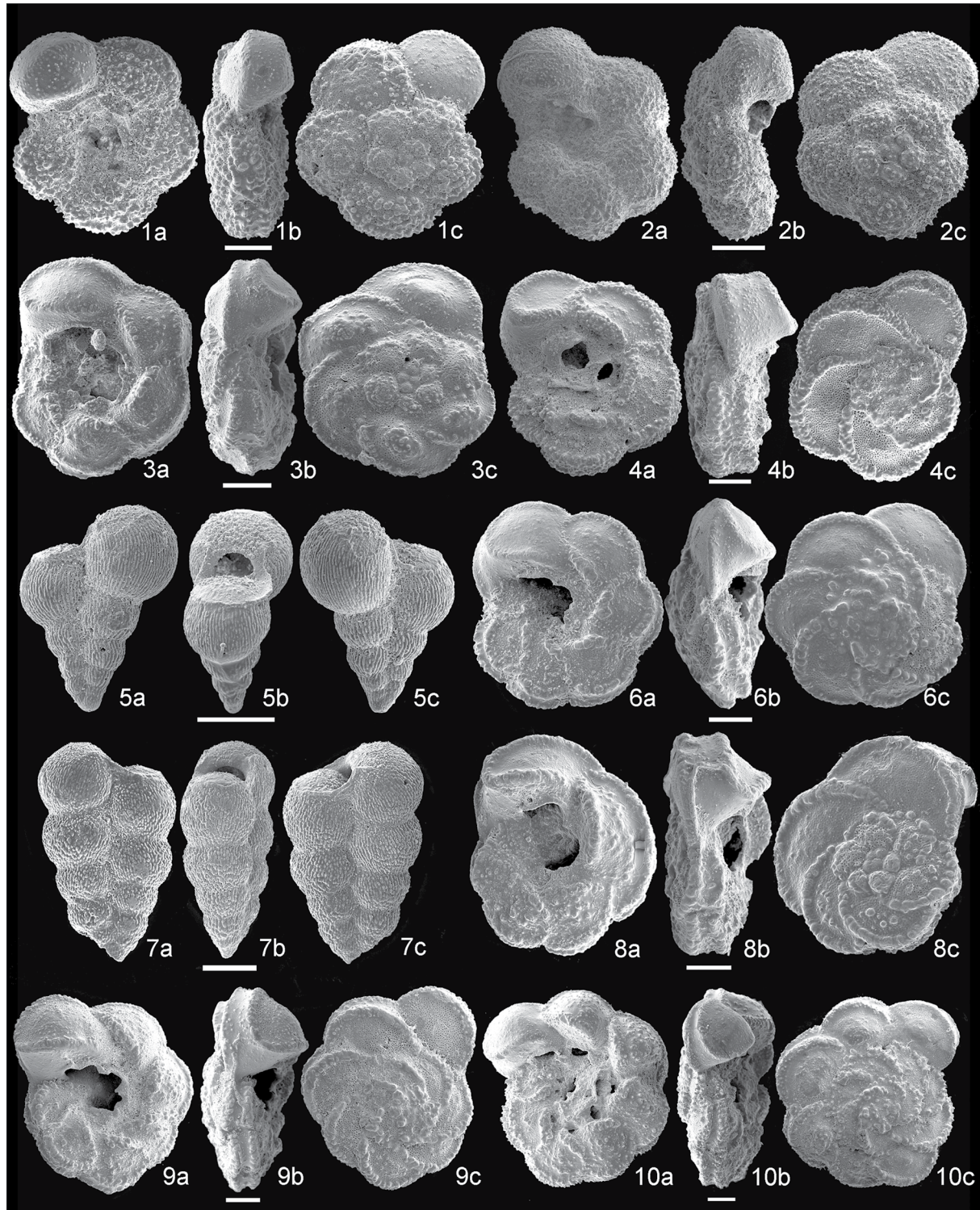
**Figure 6.** Scanning electron microscope (SEM) images of species of planktonic foraminifera. (1a–c) *Globotruncana hilli*, sample 369-U1513B-8H-5, 98–100 cm. (2a–c) *Archaeoglobigerina cretacea*, sample 369-U1513B-8H-6, 48–50 cm. (3a–c) *Globotruncana bulloides*, sample 369-U1513B-10F-1, 50–52 cm. (4a–c) *Globotruncana linneiana*, sample 369-U1513B-11F-1, 100–102 cm. (5a–c) *Planoheterohelix globulosa*, sample 369-U1513B-8H-5, 98–100 cm. (6a–c) *Globotruncana arca*, sample 369-U1513B-13F-2, 145–147 cm. (7a–c) *Planoheterohelix papula*, sample 369-U1513A-13F-1, 52–54 cm. (8a–c) *Marginotruncana pseudolinneiana*, sample 369-U1513B-14F-1, 122–124 cm. (9a–c) *Globotruncana neotricarinata*, sample 369-U1513B-14F-2, 70–74 cm. (10a–c) *Globotruncana bulloides* (=*culverensis*), sample 369-U1513B-14F-3, 22–24 cm.
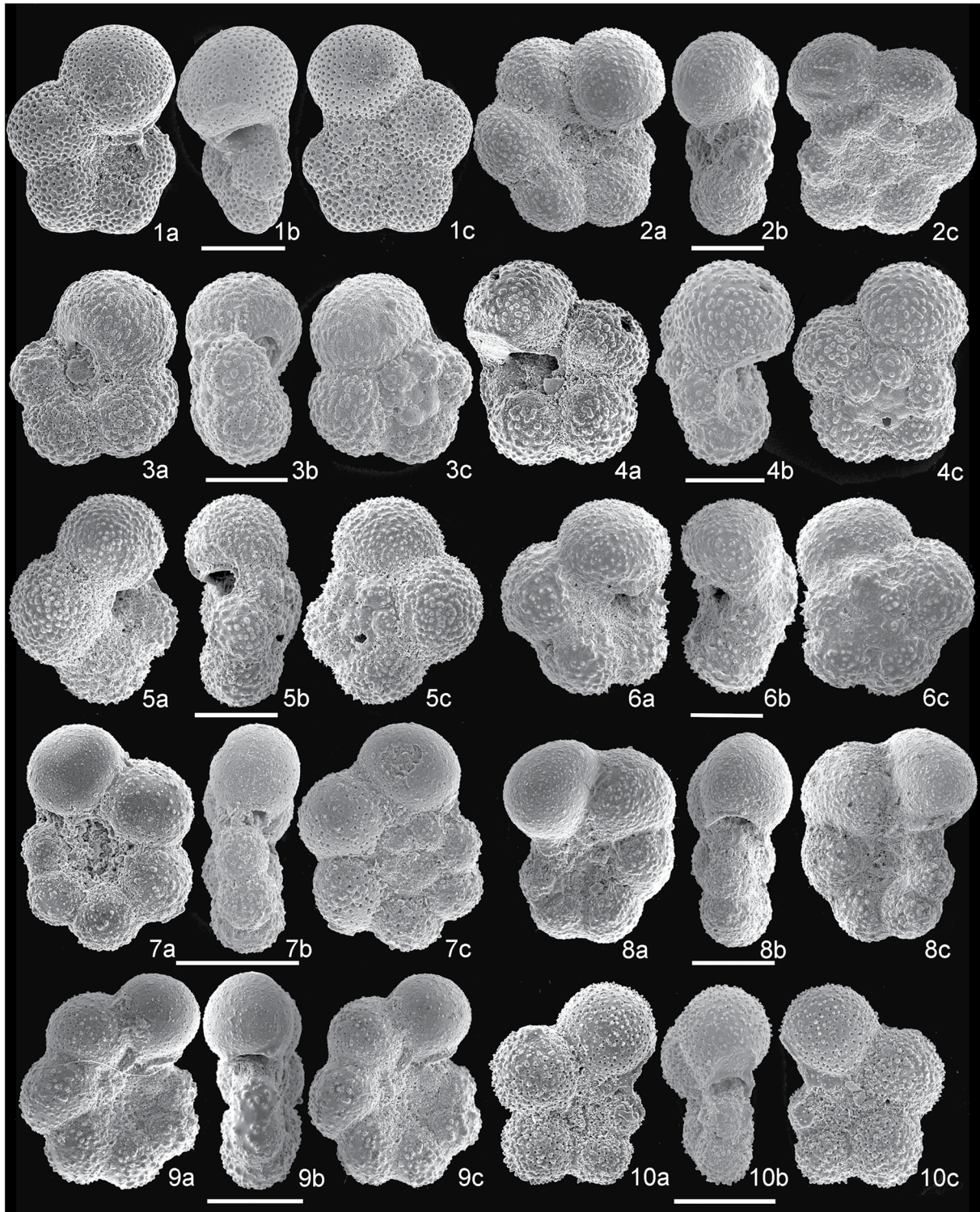
**Figure 7.** Scanning electron microscope (SEM) images of species of planktonic foraminifera. (1a–c) *Muricohedbergella crassa*, sample 369-U1513A-11F-4, 60–62 cm. (2a–c) *Muricohedbergella planispira*, sample 369-U1513B-9F-3, 30–32 cm. (3a–c) *Costellagerina* cf. *bulbosa*, sample 369-U1513A-9H-5, 145–147 cm. (4a–c) *Costellagerina* cf. *pilula*, sample 369-U1513A-9H-5, 145–147 cm. (5a–c) *Whiteinella baltica*, sample 369-U1513B-13F-5, 145–147 cm. (6a–c) *Muricohedbergella delrioensis*, sample 369-U1513B-13F-5, 95–97 cm. (7a–c) *Liuenella falklandica*, sample 369-U1513A-9H-6, 98–100 cm. (8a–c) *Globigerinelloides alvarezi*, sample 369-U1513B-10F-1, 50–52 cm. (9a–c) *Globigerinelloides ultramicrus*, sample 369-U1513B-11F-1, 100–102 cm. (10a–c) *Globigerinelloides asper*, sample 369-U1513A-11F-2, 143–145 cm.
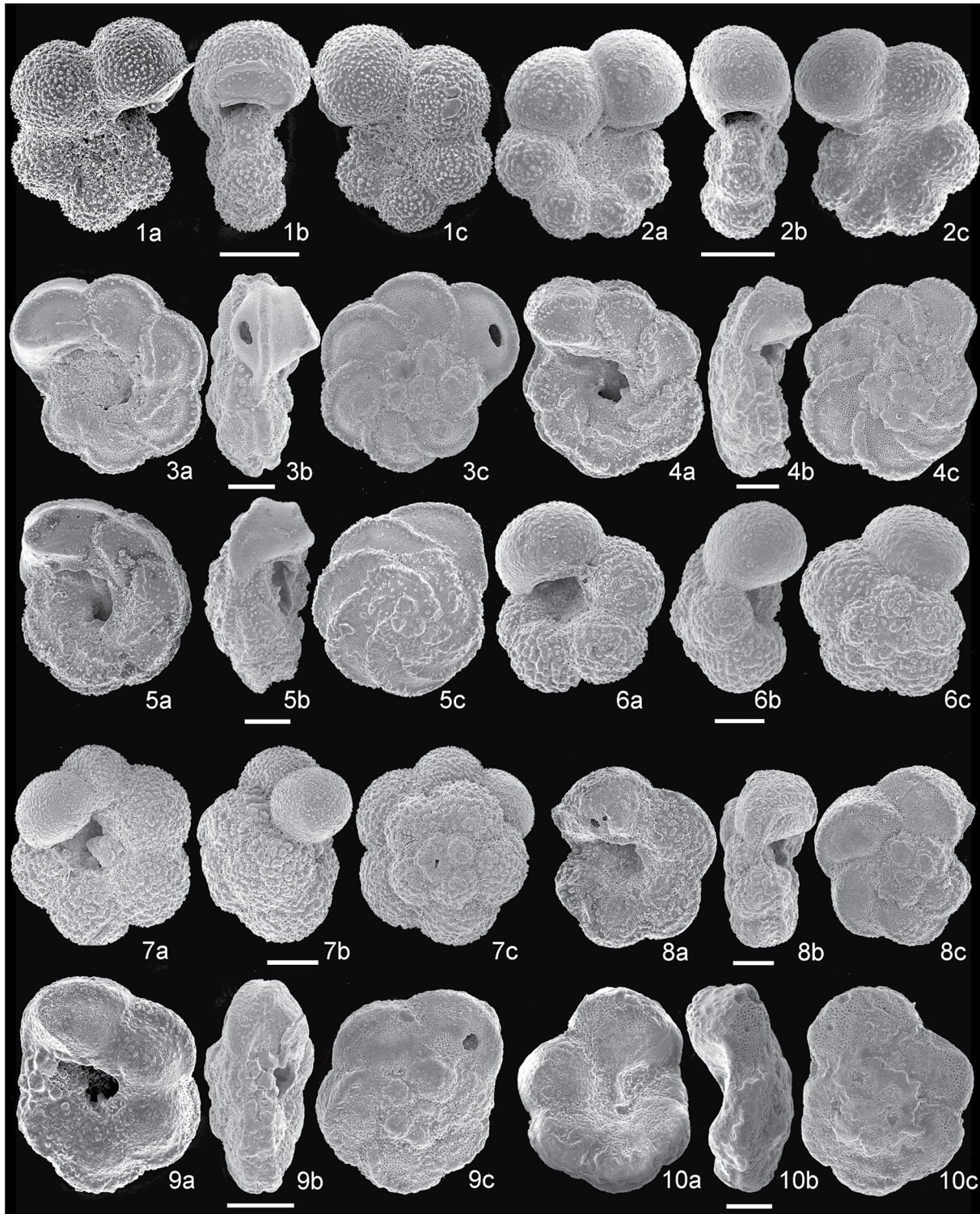
**Figure 8.** Scanning electron microscope (SEM) images of species of planktonic foraminifera. (1a–c) *Globigerinelloides prairiehillensis*, sample 369-U1513A-11F-2, 143–145 cm. (2a–c) *Globigerinelloides yaucoensis*, sample 369-U1513B-14F-2, 70–72 cm. (3a–c) *Marginotruncana pseudomarginata*, sample 369-U1513A-17X-4, 70–73 cm. (4a–c) *Marginotruncana coronata*, sample 369-U1513A-17X-4, 70–73 cm. (5a–c) *Contusotruncana morozovae*, sample 369-U1513A-17X-2, 40–43 cm. (6a–c) *Whiteinella brittonensis*, sample 369-U1513A-24X-1, 10–13 cm. (7a–c) *Whiteinella paradubia*, sample 369-U1513A-19X-3, 75–78 cm. (8a–c) *Dicarinella marginata*, sample 369-U1513A-26X-1, 88–91 cm. (9a–c) *Dicarinella hagni*, sample 369-U1513A-37X-2, 111–114 cm. (10a–c) *Falsotruncana maslakovae*, sample 369-U1513A-33X-1, 10–13 cm.
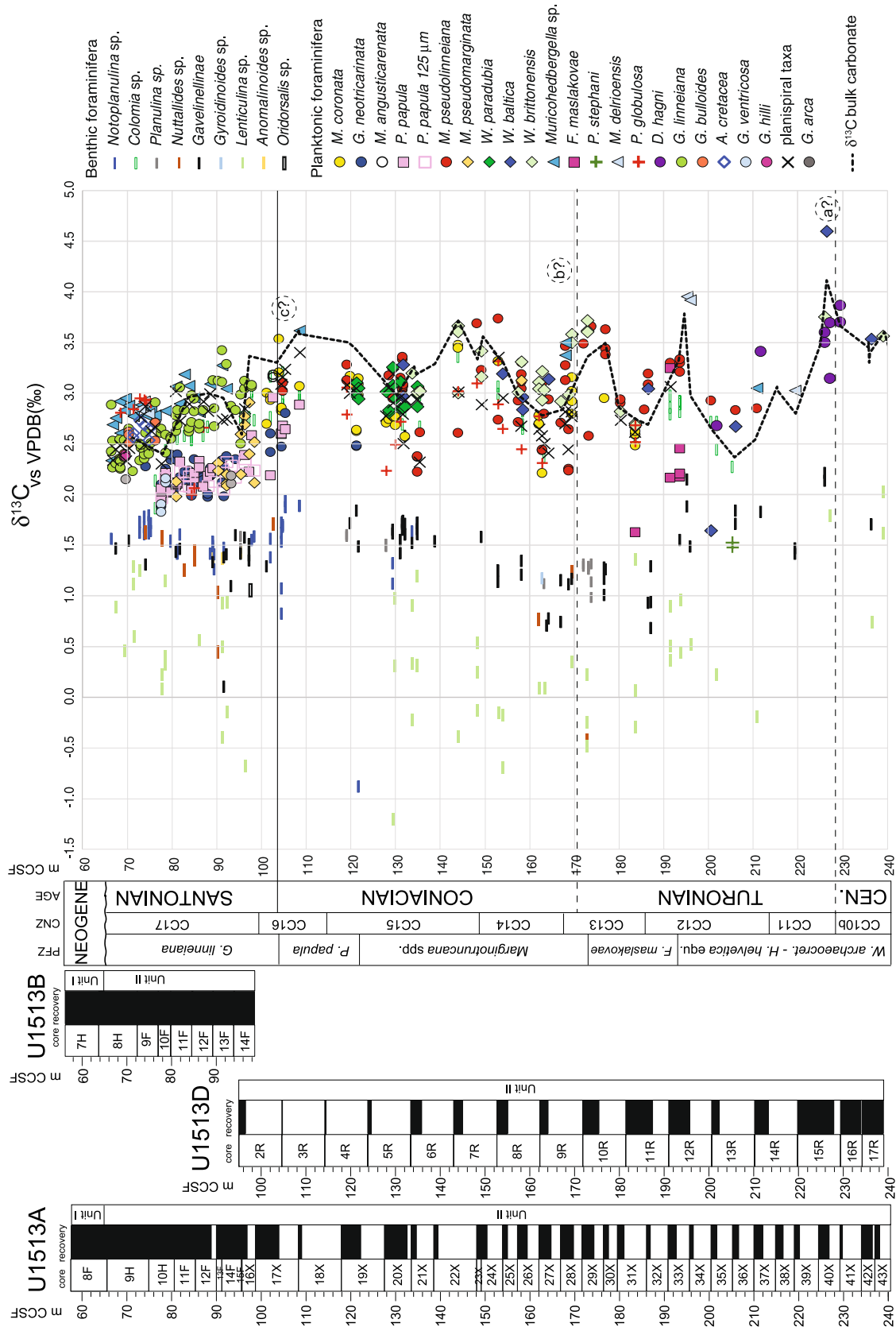
**Figure 9.** Holes U1513A, U1513B, and U1513D: δ¹³C record of bulk carbonate and benthic and planktonic foraminifera. Carbon isotope events of uncertain identification at Site U1513: a? = Cenomanian/Turonian Boundary Event, b? = Navigation Event, c? = Michel Dean Event; see Figure 1c for the carbon isotope reference curve. Core recovery, lithologic units, age, planktonic foraminiferal and calcareous nannofossils biozonations, and abbreviations as explained in the caption of Figure 2.

recovery and poor to moderate preservation of foraminifera in several samples, especially in the Turonian-Coniacian stratigraphic interval, hampered identification of other chemostratigraphic events. Even features observed across the Turonian-Coniacian boundary interval, they could reflect either carbon cycling in the austral seas or be artifacts of poor recovery. Certainly, additional high-resolution studies are needed before chemostratigraphic correlation with the European records and elsewhere can be confidently proposed for the Turonian and Coniacian.

Sediment recovery improves upward at Site U1513 and positive $\delta^{13}C$ excursions in both bulk carbonate and foraminiferal data with values approaching 3.5‰ are registered across the base of the Santonian (Figure 9) and could correspond with the Michel Dean Event identified near the base of the Coniacian/Santonian boundary in the European sections (Figure 1c) including the Santonian stratotype section (Jarvis et al., 2006; Lamolda et al., 2014; Thibault et al., 2016; Voigt et al., 2010). In the Santonian interval the carbon isotope values decline by 0.5‰ and show fluctuations toward the top of the studied stratigraphic sequence (Figure 9). This trend within the Santonian is not observable in the low latitude sections (e.g., English Chalk: Jarvis et al., 2006. German chalk: Voigt et al., 2010. Italy: Sprovieri et al., 2013. Tibet: Wendler, 2013).

## 6. Foraminiferal Stable Isotope Paleoecology and Species Depth Ranking

The relative ranking of carbon and oxygen isotope values measured from co-occurring foraminiferal taxa (data at https://doi.pangaea.de/10.1594/PANGAEA.939392) permits characterization of their relative depth habitats and can be used as a proxy for determining the thermal stratification and dissolved inorganic carbon (DIC) $\delta^{13}C$ gradient of the water column through time (e.g., Abramovich et al., 2003; Birch et al., 2013; D'Hondt & Arthur, 1995; Mulitza et al., 1997; Petrizzo et al., 2008; Rohling et al., 2004). Therefore, the species-specific $\delta^{18}O$ versus $\delta^{13}C$ values are plotted to interpret the foraminiferal depth ecology (Figure 10). Differences in $\delta^{18}O$ and $\delta^{13}C$ among samples may be influenced by (a) depth migration though ontogeny; (b) peaks in abundance during different seasons for different taxa; (c) measurement errors; (d) environmental factors (e.g., pH and alkalinity); and (e) diagenetic artifacts. To minimize ontogenetic and preservational artifacts, we analyzed only the best-preserved specimens of the most abundant species taken from a narrow size fraction.

Stable isotope analyses of bulk carbonate are also shown on the $\delta^{18}O$ versus $\delta^{13}C$ cross plots relative to foraminiferal data from the same time intervals (Figure 10). These measurements are mostly from calcareous nannofossils that lived in the photic zone, but they also include analyses of deeper dwelling calcareous nannofossil taxa as well as potential contributions from other calcareous biogenic constituents (e.g., benthic and planktonic foraminifera, echinoid spines).

### 6.1. Latest Cenomanian

The available data for the latest Cenomanian shown in the $\delta^{18}O$ versus $\delta^{13}C$ foraminiferal cross-plot (Figure 10a) indicate a clear separation between benthic and planktonic foraminifera. *Whiteinella baltica* and *W. brittonensis* yield slightly lower $\delta^{18}O$ and $\delta^{13}C$ values than *Dicarinella hagni* and bulk carbonate values show a slight negative offset in $\delta^{18}O$ and $\delta^{13}C$ relative to the planktonic species. Although the paucity of data in this interval prevents detailed interpretations, the cross-plots of planktonic foraminifera are consistent with their growth in a shallow depth habitat.

### 6.2. Turonian

The $\delta^{18}O$ versus $\delta^{13}C$ cross-plot of foraminiferal values in the Turonian (Figure 10b) indicates differences of about 2.5‰ in both $\delta^{13}C$ and $\delta^{18}O$ between benthic taxa and planktonic foraminifera exhibiting the strongest surface water signal. However, there is a lack of clear separation among species within the planktonic and benthic realm along either axis. Whereas $\delta^{13}C$ variations among benthic taxa could reflect variations in export productivity influencing the strength of the biological pump (MacLeod et al., 2001), with infaunal taxa migrating within the sediment column tracking food sources, it is difficult to explain why these changes might lead to the high variation among benthic $\delta^{18}O$ measurements. One alternative hypothesis is that large interannual variation in circulation, perhaps on millennial timescales, within a basin strongly influenced by local processes is the source of variability observed among benthic taxa. It is noteworthy that the $\delta^{13}C$ and $\delta^{18}O$ values of *Colomia*
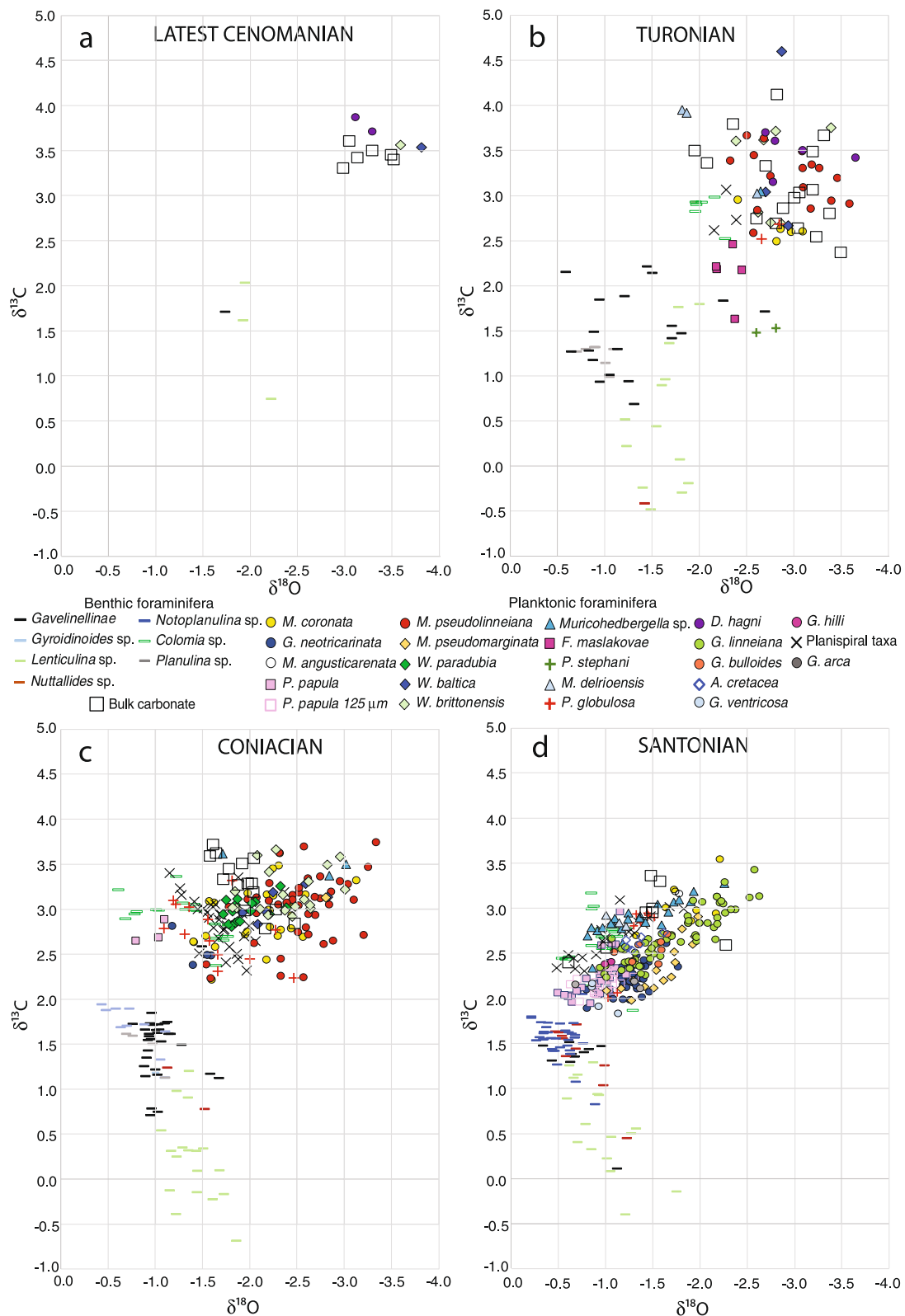
**Figure 10.** (a–d) Holes U1513A, U1513B, and U1513D: δ¹⁸O versus δ¹³C cross-plots of stable isotope values measured on bulk carbonate and well-preserved foraminiferal specimens in the latest Cenomanian (a), Turonian (b), Coniacian (c), and Santonian (d). Among planktonic foraminifera, species showing the lowest δ¹⁸O and the highest δ¹³C values are interpreted as surface dwellers whereas species displaying the highest δ¹⁸O values and the lowest δ¹³C values are interpreted as thermocline dwellers (Pearson, 1998; Pearson et al., 2001). See text for the interpretation of the depth ecologies of the taxa.

**Table 2**
*Depth Ecology of the Planktonic Foraminifera Species Occurring at Site U1513 According to Their Species-Specific $\delta^{18}O$ Versus $\delta^{13}C$ Values*

| Mixed layer | Thick mixed layer or seasonal thermocline | Permanent thermocline |
|---|---|---|
| **Surface dwellers** | **Intermediate dwellers** | **Thermocline dwellers** |
| TURONIAN | | |
| *Whiteinella brittonensis* | *Marginotruncana pseudolinneiana* | *Marginotruncana coronata* |
| *Dicarinella hagni* | *Whiteinella baltica* | *Falsotruncana maslakovae* |
| | *Muricohedbergella* | *Praeglobotruncana stephani* |
| | | Biserial taxa |
| | | Planispiral taxa |
| | | |
| CONIACIAN | | |
| *Muricohedbergella* | *Whiteinella baltica* | *Globotruncana neotricarinata* |
| *Marginotruncana pseudolinneiana* | *Whiteinella paradubia* | *Planoheterohelix papula* |
| *Whiteinella brittonensis* | *Marginotruncana coronata* | Biserial taxa |
| | | Planispiral taxa |
| | | |
| SANTONIAN | | |
| *Muricohedbergella* | *Archaeoglobigerina cretacea* | *Globotruncana neotricarinata* |
| *Marginotruncana coronata* | *Globotruncana bulloides* | *Planoheterohelix papula* |
| *Globotruncana linneiana* | | *Globotruncana hilli* |
| *Marginotruncana angusticarenata* | | *Globotruncana arca* |
| | | *Globotruncana ventricosa* |
| | | *Marginotruncana pseudomarginata* |
| | | Biserial taxa |
| | | Planispiral taxa |

*Note.* See text for further explanation.

are higher than co-occurring benthic taxa because of its aragonitic test composition (Bandy, 1954; Loeblich & Tappan, 1984; Wendler et al., 2011).

Large interannual and/or seasonal variations in the surface water conditions could explain overlap among planktonic foraminiferal and the wide scatter of bulk carbonate data. Petrizzo et al. (2008) and Ando et al. (2010) recognized the influence of seasonal variations in planktonic foraminiferal data from Albian-Cenomanian sediments recovered in western North Atlantic (Blake Nose, ODP Sites 1050 and 1052) and suggested that stable isotope separation among planktonic species reflects species proliferation during their seasonal optima. Specifically, the thin summer mixed layer is expected to experience relatively large and frequent short-term perturbations in temperature and salinity. This difference should be reflected in greater variability in $\delta^{18}O$ values in analyses of taxa that lived in the summer mixed layer than observed for analyses of taxa that lived in the thick winter mixed layer or below the seasonal thermocline (in addition to surface dwelling taxa having generally low $\delta^{18}O$ values and high $\delta^{13}C$ values; Petrizzo et al., 2008).

Applying this model, we propose that *W. brittonensis* and *D. hagni* in the Turonian interval (Figure 10b; Table 2) were summer mixed-layer dwellers as interpreted for nearby Site U1516 in the Mentelle Basin (Petrizzo et al., 2020, 2021). These taxa exhibit relatively high variability in $\delta^{18}O$ and $\delta^{13}C$ among samples and show the lowest $\delta^{18}O$ and highest $\delta^{13}C$ values. *Whiteinella baltica* and *Marginotruncana pseudolinneiana* also shows relatively high variability among samples but have slightly lower $\delta^{13}C$ values suggesting that they lived near the seasonal thermocline or in the thick winter mixed layer. *Marginotruncana coronata*, *P. globulosa*, and planispiral taxa have isotopic values with relatively little variation among samples and are hypothesized to have lived below

the seasonal thermocline in agreement with previous data from other southern high latitudes sites (Falkland Plateau Site 511, Mentelle Basin Site 258 and Site U1516; Huber et al., 1995, 2018; Petrizzo et al., 2020; Figure 1a). Low $\delta^{13}C$ values are typical for Cretaceous biserial taxa (*P. globulosa*; Huber et al., 1995, 1999; MacLeod et al., 2000, 2001; 2005) and may reflect stronger disequilibrium fractionation due to their presumed faster growth rate, which has been inferred for opportunistic groups (e.g., Bornemann & Norris, 2007; Hart, 1980; Leckie, 1987; Premoli Silva & Sliter, 1999). The stable isotope record of *F. maslakovae* and *Praeglobotruncana stephani* is consistent with previous interpretations (Mentelle Basin Site U1516: Petrizzo et al., 2020; Falkland Plateau Site 511: Huber et al., 1995; Tanzania: Wendler et al., 2013) that show relatively little variability between samples, with the highest $\delta^{18}O$ values and usually the lowest $\delta^{13}C$ values, suggesting that they probably lived below the seasonal thermocline, possibly near the permanent thermocline. The depth ecology of *Muricohedbergella*'s species is more difficult to interpret because of the variability in $\delta^{18}O$ and $\delta^{13}C$ values among samples, although its variable $\delta^{13}C$ values could indicate seasonal variations in the surface waters.

### 6.3. Coniacian

In the Coniacian, the $\delta^{18}O$ versus $\delta^{13}C$ cross plot (Figure 10c) indicates differences of about 2.0‰ between epibenthic foraminifera and planktonic foraminiferal species with the latter exhibiting the strongest surface water signal. In both $\delta^{13}C$ and $\delta^{18}O$ values there is good separation between planktonic and benthic values. In addition, benthic $\delta^{18}O$ values span a much smaller range and the degree of correlation between $\delta^{18}O$ and $\delta^{13}C$ values of planktonic foraminiferal species is higher compared to the Turonian data. These changes suggest increased stratification of the water column and lower interannual variation in sea floor waters. However, planktonic foraminiferal data still show moderate overlap among species that could indicate large interannual and/or seasonal variations in the surface water conditions.

*Muricohedbergella* show low $\delta^{18}O$ and high $\delta^{13}C$ values and are interpreted as summer, mixed-layer dwellers (Figure 10c; Table 2). *Marginotruncana pseudolinneiana* shows the lowest $\delta^{18}O$ and the highest $\delta^{13}C$ values and is interpreted as summer mixed-layer dweller. It also has high intra-specific variability among samples consistent with relatively large and frequent short-term perturbations in temperature and nutrient concentrations. Similarly, *M. coronata* exhibits relatively high variability in $\delta^{18}O$ and $\delta^{13}C$ among samples suggesting that it lived in the thick winter mixed layer, and it may also have lived in deeper ecological niches during its ontogeny or had the potential to expand its numbers early in the spring before significant warming and $^{12}C$ depletion of surface water DIC had occurred. *Whiteinella baltica* and *Whiteinella paradubia*, show a slightly higher $\delta^{18}O$ and lower $\delta^{13}C$ values indicating a depth habitat near the seasonal thermocline or in the winter mixed layer, or population blooms early in the season before surface waters are depleted in $^{12}C$. *Whiteinella brittonensis,* in contrast, shows a similar degree of variability but higher $\delta^{13}C$ and lower $\delta^{18}O$ values suggesting its preference for growth during the summer season. Planispiral and biserial (*P. globulosa*) taxa register small $\delta^{18}O$ and high $\delta^{13}C$ intra-specific variability among samples indicating a depth habitat below the seasonal thermocline or near the permanent thermocline. A habitat in the permanent thermocline is inferred for *G. neotricarinata,* which yields the highest $\delta^{18}O$ and nearly the lowest $\delta^{13}C$ values and for *P. papula* that exhibits the highest $\delta^{18}O$ and relatively low $\delta^{13}C$ values. Bulk carbonate cross-plots are intermediate between those of the upper surface dwelling and thermocline dwelling planktonic species.

### 6.4. Santonian

The depth ecology of Santonian foraminifera is consistent with previous stable isotopic interpretations from Site U1513 (Petrizzo et al., 2020) that reveal they lived in a well stratified water column. There is a clear separation in isotopic values between planktonic and benthic species as well as good separation among taxa living within the surface waters (Figure 10d; Table 2). Differences between planktonic foraminifera and epibenthic foraminifera remain about 2.0‰ in both $\delta^{13}C$ and $\delta^{18}O$, similar to the Coniacian data. Planktonic foraminifera exhibit high inter-specific variability in $\delta^{18}O$ and $\delta^{13}C$ values, but the overlap in fields occupied by different taxa is reduced relative to earlier time slices and correlation between $\delta^{18}O$ versus $\delta^{13}C$ is increased (Figure 10d). Separation among Santonian taxa is arguably even more apparent in the stratigraphic plots (Figures 9, 11, and 12) than the cross-plots (Figure 10d) as declining trends in both isotopic measurements for all taxa through time are masked when the data are all plotted on the same isotopic axes. Regardless of the visualization scheme, these data indicate
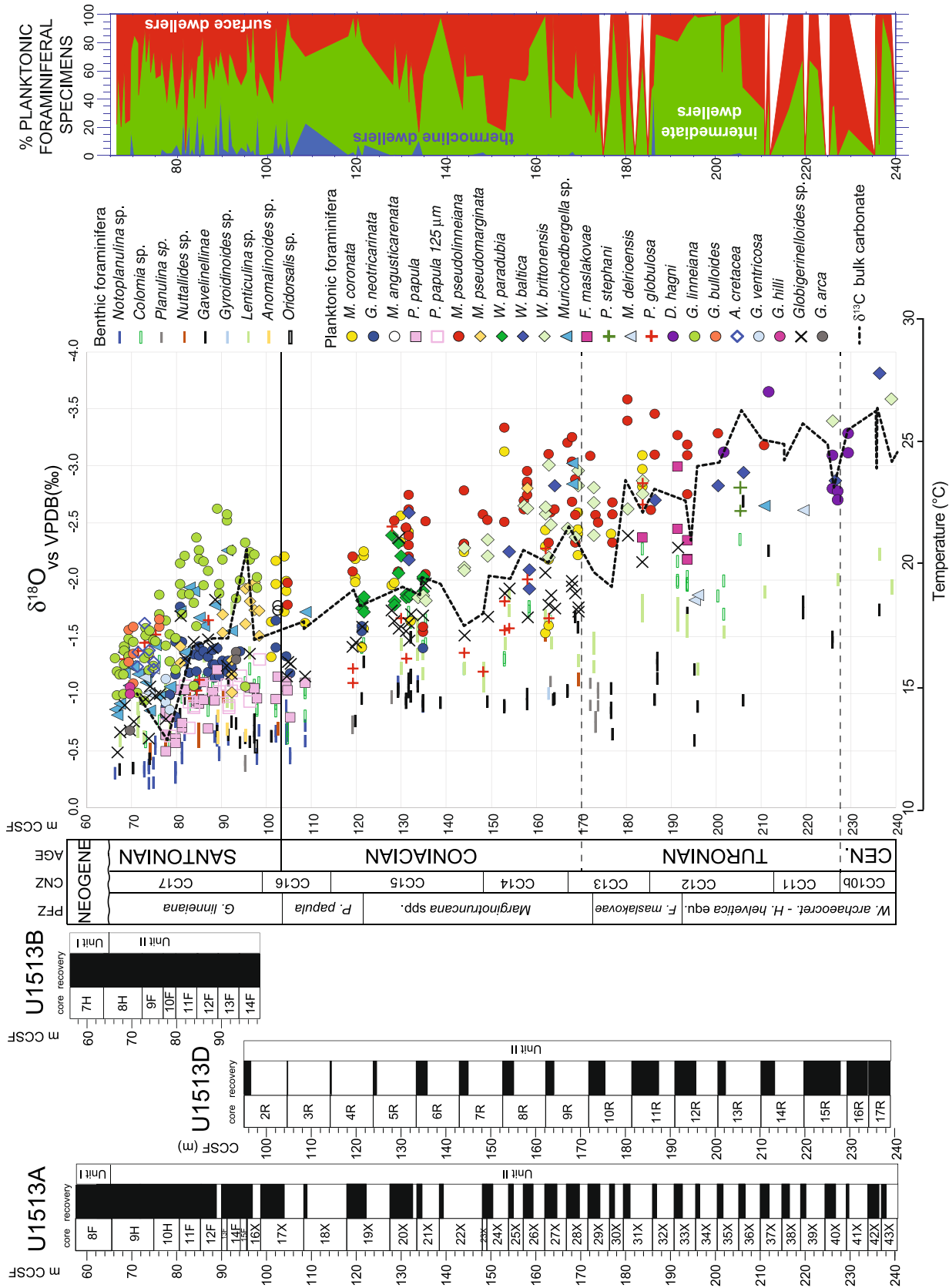
**Figure 11.** Holes U1513A, U1513B, and U1513D: δ^{18}O record of bulk carbonate and foraminifera compared with the percent distribution of thermocline (blue), intermediate (green), and surface dweller (red) planktonic foraminifera; barren samples are shown in white. Core recovery, lithologic units, age, planktonic foraminiferal and calcareous nannofossils biozonations, and abbreviations as explained in the caption of Figure 2.
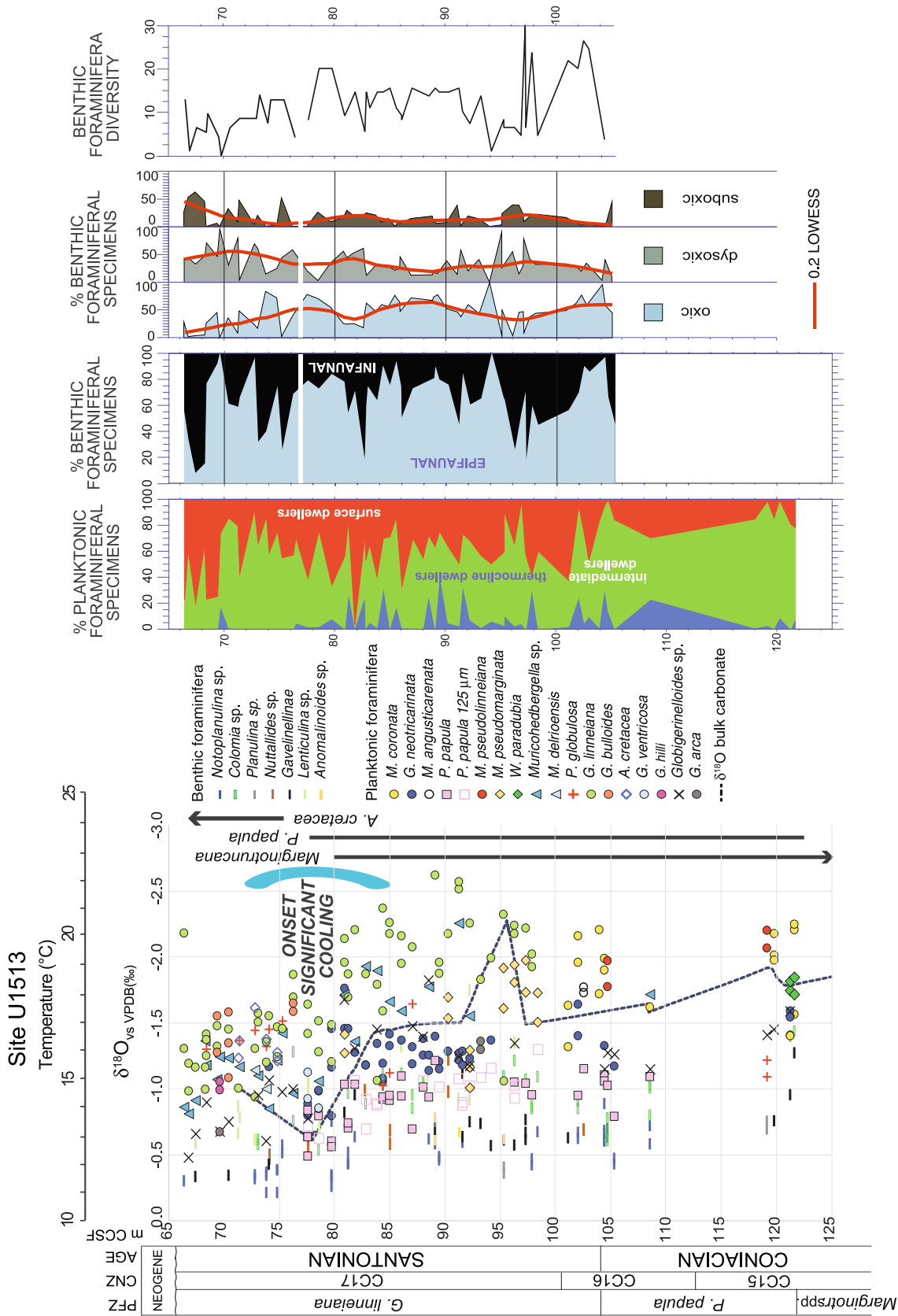
**Figure 12.** The upper Coniacian-Santonian interval at Site U1513: δ¹⁸O record of bulk carbonate and foraminifera. Percent abundance of thermocline (blue), intermediate (green), and surface dweller (red) planktonic foraminifera. Percent abundance of epifaunal (light blue), infaunal (black), oxic, dysoxic, suboxic benthic foraminifera, and taxa diversity. The stratigraphic distribution of *Marginotruncana*, *Archaeoglobigerina cretacea*, and *Planoheterohelix papula* is shown. The onset of the significant cooling in the Santonian is placed at the abrupt decline in the δ¹⁸O values of the surface dweller planktonic foraminiferal and calcareous nannofossils biozonations, and abbreviations as explained in the caption of Figure 2. See text for further explanation.

well-developed stratification, with a stable and relatively well-developed thermocline distinct from the surface mixed layer.

*Marginotruncana coronata* shows the lowest $\delta^{18}O$ and the highest $\delta^{13}C$ values suggesting this species was a summer mixed-layer dweller at high latitudes during the Santonian. *Globotruncana linneiana* and *Muricohedbergella* exhibit very high variability in $\delta^{18}O$ and $\delta^{13}C$ of more than 1‰ among samples indicating they had peak population numbers spanning two or more seasons or were changing depth habitats within the mixed layer probably because of variations in temperatures and nutrients supplies. *Archaeoglobigerina cretacea* and *Globotruncana bulloides*, show a low isotopic variability that suggests they lived in the thick winter mixed layer. *Planoheterohelix globulosa* and planispiral taxa exhibit isotopic values indicating a depth habitat below the seasonal thermocline. The highest $\delta^{18}O$ values and lowest $\delta^{13}C$ values of *P. papula*, *G. neotricarinata*, *G. hilli*, *Globotruncana arca*, *Globotruncana ventricosa*, and *Marginotruncana pseudomarginata* suggest a depth habitat within or below the thermocline. The bulk carbonate cross-plots are closer to those of surface mixed layer species than thermocline species.

### 6.5. Additional Remarks

Especially evident in the present planktonic foraminiferal data set is the depth distribution of *M. coronata*, which shows an isotopic signature indicative of a relatively deep and cold habitat in the Turonian (Figure 10b). Then, in the Coniacian (Figure 10c), isotopic values indicate *M. coronata* increasingly lived in water with a summer surface water signature suggesting it migrated toward sharing the ecological niches in the mixed layer occupied by *M. pseudolinneiana*. In the Santonian (Figure 10d), immediately before the time of its extinction, its isotopic values overlap with the surface-dwelling *G. linneiana*.

The low isotopic values with large scatter in $\delta^{13}C$ of *Lenticulina* in all time intervals are consistent with its inferred epifaunal to infaunal habitat and a strong vital effect, possibly related to a fast metabolism, reproduction and calcification (Wendler et al., 2013). Large epifaunal benthic foraminifera, gavelinellids, and *Notoplanulina* sp. show similar $\delta^{13}C$ and $\delta^{18}O$ values, and the values of the gavelinellids fall in the range of the *Notoplanulina* sp. that exhibit a slightly broader variability in the $\delta^{13}C$ values.

## 7. Paleotemperature Estimates

Late Cenomanian-Santonian foraminifera from Site U1513 yield oxygen isotope ratios that suggest warmest temperatures during the latest Cenomanian-early Turonian, followed by a plateau of warm temperatures in the Turonian-early Coniacian before a progressive decline throughout the Coniacian, reaching coolest temperatures in the interval studied within the Santonian (Figure 11). These data nicely mirror previous paleotemperature estimates (Figure 1c; see for instance Friedrich et al., 2012; Huber et al., 2018; O'Brien et al., 2017; and references herein).

In the uppermost Cenomanian sediments (239.06–229.47 m CCSF), $\delta^{18}O$ for planktonic foraminifera are notable for their remarkably low values of −3.8‰ that suggest paleotemperatures of 27°C in the surface waters. In the same stratigraphic interval, epifaunal benthic foraminiferal $\delta^{18}O$ values range from −1.7 to −2.3‰ (18°C–20°C).

Throughout the Turonian (229.47–172.10 m CCSF), apparent temperatures remain quite high with the lowest $\delta^{18}O$ values consistently falling between −3.0‰ and −3.5‰. The range of planktonic foraminifera $\delta^{18}O$ values in the Turonian varies from −1.8‰ to −3.7‰ (18°C–27°C). Benthic foraminifera $\delta^{18}O$ values are between −0.5‰ and −2.6‰ and seem to indicate a high variability (12°C–22°C) which is difficult to interpret. Variation could be related to changes in the pattern of the deep-water circulation in a basin influenced by local processes complicated by factors such as depth in the sediment taxa live and variations in carbonate ion concentrations especially in pore waters.

There is a long-term gradual increase in planktonic foraminifera $\delta^{18}O$ values by 0.5‰–1.0‰ through the Coniacian (172.10–104.45 m CCSF). The lowest measured value in lower Coniacian is −3.3‰ (25°C) at 153.00 m CCSF and values increase to −2.2‰ (20°C) in the youngest Coniacian samples. The upward increase of the mean foraminiferal $\delta^{18}O$ values is confirmed by the similar trend of the bulk carbonate data. Over the same interval, maximum planktonic $\delta^{18}O$ values increase from −1.7‰ to −0.7‰. Benthic foraminifera $\delta^{18}O$ values are between −0.6‰ and −1.8‰ and are largely unchanged through most of the Coniacian (172.10–119.16 m CCSF); they

increase by 0.5‰ in the upper 10 m of the Stage. The difference in trends between planktonic and benthic taxa results in a progressive decrease of the surface to seafloor $\delta^{18}O$ gradient suggesting a decreased vertical temperature gradient through time.

Oxygen isotope ratios for both planktonic and benthic foraminifera increase to higher values in the Santonian (Figure 11). Sea surface paleotemperatures estimated from the shallow dwelling planktonic foraminifera shift from 20°C near the base of the Santonian at 104 m CCSF to 23°C at 90 m CCSF before decreasing to 14°C at the top of the studied interval (66.40 m CCSF). Much of this change occurs between 85.38 and 72.79 m CCSF (Figures 11 and 12). As in the Coniacian, bulk carbonate $\delta^{18}O$ values parallel those of surface water, planktonic foraminiferal trends. The highest $\delta^{18}O$ values of planktonic taxa indicate cooler temperatures varying only slightly from 15°C to 12°C in the thermocline during the Santonian, and benthic temperatures are estimated to have fallen only slightly from 12°C to 10°C across the interval. All together these values suggest continued cooling during the Santonian that accelerated during the middle portion of the Stage and affected the upper part of the water column more strongly than the deeper surface waters and the seafloor.

Comparison of the planktonic and benthic foraminiferal $\delta^{18}O$ record and the paleotemperature estimates at Site U1513 with the data from DSDP Site 258 (Huber et al., 2018) which is located 1.1 km west-northwest from Site U1513, show a good correspondence of values between the two sites in the interval from the earliest Cenomanian to the Coniacian. In the Santonian the low recovery of sediments and low diversity of the calcareous plankton assemblages at Site 258 (Herb, 1974; Huber et al., 2018) prevent the observation of the onset of the cooling in both surface waters and seafloor as documented at Site U1513.

## 8. Paleoceanography and Onset of the Long-Term Cooling in the Santonian

### 8.1. Planktonic Foraminiferal Patterns

The patterns of the planktonic foraminiferal assemblages in terms of diversity, depth habitats and paleotemperatures described above and illustrated in Figures 9–11 reveal some differences throughout the studied stratigraphic interval that are used to interpret variations in the vertical structure of the water column. The Cenomanian-Turonian boundary interval is characterized by high sea surface paleotemperatures of about 27°C (Figure 11), by the dominance of surface-dwelling taxa that alternate with taxa dwelling at intermediate water depths, and by an apparent absence of obligate thermocline dwellers (Figure 11). Moreover, typical Tethyan species are absent at Site U1513, including the zonal marker and intermediate dweller *H. helvetica* that is commonly recorded from low latitudes to as far south as 50°S at the Kerguelen Plateau (Petrizzo et al., 2020). These observations together with the paleotemperature values inferred from $\delta^{18}O$ foraminiferal data, might indicate a reduced vertical temperature gradient between mixed layer and thermocline waters. The occurrence of common microhedbergellids (Figure 4), interpreted as opportunistic species because of their small size and high reproductive potential, further suggests a paleoceanographic regime affected by episodes of enhanced eutrophy, in agreement with data from across the Cenomanian-Turonian boundary interval at Site U1516 which is located only few kilometers distant from Site U1513 (Figure 1b; Petrizzo et al., 2021).

Surface dwelling taxa continue to dominate in the lower Turonian (Figure 11) until they are replaced in abundance by the intermediate and thermocline depth dwellers *Marginotruncana* and planispiral taxa that together with the thermocline dwellers *Falsotruncana* and *Praeglobotruncana* comprise the mid-to late Turonian assemblages (Figure 4). The fluctuation in abundance of the surface, intermediate, and thermocline dwellers observed in the Turonian and Coniacian point to a relatively stable paleoceanographic setting with a thermal gradient in the surface waters. In the Coniacian-Santonian interval, fluctuations in abundance of the trophic groups (Figure 11) are associated with the progressive decrease of paleotemperatures in the surface water as recorded by the bulk carbonate and foraminiferal $\delta^{18}O$ values.

The distribution of the trophic groups at Site U1513 during the Turonian-Santonian is comparable with the foraminiferal record reported from the Northeast Georgia Rise and the Kerguelen Plateau (Petrizzo et al., 2020), located in the southern Indian Ocean at 58°S and 50°S of paleolatitude, respectively (Figure 1a). The composition of the assemblages also reflects the presence of a well-defined thermocline or a thick mixed layer suitable to accommodate a large number of ecological niches. In addition, the presence of Tethyan species at Site U1513, albeit only in low abundance, is consistent with the Mentelle Basin (about 60°S of paleolatitudes) being just south of

the Tethyan Bioprovince. This Bioprovince reached its maximum poleward expansion during the Turonian-early Santonian hot greenhouse climate (Petrizzo et al., 2020).

The Tethyan affinity of the Turonian-Santonian planktonic foraminifera at Site U1513 is also in agreement with the presence of a subtropical gyre inferred to pass along the southern edge of India and eastward to the northwestern edge of Australia, and of a subantarctic gyre inferred to flow northward along Antarctica and then eastward into the southern Indian Ocean (Figure 1a; Huber, 1992; Pucéat et al., 2005). North-south migration of the boundary between these two gyres flowing near Site U1513 may explain the fluctuations in abundance and composition of the three trophic groups responding to the variation in the relative local importance of either the warmer, northern or colder, southern gyre (Figure 11).

The topmost sedimentary sequence in the Santonian contains planktonic foraminiferal assemblages characterized by the loss of most Tethyan thermocline species. This change in composition of the assemblages is similar to the record previously observed at the Northeast Georgia Rise and Kerguelen Plateau (Figure 1a). At these localities the changes in the foraminiferal population dynamics have been interpreted to coincide with the development of the Transitional Bioprovince at mid-high latitudes and to the onset of the surface water cooling in the latest Santonian (Petrizzo et al., 2020). The onset of cooling in the Santonian was also documented at mid-latitudes in the Exmouth Plateau (Indian Ocean, NW Australia; 47°S of paleolatitudes, Figure 1a) by observed changes in species composition of the planktonic foraminiferal assemblages and foraminiferal stable isotope values (Falzoni et al., 2016; Petrizzo, 2002; Petrizzo et al., 2020).

In terms of composition of the planktonic foraminiferal assemblages, the interval of relatively rapid cooling (Figure 12) includes (a) the extinctions of *P. papula* at 77.60 m CCSF and all species of the genus *Marginotruncana* (79.75 m CCSF), (b) the appearance of *A. cretacea* (75.29 m CCSF), and (c) an increase in abundance of *G. bulloides*. The extinction of *Marginotruncana* in the Santonian might be explained by the stress of cooling combined with likely competition exerted by species of the diversifying *Globotruncana* lineage which occupied similar depth habitats as species of *Marginotruncana*, a possibility previously postulated by Falzoni et al. (2018).

The composition of the planktonic foraminiferal assemblages and the isotopic record at Site U1513 clearly document the first representatives of species within the genus *Globotruncana* (*G. neotricarinata*, *G. ventricosa*, and *G. arca*) in the Coniacian, which represent taxa that diverged from their keeled shallow-dwelling marginotruncanid ancestors and occupied a deeper/colder habitat (Figures 10–12). Subsequently, *Globotruncana*'s species migrated upward in the water column as their ancestors disappeared and surface-ocean temperatures decreased. An exception is *G. linneiana* that inhabited the same shallow ecological niches of its ancestor *M. pseudolinneiana* (Figures 10–12). Therefore, the onset of significant cooling during the Santonian fostered the expansion of the deep/cold ecological niches that favored the proliferation in number of species of the globotruncanids (including *A. cretacea*). These species started a major phase of diversification in this time interval (e.g., Caron & Homewood, 1983; Hart, 1999; Petrizzo, 2000; Premoli Silva & Sliter, 1999), and negatively affected all shallow-dwelling taxa that had evolved during hotter greenhouse times (Turonian-Coniacian) such as species of *Marginotruncana*. In this paleoceanographic context, the extinction of the biserial and deeper *P. papula* could be ascribed to competition with the evolving globotruncanids in the cooler ecological niches.

### 8.2. Benthic Foraminiferal Patterns in the Santonian

The paleoceanographic signal of foraminiferal $\delta^{18}O$ and $\delta^{13}C$ values in the interval recording the cooling is also reflected by changes in the composition of the benthic foraminiferal assemblages (Figure 12). In general, throughout the Santonian, benthic foraminiferal specimens decrease in absolute abundance and in diversity with values for species richness decreasing from 25 species to 10 species at the top of the stratigraphic sequence (Figures 3 and 12). At the Coniacian-Santonian transition, epifaunal and oxic taxa dominate the assemblages, whereas throughout the Santonian to 92.30 m CCSF, a significant decline in oxic benthic foraminifera is observed balanced by the marked relative increase of infaunal dysoxic taxa and a slight increase of suboxic taxa. This shift is followed by the occurrence of a more stable foraminiferal assemblage dominated by epifaunal, oxic taxa until 76.50 m CCSF (Figure 12). The overlying stratigraphic interval registers an increase in agglutinated and opportunist benthic taxa that are tolerant of oxygen undersaturated environments (e.g., marginulinids, gyroidinids, and polymorphinids), together with a progressive decline of epifaunal, oxic benthic foraminifera (Figure 12).

A combination of environmental factors might have influenced the benthic foraminiferal communities including temperature, paleocurrents, and associated changes in their behavior and nature, as well as changes in paleodepth and ocean chemistry. The proximity of Site U1513 to the west Australian continental margin and the possible terrigenous input is a factor that could significantly influence the distribution of the benthic foraminifera. However, the long-term record of benthic foraminifera across the Santonian interval does not strictly indicate episodes of increased continental weathering that could trigger low oxygen conditions for short periods.

A possible explanation for the stepwise decline of the benthic foraminiferal abundance and diversity toward the top of the Santonian (Figures 3 and 12), and the gradual shifts in the assemblage composition from abundant oxic taxa to more dysoxic and suboxic taxa in the interval across the onset of cooling (Figure 12), could be changes in water circulation. The configuration of a tropical to subtropical gyre system that facilitated the Tethyan influence during the Turonian-Santonian interval (Huber, 1992; Petrizzo et al., 2020; Pucéat et al., 2005) and the convergence of two oceanic gyres in the surface water (Figure 1a) might have had a decisive influence on the bottom water and, thus, on the distribution of epifaunal oxic benthic taxa at Site U1513. A possible gradual change from the influence of Tethyan paleocurrents to a more pronounced austral influence, would have resulted in cooler waters at the sea floor, a possibility consistent with a shift from older to younger water masses carrying less oxygen (Southern Component water: e.g., Donnadieu et al., 2016; Ladant et al., 2020; Moiroud et al., 2016; Pucéat et al., 2005; Robinson et al., 2010).

### 8.3. Remarks on the Onset of Cooling

The oxygen isotope data from Site U1513 provide a detailed record of the timing and pattern of the cooling phase in the Southern Hemisphere at about 60°S indicating that cooling began by the start of the Coniacian (Figure 11) in agreement with many paleotemperature compilations (e.g., Ando et al., 2013; Falzoni et al., 2016; Friedrich et al., 2012; Huber et al., 2002, 2018; Li & Keller, 1999; Linnert et al., 2014; O'Brien et al., 2017; Scotese et al., 2021; Figure 1c). Change was gradual over most of this interval at Site U1513, but a relatively brief interval of pronounced cooling marking a potential tipping point in the climatic transition from the Late Cretaceous hot to coolhouse occurred in the Santonian. This cooling step coincides with a significant increase in the Cretaceous latitudinal paleotemperature gradient.

The δ18O values of benthic and planktonic foraminifera show convergence near the top of the Santonian. Specifically, at Site U1513 in the interval from 85.38 to 72.79 m CCSF (Figures 11 and 12), the onset of significant cooling in the water column is nicely registered by the isotopic record of benthic and planktonic foraminifera, which indicates a decrease in temperature of about 6°C and 3°C in surface and sea floor waters, respectively. Specifically, data indicate a mean paleotemperature decrease by about 2°C–4°C in the entire water column that is more pronounced in the shallower part of the surface waters (Figures 11 and 12).

A small vertical δ18O and δ13C gradient is observable in this interval as the extremes of benthic and planktonic foraminifera values and the wide range of values in both isotope systems are reduced compared to the interval below (Figures 9 and 11). Moreover, the overlap of values of deeper planktonic (*P. papula*, *G. neotricarinata*, and planispiral taxa) and benthic foraminifera indicates a small separation between the lower sea surface and the seafloor waters (Figures 9, 11, and 12). In the same stratigraphic interval, the summer mixed layer dwellers *G. linneiana* and *Muricohedbergella* show an increase of 1.0‰ of the δ18O values and the thermocline *P. papula* and the benthic foraminifera shift to higher values by 0.5‰. This observation points to increasing mixing in the water column with loss of the stratified habitats of many planktonic foraminiferal taxa and reduction of the bioproduction in benthic foraminifera which declined in abundance.

The record of a significant decrease of the sea surface temperatures by 2°C in the late Santonian was also derived from TEX86 data obtained from sediments of the Demerara Rise in the western equatorial Atlantic Ocean (Forster et al., 2007) at 2°N–3°N of paleolatitude (Sagumana & Ogg, 2006). Additionally, a decrease in paleotemperature of about 2°C–3°C was observed in the bulk carbonate oxygen isotopes record of the late Santonian sediments from the English Chalk (Southern England) in the pioneering work by Jenkyns et al. (1994). A cooling trend was also shown for the late Santonian to early Campanian Mooreville Chalk sequence in the northeastern Gulf of Mexico (Liu, 2009). Conversely, the climatic transition from the hot to the coolhouse is placed within the first 3–4 Myr of the Campanian by Ando et al. (2013) based on the isotope record of benthic foraminifera from Shatsky Rise (IODP Site U1348, NW Pacific) located near the equator in the Late Cretaceous (Sager et al., 2005).

A similar observation that infers the onset of cooling in the early Campanian is reported from Falkland Plateau (DSDP Site 511: paleolatitude about 61°S–56°S; Figure 1a) based on the foraminiferal isotopic record (Huber et al., 2018). Therefore, the beginning of the significant cooling seems to be diachronous among localities, even at similar paleolatitudes. Potential reasons for this are true diachroneity or imprecision in dating related to the different age models used in each study.

The changes in composition of the foraminiferal assemblages at Site U1513 might indicate that the onset of the cooling was more pronounced at this site than in lower latitudes. For instance, the extinction of the genus *Marginotruncana* at Site U1513 and at the Exmouth Plateau (Petrizzo, 2000) is recorded in the Santonian, thus, at a time earlier compared to the tropical Tethyan record that document the faunal turnover of the keeled taxa in the early Campanian (e.g., Coccioni & Premoli Silva, 2015; Robaszynski & Caron, 1995). This observation is not surprising considering the high latitude amplification of responses to greenhouse forcing.

## 9. Conclusions

Site U1513 in the Mentelle Basin recovered a latest Cenomanian to Santonian sedimentary sequence deposited at about 60°S in the Late Cretaceous (Hay et al., 1999; Müller et al., 2016; Scotese, 2016; van Hinsbergen et al., 2015). Biostratigraphic results based on planktonic foraminifera and calcareous nannofossils reveal a Tethyan affinity for some of the assemblages and confirms the reliability of the mid-to high latitude biozonation for planktonic foraminifera (Petrizzo et al., 2020) except in the latest Cenomanian-early Turonian when Tethyan marker species were absent at Site U1513.

The carbon isotope record at Site U1513 shows a positive excursion correlated with the plateau of high carbon isotopic values documented across the Cenomanian-Turonian boundary interval in stratigraphic sections located at low (e.g., English Chalk: Jarvis et al., 2006) and high latitudes (Site U1516: Petrizzo et al., 2021). However, the carbon isotope curve from the late Turonian to Santonian at Site U1513 is difficult to interpret and to correlate across latitudes because of its low resolution due to low sediment recovery in the Coniacian interval, and the very different paleoceanographic setting of Mentelle Basin compared to the European chalk sea and other low latitude sedimentary basins.

Carbon and oxygen isotope values measured on planktonic foraminiferal taxa provide good constraints on the paleoecological preferences and depth habitats of several species. Ecological information for some species is reported for the first time in this study. The isotopic data allow interpretation of the evolution of surface water stratification through the Late Cretaceous and show fluctuations in relative thickness of the mixed layer and thermocline. Particularly interesting is documentation that *M. coronata*'s preferred habitat migrated from deeper waters in the Turonian to shallower water in the Santonian.

Paleotemperature estimates based on the δ¹⁸O ratios of foraminiferal tests nicely document warmest temperature of the surface (27°C) and bottom water (20°C) in the latest Cenomanian-early Turonian, that progressively decrease thought time and reach minimum values of 14°C and 11°C at the surface and sea floor, respectively, in the Santonian.

Finally, the foraminiferal and stable isotope data presented in this paper reveal that the climatic transition from the Cretaceous hot to the coolhouse was not smoothly gradual. Cooling began by the beginning of the Coniacian and was gradual during the Stage but exhibits an accelerated step within the Santonian. The Santonian cooling event affected both surface and bottom water masses according to changes in the composition and abundance of the foraminiferal assemblages, although the cooling was more dramatic in the surface waters than at the sea floor.

Planktonic foraminifera underwent extinctions of both deep (*P. papula*) and surface (*Marginotruncana*) dwellers during the Santonian indicating a loss of ecological niches resulting from reduction of the vertical thermal gradient and of possible increased mixing within the upper water column. Benthic foraminifera document a transition from oxic to dysoxic conditions at the seafloor, and an increase in opportunistic taxa and decrease in diversity reflecting a decline in oxygenation and organic flux at the seafloor. The convergence of the subtropical and subantarctic gyres nearby Site U1513 could explain the paleotemperatures and the foraminiferal community changes registered in the surface and bottom water. At a wider paleoceanographic scale, the results of this study corroborate the hypothesis that the onset in the Santonian of the Late Cretaceous long-term cooling was caused

by changes in oceanic circulation and enhanced meridional exchanges presumably coupled with decreased $CO_2$ in the atmosphere and an increase of the temperature gradient between low and high latitudes.

## Data Availability Statement

The list the planktonic and benthic foraminiferal species, the distribution chart and absolute abundances of planktonic and benthic foraminifera, the distribution chart of calcareous nannofossils, and the bulk carbonate and foraminifera carbon and oxygen stable isotopes data are available in the Supporting Information S1 and in the PANGAEA Data Publisher for Earth & Environmental Science at https://doi.pangaea.de/10.1594/PANGAEA.939392.

## References

Abramovich, S., Keller, G., Stüben, D., & Berner, Z. (2003). Characterization of late Campanian and Maastrichtian planktonic foraminiferal depth habitats and vital activities based on stable isotopes. *Palaeogeography, Palaeoclimatology, Palaeoecology*, *202*, 1–29. https://doi.org/10.1016/s0031-0182(03)00572-8

Alegret, L., Molina, E., & Thomas, E. (2003). Benthic foraminiferal turnover across the Cretaceous/Paleogene boundary at Agost (southeastern Spain): Paleoenvironmental inferences. *Marine Micropaleontology*, *48*(3-4), 251–279. https://doi.org/10.1016/s0377-8398(03)00022-7

Alegret, L., & Thomas, E. (2007). Deep-sea environments across the Cretaceous/Paleogene boundary in the eastern South Atlantic Ocean (ODP leg 208, Walvis Ridge). *Marine Micropaleontology*, *64*(1-2), 1–17.

Ando, A., Huber, B. T., & MacLeod, K. G. (2010). Depth-habitat reorganization of planktonic foraminifera across the Albian/Cenomanian boundary. *Paleobiology*, *36*, 357–373. https://doi.org/10.1666/09027.1

Ando, A., Woodard, S. C., Evans, H. F., Littler, K., Herrmann, S., MacLeod, K. G., et al. (2013). An emerging palaeoceanographic 'missing link': Multidisciplinary study of rarely recovered parts of deep-sea Santonian-Campanian transition from Shatsky Rise. *Journal of the Geological Society*, *170*, 381–384. https://doi.org/10.1144/jgs2012-137

Arthur, M. A., & Schlanger, S. O. (1979). Cretaceous "oceanic anoxic events" as causal factors in development of reef reservoired giant oil fields. *AAPG Bulletin*, *63*, 870–885. https://doi.org/10.1306/2f91848c-16ce-11d7-8645000102c1865d

Bandy, O. L. (1954). Aragonite tests among the foraminifera. *Journal of Sedimentary Petrology*, *24*, 60–61. https://doi.org/10.1306/d4269652-2b26-11d7-8648000102c1865d

Barclay, R. S., McElwain, J. C., & Sageman, B. B. (2010). Carbon sequestration activated by a volcanic $CO_2$ pulse during Ocean Anoxic Event 2. *Nature Geoscience*, *3*, 205–208. https://doi.org/10.1038/ngeo757

Barrera, E., & Savin, S. M. (1999). Evolution of late Campanian–Maastrichtian marine climates and oceans. In E. Barrera & C. C. Johnson (Eds.), *Evolution of the Cretaceous ocean-climate system* (Vol. 332, pp. 245–282). Geological Society of America Special Paper. https://doi.org/10.1130/0-8137-2332-9.245

Barrera, E., Savin, S. M., Thomas, E., & Jones, C. E. (1997). Evidence for thermohaline-circulation reversals controlled by sea-level change in the latest Cretaceous. *Geology*, *25*, 715–718. https://doi.org/10.1130/0091-7613(1997)025<0715:eftcrc>2.3.co;2

Barron, E. J. (1983). A warm, equable Cretaceous: The nature of the problem. *Earth-Science Reviews*, *19*, 305–338. https://doi.org/10.1016/0012-8252(83)90001-6

Barron, E. J., Fawcett, P. J., Peterson, W. H., Pollard, D., & Thompson, S. L. (1995). A 'simulation' of mid-Cretaceous climate. *Paleoceanography*, *10*, 953–962. https://doi.org/10.1029/95pa01624

Bemis, B. E., Spero, H. J., Bijma, J., & Lea, D. W. (1998). Reevaluation of the oxygen isotopic composition of planktonic foraminifera: Experimental results and revised paleotemperature equations. *Paleoceanography*, *13*, 150–160. https://doi.org/10.1029/98pa00070

Bergen, J. A., & Sikora, P. J. (1999). Microfossil diachronism in southern Norwegian north sea chalks: Valhall and Hod fields. In R. W. Jones & M. D. Simmons (Eds.), *Biostratigraphy in production and development geology* (Vol. 152, pp. 85–111). Geological Society, London, Special Publications. https://doi.org/10.1144/gsl.sp.1999.152.01.06

Berner, R. A. (2004). *The Phanerozoic carbon cycle* (p. 150). Oxford University Press.

Berner, R. A., Lasaga, A. C., & Garrels, R. M. (1983). The carbonate–silicate geochemical cycle and its effect on atmospheric carbon dioxide over the past 100 million years. *American Journal of Science*, *283*, 641–683. https://doi.org/10.2475/ajs.283.7.641

Bice, K. L., Birgel, D., Meyers, P. A., Dahl, K. A., Hinrichs, K. U., & Norris, R. D. (2006). A multiple proxy and model study of Cretaceous upper ocean temperatures and atmospheric $CO_2$ concentrations. *Paleoceanography*, *21*, PA2002. https://doi.org/10.1029/2005pa001203

Bice, K. L., & Norris, R. D. (2002). Possible atmospheric $CO_2$ extremes of the middle Cretaceous (late Albian–Turonian). *Paleoceanography*, *17*, 1070. https://doi.org/10.1029/2002PA000778

Birch, H., Coxall, H. K., Pearson, P. N., Kroon, D., & O'Regan, M. (2013). Planktonic foraminifera stable isotopes and water column structure: Disentangling ecological signals. *Marine Micropaleontology*, *101*, 127–145. https://doi.org/10.1016/j.marmicro.2013.02.002

Blair, S. A., & Watkins, D. K. (2009). High-resolution calcareous nannofossil biostratigraphy for the Coniacian/Santonian stage boundary, Western Interior Basin. *Cretaceous Research*, *30*, 367–384. https://doi.org/10.1016/j.cretres.2008.07.016

Bolli, H. M., Beckmann, J. P., & Saunders, J. B.(1994). *Benthic foraminiferal biostratigraphy of the southern Caribbean region*. Cambridge University Press.

Bornemann, A., & Norris, R. D. (2007). Size-related stable isotope changes in Late Cretaceous planktic foraminifera: Implications for paleoecology and photosymbiosis. *Marine Micropaleontology*, *65*(1–2), 32–42. https://doi.org/10.1016/j.marmicro.2007.05.005

Bornemann, A., Norris, R. D., Friedrich, O., Beckmann, B., Schouten, S., Sinninghe Damsté, J. S., et al. (2008). Isotopic evidence for glaciation during the Cretaceous supergreenhouse. *Science*, *319*(5860), 189–192. https://doi.org/10.1126/science.1148777

Boyce, C. K., Brodribb, T. J., Feild, T. S., & Zwieniecki, M. A. (2009). Angiosperm leaf vein evolution was physiologically and environmentally transformative. *Proceedings of the Royal Society B Biological Sciences*, *276*, 1771–1776. https://doi.org/10.1098/rspb.2008.1919

Burnett, J. A. (1998). Upper Cretaceous. In P. R. Bown (Ed.), *Calcareous nannofossil biostratigraphy* (pp. 132–199). British Micropalaeontological Society Publication Series. https://doi.org/10.1007/978-94-011-4902-0_6

Caron, M. (1981). Un nouveau genre de foraminifère planctonique du Crétacé: *Falsotruncana* nov. gen. *Eclogae Geologicae Helvetiae*, *74*, 65–73. https://doi.org/10.5169/seals-165091

Caron, M., Dall'Agnolo, S., Accarie, H., Barrera, E., Kauffman, E. G., Amédro, F., & Robaszynski, F. (2006). High-resolution stratigraphy of the Cenomanian-Turonian boundary interval at Pueblo (USA) and Wadi Bahloul (Tunisia): Stable isotope and bio-events correlation. *Geobios*, *39*, 171–200. https://doi.org/10.1016/j.geobios.2004.11.004

Caron, M., & Homewood, P. (1983). Evolution of early planktic foraminifers. *Marine Micropaleontology*, *7*, 453–462. https://doi.org/10.1016/0377-8398(83)90010-5

Chenot, E., Deconinck, J. F., Pucéat, E., Pellenard, P., Guiraud, M., Jaubert, M., et al. (2018). Continental weathering as a driver of Late Cretaceous cooling: New insights from clay mineralogy of Campanian sediments from the southern Tethyan margin to the Boreal realm. *Global and Planetary Change*, *162*, 292–312. https://doi.org/10.1016/j.gloplacha.2018.01.016

Clarke, L. J., & Jenkyns, H. C. (1999). New oxygen isotope evidence for long-term Cretaceous climatic change in the southern hemisphere. *Geology*, *27*, 699–702. https://doi.org/10.1130/0091-7613(1999)027<0699:noiefl>2.3.co;2

Coccioni, R., & Premoli Silva, I. (2015). Revised Upper Albian–Maastrichtian planktonic foraminiferal biostratigraphy and magnetostratigraphy of the classical Tethyan Gubbio section (Italy). *Newsletters on Stratigraphy*, *48*, 47–90. https://doi.org/10.1127/nos/2015/0055

Cogné, J. P., & Humler, E. (2006). Trends and rhythms in global seafloor generation rate. *Geochemistry, Geophysics, Geosystems*, *7*(3), Q03011. https://doi.org/10.1029/2005GC001148

Corbett, M. J., & Watkins, D. K. (2014). Transitional forms in the *Eprolithus-Lithastrinus* lineage: A taxonomic revision of Turonian through Santonian species. *Micropaleontology*, *60*, 175–193.

Corbett, M. J., Watkins, D. K., & Pospichal, J. J. (2014). A quantitative analysis of calcareous nannofossil bioevents of the Late Cretaceous (late Cenomanian-Coniacian) Western Interior Seaway and their reliability in established zonation schemes. *Marine Micropaleontology*, *109*, 30–45. https://doi.org/10.1016/j.marmicro.2014.04.002

Craggs, H. J., Valdes, P. J., & Widdowson, M. (2012). Climate model predictions for the latest Cretaceous: An evaluation using climatically sensitive sediments as proxy indicators. *Palaeogeography, Palaeoclimatology, Palaeoecology*, *315*, 12–23. https://doi.org/10.1016/j.palaeo.2011.11.004

Cramer, B. D., & Jarvis, I. (2020). Carbon isotope stratigraphy. In F. M., Gradstein, J. G., Ogg, M. D., Schmitz, & G. M., Ogg (Eds.), *Geologic time scale 2020* (pp. 309–343). Elsevier. https://doi.org/10.1016/b978-0-12-824360-2.00011-5

Cramer, B. S., Miller, K. G., Barrett, P. J., & Wright, J. D. (2011). Late Cretaceous–Neogene trends in deep ocean temperature and continental ice volume: Reconciling records of benthic foraminiferal geochemistry ($\delta^{18}$O and Mg/Ca) with sea level history. *Journal of Geophysical Research: Oceans*, *116*, C12023. https://doi.org/10.1029/2011jc007255

Cramer, B. S., Toggweiler, J. R., Wright, J. D., Katz, M. E., & Miller, K. G. (2009). Ocean overturning since the Late Cretaceous: Inferences from a new benthic foraminiferal isotope compilation. *Paleoceanography*, *24*, PA4216. https://doi.org/10.1029/2008PA001683

Crowley, T. J., & Berner, R. A. (2001). $CO_2$ and climate change. *Science*, *292*, 870–872. https://doi.org/10.1126/science.1061664

Desmares, D., Grosheny, D., Beaudoin, B., Gardin, S., & Gauthier-Lafaye, F. (2007). High resolution stratigraphic record constrained by volcanic ashes layers at the Cenomanian-Turonian boundary in the Western Interior Basin, USA. *Cretaceous Research*, *28*, 561–582. https://doi.org/10.1016/j.cretres.2006.08.009

D'Hondt, S., & Arthur, M. A. (1995). Interspecies variation in stable isotopic signals of Maastrichtian planktonic foraminifera. *Paleoceanography*, *10*(1), 123–135. https://doi.org/10.1029/94pa02671

Dickson, A. J., Saker-Clarket, M., Jenkyns, H. C., Bottini, C., Erba, E., Russo, F., et al. (2017). A Southern Hemisphere record of global trace-metal drawdown and orbital modulation of organic-matter burial across the Cenomanian-Turonian boundary (Ocean Drilling Program Site 1138, Kerguelen Plateau). *Sedimentology*, *64*, 186–203. https://doi.org/10.1111/sed.12303

Donnadieu, Y., Pierrehumbert, R., Jacob, R., & Fluteau, F. (2006). Modelling the primary control of paleogeography on Cretaceous climate. *Earth and Planetary Science Letters*, *248*, 426–437. https://doi.org/10.1016/j.epsl.2006.06.007

Donnadieu, Y., Pucéat, E., Moiroud, M., Guillocheau, F., & Deconinck, J.-F. (2016). A better-ventilated ocean triggered by Late Cretaceous changes in continental configuration. *Nature Communications*, *7*, 1–12. https://doi.org/10.1038/ncomms10316

Douglas, R. G., & Savin, S. M. (1975). Oxygen and carbon isotope analyses of Tertiary and Cretaceous microfossils from Shatsky Rise and other sites in the north Pacific Ocean. *Initial Reports of the Deep Sea Drilling Project*, *32*(50), 520. https://doi.org/10.2973/dsdp.proc.32.115.1975

Elderbak, K., & Leckie, R. M. (2016). Paleocirculation and foraminiferal assemblages of the Cenomanian–Turonian Bridge Creek limestone bedding couplets: Productivity vs. dilution during OAE2. *Cretaceous Research*, *60*, 52–77. https://doi.org/10.1016/j.cretres.2015.11.009

Eldrett, J. S., Ma, C., Bergman, S. C., Lutz, B., Gregory, F. J., Dodsworth, P., et al. (2015). An astronomically calibrated stratigraphy of the Cenomanian, Turonian and earliest Coniacian from the Cretaceous Western Interior Seaway, USA: Implications for global chronostratigraphy. *Cretaceous Research*, *56*, 316–344. https://doi.org/10.1016/j.cretres.2015.04.010

Eldrett, J. S., Vieira, M., Gallagher, L., Hampton, M., Blaauw, M., & Swart, P. K. (2021). Late Cretaceous to Palaeogene carbon isotope, calcareous nannofossil and foraminifera stratigraphy of the Chalk Group, central North Sea. *Marine and Petroleum Geology*, *124*, 104789. https://doi.org/10.1016/j.marpetgeo.2020.104789

Falzoni, F., & Petrizzo, M. R. (2020). Patterns of planktonic foraminiferal extinctions and eclipses during Oceanic Anoxic Event 2 at Eastbourne (SE England) and other mid-low latitude locations. *Cretaceous Research*, *116*, 104593. https://doi.org/10.1016/j.cretres.2020.104593

Falzoni, F., Petrizzo, M. R., Caron, M., Leckie, R. M., & Elderbak, K. (2018). Age and synchronicity of planktonic foraminiferal bioevents across the Cenomanian–Turonian boundary interval (Late Cretaceous). *Newsletters on Stratigraphy*, *51*, 343–380. https://doi.org/10.1127/nos/2018/0416

Falzoni, F., Petrizzo, M. R., Clarke, L. C., MacLeod, K. G., & Jenkyns, H. J. (2016). Long-term Late Cretaceous carbon- and oxygen-isotope trends and planktonic foraminiferal turnover: A new record from the southern mid-latitudes. *Geological Society of America Bulletin*, *128*, 1725–1735. https://doi.org/10.1130/B31399.1

Fletcher, B. J., Brentnall, S. J., & Anderson, C. W. (2008). Atmospheric carbon dioxide linked with Mesozoic and early Cenozoic climate change. *Nature Geoscience*, *1*, 43–48. https://doi.org/10.1038/ngeo.2007.29

Fluteau, F., Ramstein, G., Besse, J., Guiraud, R., & Masse, J. P. (2007). Impacts of palaeogeography and sea level changes on mid-Cretaceous climate. *Palaeogeography, Palaeoclimatology, Palaeoecology*, *247*, 357–381. https://doi.org/10.1016/j.palaeo.2006.11.016

Forster, A., Schouten, S., Baas, M., & Sinninghe Damsté, J. S. (2007). Mid-Cretaceous (Albian–Santonian) sea surface temperature record of the tropical Atlantic Ocean. *Geology*, *35*, 919–922. https://doi.org/10.1130/g23874a.1

Foster, G. L., Royer, D. L., & Lunt, D. J. (2017). Future climate forcing potentially without precedent in the last 420 million years. *Nature Communications*, *8*, 14845. https://doi.org/10.1038/ncomms14845

Frank, T., & Arthur, M. A. (1999). Tectonic forcing of Maastrichtian ocean-climate evolution. *Paleoceanography*, *14*, 103–117. https://doi.org/10.1029/1998pa900017

Friedrich, O., & Erbacher, J. (2006). Benthic foraminiferal assemblages from Demerara rise (ODP Leg 207, western tropical Atlantic): Possible evidence for a progressive opening of the equatorial Atlantic gateway. *Cretaceous Research*, *27*, 377–397. https://doi.org/10.1016/j.cretres.2005.07.006

Friedrich, O., Herrle, J. O., Cooper, M. J., Erbacher, J., Wilson, P. A., & Hemleben, C. (2009). The early Maastrichtian carbon cycle perturbation and cooling event: Implications from the South Atlantic Ocean. *Paleoceanography*, *24*, PA221. https://doi.org/10.1029/2008pa001654

Friedrich, O., Norris, R. D., & Erbacher, J. (2012). Evolution of middle to Late Cretaceous oceans – A 55 my record of Earth's temperature and carbon cycle. *Geology*, *40*(2), 107–110. https://doi.org/10.1130/g32701.1

Friedrich, O., Schmiedl, G., & Erlenkeuser, H. (2006). Stable isotope composition of Late Cretaceous benthic foraminifera from the southern South Atlantic: Biological and environmental effects. *Marine Micropaleontology*, *58*, 135–157. https://doi.org/10.1016/j.marmicro.2005.10.005

Gaer, B. T., & Watkins, D. K. (2020). A biometric analysis of the *Eiffellithus eximius* species complex and its biostratigraphic implications. *Marine Micropaleontology*, *157*, 101876. https://doi.org/10.1016/j.marmicro.2020.101876

Gale, A. S., Jenkyns, H. C., Tsikos, H., van Breugel, Y., Sinninghe Damsté, J. S., Bottini, C., et al. (2019). High-resolution bio- and chemostratigraphy of an expanded record of Oceanic Anoxic Event 2 (late Cenomanian-early Turonian) at Clot Chevalier, near Barrême, SE France (Vocontian basin, SE France). *Newsletters on Stratigraphy*, *52*, 97–129. https://doi.org/10.1127/nos/2018/0445

Gale, A. S., Kennedy, W. J., Lees, J. A., Petrizzo, M. R., & Walaszczyk, I. (2007). An integrated study (inoceramid bivalves, ammonites, calcareous nannofossils, planktonic foraminifera, stable carbon isotopes) of the Ten Mile Creek section, Lancaster, Dallas County, north Texas, a candidate Global boundary Stratotype Section and Point for the base of the Santonian Stage. *Acta Geologica Polonica*, *57*, 113–160.

Gale, A. S., Mutterlose, J., Batenburg, S., Gradstein, F. M., Agterberg, F. P., Ogg, J. G., & Petrizzo, M. R. (2020). The Cretaceous period. In F. M. Gradstein, J. G. Ogg, M. D. Schmitz, & G. M. Ogg (Eds.), *Geologic time scale 2020* (Vol. 2, pp. 1023–1086). Elsevier B.V. chapter 27. https://doi.org/10.1016/B978-0-12-824360-2.00027-9

Gradstein, F. M., Ogg, J. G., Schmitz, M. D., & Ogg, G. M. (2012). *The geologic time scale 2012* (p. 1144). Elsevier.

Gradstein, F. M., Ogg, J. G., Schmitz, M. D., & Ogg, G. M. (2020). *Geologic time scale 2020* (p. 1357). Elsevier.

Hallam, A. (1985). A review of Mesozoic climates. *Journal of the Geological Society*, *142*(3), 433–445. https://doi.org/10.1144/gsjgs.142.3.0433

Hampton, M. J., Bailey, H. W., Gallagher, L. T., Mortimore, R. N., & Wood, C. J. (2007). The biostratigraphy of Seaford Head, Sussex, southern England; an international reference section for the basal boundaries for the Santonian and Campanian Stages in chalk facies. *Cretaceous Research*, *28*, 46–60. https://doi.org/10.1016/j.cretres.2006.05.025

Haq, B. U. (2014). Cretaceous eustasy revisited. *Global and Planetary Change*, *113*, 44–58. https://doi.org/10.1016/j.gloplacha.2013.12.007

Hart, M. B. (1980). The recognition of mid-Cretaceous sea-level changes by means of foraminifera. *Cretaceous Research*, *1*(4), 289–297. https://doi.org/10.1016/0195-6671(80)90040-3

Hart, M. B. (1999). The evolution and biodiversity of Cretaceous Foraminiferida. *Geobios*, *32*, 247–255. https://doi.org/10.1016/s0016-6995(99)80038-2

Hart, M. B., & Bailey, H. W. (1979). The distribution of planktonic Foraminiferida in the mid-Cretaceous of NW Europe. *Aspekte der Kreide Europas*, *6*, 527–542.

Hay, W. W. (2008). Evolving ideas about the Cretaceous climate and ocean circulation. *Cretaceous Research*, *29*, 725–753. https://doi.org/10.1016/j.cretres.2008.05.025

Hay, W. W., Deconto, R., Wold, C. N., Wilson, K. M., Voigt, S., Schulz, M., et al. (1999). Alternative global Cretaceous paleogeography. In E. Barrera & C. C. Johnson (Eds.), *The evolution of the Cretaceous ocean/climate system* (pp. 1–47). Geological Society of America Special Paper 332. https://doi.org/10.1130/0-8137-2332-9.1

Hay, W. W., & Floegel, S. (2012). New thoughts about the Cretaceous climate and oceans. *Earth-Science Reviews*, *115*, 262–272. https://doi.org/10.1016/j.earscirev.2012.09.008

Haynes, S. J., MacLeod, K. G., Ladant, J.-B., Vande Guchte, A., Rostami, M. A., Poulsen, C. J., & Martin, E. E. (2020). Constraining sources and relative flow rates of bottom waters in the Late Cretaceous Pacific Ocean. *Geology*, *48*, 509–513. https://doi.org/10.1130/g47197.1

Herb, R. (1974). Cretaceous planktonic foraminifera from the eastern Indian Ocean. In *Initial report of the Deep Sea Drilling Project* (Vol. 26, pp. 745–770). U.S. Government Printing Office. https://doi.org/10.2973/dsdp.proc.26.132.1974

Howe, R. W., Sikora, P. J., Gale, A. S., & Bergen, J. A. (2007). Calcareous nannofossil and planktonic foraminiferal biostratigraphy of proposed stratotypes for the Coniacian/Santonian boundary: Olazagutia, northern Spain; Seaford Head, southern England; and Ten Mile Creek, Texas, USA. *Cretaceous Research*, *28*(1), 61–92.

Huber, B. T. (1992). Paleobiogeography of Campanian-Maastrichtian foraminifera in the southern high latitudes. *Palaeogeography, Palaeoclimatology, Palaeoecology*, *92*, 325–360. https://doi.org/10.1016/0031-0182(92)90090-r

Huber, B. T., Hobbs, R. W., Bogus, K. A., Batenburg, S. J., Brumsack, H.-J., do Monte Guerra, R., et al. & the Expedition 369 Scientists. (2019a). Site U1513. In R. W. Hobbs, B. T. Huber, K. A. Bogus (Eds.), *Australia Cretaceous Climate and Tectonics*. *Proceedings of the International Ocean Discovery Program* (Vol. 369). International Ocean Discovery Program. https://doi.org/10.14379/iodp.proc.369.104.2019

Huber, B. T., Hobbs, R. W., Bogus, K. A., Batenburg, S. J., Brumsack, H.-J., do Monte Guerra, R., et al. & the Expedition 369 Scientists. (2019b). Expedition 369 methods. In R. W. Hobbs, B. T. Huber & K. A. Bogus (Eds.), *Australia Cretaceous Climate and Tectonics*. *Proceedings of the International Ocean Discovery Program* (Vol. 369). International Ocean Discovery Program. https://doi.org/10.14379/iodp.proc.369.102.2019

Huber, B. T., Hodell, D. A., & Hamilton, C. P. (1995). Middle-Late Cretaceous climate of the southern high latitudes: Stable isotopic evidence for minimal equator-to-pole thermal gradients. *Geological Society of America Bulletin*, *107*, 1164–1191. https://doi.org/10.1130/0016-7606(1995)107<1164:MLCCOT>2.3.CO;2

Huber, B. T., Leckie, R. M., Norris, R. D., Bralower, T. J., & CoBabe, E. (1999). Foraminiferal assemblage and stable isotopic change across the Cenomanian–Turonian boundary in the subtropical North Atlantic. *Journal of Foraminiferal Research*, *29*, 392–417.

Huber, B. T., MacLeod, K. G., Watkins, D. K., & Coffin, M. F. (2018). The rise and fall of the Cretaceous Hot Greenhouse climate. *Global and Planetary Change*, *167*, 1–23. https://doi.org/10.1016/j.gloplacha.2018.04.004

Huber, B. T., Norris, R. D., & MacLeod, K. G. (2002). Deep-sea paleotemperature record of extreme warmth during the Cretaceous. *Geology*, *30*, 123–126. https://doi.org/10.1130/0091-7613(2002)030<0123:dsproe>2.0.co;2

Huber, B. T., Petrizzo, M. R., Watkins, D. K., Haynes, S. J., & MacLeod, K. G. (2017). Correlation of Turonian continental margin and deep-sea sequences in the subtropical Indian Ocean sediments by integrated planktonic foraminiferal and calcareous nannofossil biostratigraphy. *Newsletters on Stratigraphy*, *50*(2), 141–185. https://doi.org/10.1127/nos/2017/0373

Huber, B. T., Petrizzo, M. R., Young, J., Falzoni, F., Gilardoni, S., Bown, P. R., & Wade, B. S. (2016). Pforams@mikrotax: A new online taxonomic database for planktonic foraminifera. *Micropaleontology*, *62*, 429–438.

Jarvis, I. A. N., Gale, A. S., Jenkyns, H. C., & Pearce, M. A. (2006). Secular variation in Late Cretaceous carbon isotopes: A new $\delta^{13}C$ carbonate reference curve for the Cenomanian–Campanian (99.6–70.6 Ma). *Geological Magazine*, *143*(5), 561–608. https://doi.org/10.1017/s0016756806002421

Jarvis, I. A. N., Lignum, J. S., Gröcke, D. R., Jenkyns, H. C., & Pearce, M. A. (2011). Black shale deposition, atmospheric $CO_2$ drawdown, and cooling during the Cenomanian–Turonian Oceanic Anoxic Event. *Paleoceanography*, *26*, PA3201. https://doi.org/10.1029/2010PA002081

Jarvis, I. A. N., Pearce, M., Püttmann, T., Voigt, S., & Walaszczyk, I. (2021). Palynology and calcareous nannofossil biostratigraphy of the Turonian–Coniacian boundary: The proposed boundary stratotype at Salzgitter-Salder, Germany and its correlation in NW Europe. *Cretaceous Research*, *123*, 104782. https://doi.org/10.1016/j.cretres.2021.104782

Jenkyns, H. C. (1980). Cretaceous anoxic events: From continents to oceans. *Journal of the Geological Society*, *137*, 171–188. https://doi.org/10.1144/gsjgs.137.2.0171

Jenkyns, H. C., Forster, A., Schouten, S., & Sinninghe Damsté, J. S. (2004). High temperatures in the Late Cretaceous Arctic Ocean. *Nature*, *432*, 888–892. https://doi.org/10.1038/nature03143

Jenkyns, H. C., Gale, A. S., & Corfield, R. M. (1994). Carbon-and oxygen-isotope stratigraphy of the English Chalk and Italian Scaglia and its palaeoclimatic significance. *Geological Magazine*, *131*(1), 1–34. https://doi.org/10.1017/s0016756800010451

Jones, E. J. W., Cande, S. C., & Spathopoulos, F. (1995). Evolution of a major oceanographic pathway: The equatorial Atlantic. In R. A. Scrutton, M. S. Stoker, G. B. Shimmield, & A. W. Tudhope (Eds.), *The tectonics, sedimentation and palaeoceanography of the North Atlantic region* (Vol. 90, pp. 199–213). Geological Society of London Special Publication. https://doi.org/10.1144/GSL.SP.1995.090.01.12

Jorissen, F. J., Fontanier, C., & Thomas, E. (2007). Paleoceanographical proxies based on deep-sea benthic foraminiferal assemblage characteristics. In C. Hillaire-Marcel, & A. De Vernal (Eds.), *Proxies in Late Cenozoic Paleoceanography. Developments in Marine Geology* (Vol. 1, pp. 263–325). Elsevier.

Keller, G., Han, Q., Adatte, T., & Burns, S. (2001). Paleoenvironment of the Cenomanian-Turonian transition at Eastbourne, England. *Cretaceous Research*, *22*, 391–422. https://doi.org/10.1006/cres.2001.0264

Kennedy, W. J., Walaszczyk, I., & Cobban, W. A. (2000). Pueblo, Colorado, USA, candidate global boundary stratotype section and point for the base of the Turonian stage of the Cretaceous, and for the base of the middle Turonian Substage, with a revision of the Inoceramidae (Bivalvia). *Acta Geologica Polonica*, *5*(3), 295–334.

Kennedy, W. J., Walaszczyk, I., & Cobban, W. P. (2005). The global boundary stratotype section and point for the base of the Turonian stage of the Cretaceous: Pueblo, Colorado, USA. *Episodes*, *28*, 93–104. https://doi.org/10.18814/epiiugs/2005/v28i2/003

Kent, D. V., & Muttoni, G. (2013). Modulation of Late Cretaceous and Cenozoic climate by variable drawdown of atmospheric $pCO_2$ from weathering of basaltic provinces on continents drifting through the equatorial humid belt. *Climate of the Past*, *9*(2), 525–546. https://doi.org/10.5194/cp-9-525-2013

Kim, S.-T., & O'Neil, J. R. (1997). Equilibrium and nonequilibrium oxygen isotope effects in synthetic carbonates. *Geochimica et Cosmochimica Acta*, *61*, 3461–3475. https://doi.org/10.1016/s0016-7037(97)00169-5

Kita, Z. A., Watkins, D. K., & Sageman, B. B. (2017). High-resolution calcareous nannofossil biostratigraphy of the Santonian/Campanian stage boundary, Western Interior Basin, USA. *Cretaceous Research*, *69*, 49–55. https://doi.org/10.1016/j.cretres.2016.08.015

Ladant, J. B., & Donnadieu, Y. (2016). Palaeogeographic regulation of glacial events during the Cretaceous supergreenhouse. *Nature Communications*, *7*, 12771. https://doi.org/10.1038/ncomms12771

Ladant, J. B., Poulsen, C. J., Fluteau, F., Tabor, C. R., MacLeod, K. G., Martin, E. E., et al. (2020). Paleogeographic controls on the evolution of Late Cretaceous ocean circulation. *Climate of the Past*, *16*(3), 973–1006. https://doi.org/10.5194/cp-16-973-2020

Lamolda, M. A., Paul, C. R. C., Peryt, D., & Pons, J. M. (2014). The global boundary stratotype and section point (GSSP) for the base of the Santonian Stage, "Cantera de Margas", Olazagutia, northern Spain. *Episodes*, *37*(1), 2–13. https://doi.org/10.18814/epiiugs/2014/v37i1/001

Leckie, R. M. (1987). Paleoecology of mid-Cretaceous planktonic foraminifera; a comparison of open ocean and epicontinental sea assemblages. *Micropaleontology*, *33*(2), 164–176. https://doi.org/10.2307/1485491

Lees, J. A. (2008). The calcareous nannofossil record across the Late Cretaceous Turonian/Coniacian boundary, including new data from Germany, Poland, the Czech Republic and England. *Cretaceous Research*, *29*, 40–64. https://doi.org/10.1016/j.cretres.2007.08.002

Li, L., & Keller, G. (1999). Variability in Late Cretaceous climate and deep waters: Evidence from stable isotopes. *Marine Geology*, *161*(2–4), 171–190. https://doi.org/10.1016/s0025-3227(99)00078-x

Linnert, C., Mutterlose, J., & Erbacher, J. (2010). Calcareous nannofossils of the Cenomanian/Turonian boundary interval from the Boreal realm (Wunstorf, northwest Germany). *Marine Micropaleontology*, *74*(1–2), 38–58. https://doi.org/10.1016/j.marmicro.2009.12.002

Linnert, C., Mutterlose, J., & Mortimore, R. (2011). Calcareous nannofossils from Eastbourne (southeastern England) and the paleoceanography of the Cenomanian–Turonian boundary interval. *PALAIOS*, *26*, 298–313. https://doi.org/10.2110/palo.2010.p10-130r

Linnert, C., Robinson, S., Lees, J., Bown, P., Pérez-Rodríguez, I., Petrizzo, M. R., et al. (2014). Evidence for global cooling in the Late Cretaceous. *Nature Communications*, *5*, 4194. https://doi.org/10.1038/ncomms5194

Linnert, C., Robinson, S. A., Lees, J. A., Pérez-Rodríguez, I., Jenkyns, H. C., Petrizzo, M. R., et al. (2018). Did Late Cretaceous cooling trigger the Campanian-Maastrichtian boundary event? *Newsletters on Stratigraphy*, *51*(2), 145–166. https://doi.org/10.1127/nos/2017/0310

Littler, K., Robinson, S. A., Bown, P. R., Nederbragt, A. J., & Pancost, R. D. (2011). High seasurface temperatures during the early Cretaceous epoch. *Nature Geoscience*, *4*, 169–172. https://doi.org/10.1038/ngeo1081

Liu, K. (2009). Oxygen and carbon isotope analysis of the Mooreville Chalk and late Santonian-early Campanian sea level and sea surface temperature changes, northeastern Gulf of Mexico, U.S.A. *Cretaceous Research*, *30*, 980–990. https://doi.org/10.1016/j.cretres.2009.02.008

Loeblich, A. R., Jr, & Tappan, H. (1984). Suprageneric classification of the Foraminiferida (Protozoa). *Micropaleontology*, *30*, 1–70. https://doi.org/10.2307/1485456

Lunt, D. J., Farnsworth, A., Loptson, C., Foster, G. L., Markwick, P., O'Brien, C. L., et al. (2016). Palaeogeographic controls on climate and proxy interpretation. *Climate of the Past*, *11*, 5683–5725. https://doi.org/10.5194/cp-12-1181-2016

Luyendyk, B. P., & Davies, T. A. (1974). Results of DSDP Leg 26 and the geologic history of the Southern Indian Ocean. In T. A. Davies, B. P. Luyendyk, K. S. Rodolfo, D. R. C. Kempe, B. C. McKelvey, R. D. Leidy, et al. (Eds.), *Initial Reports of the Deep Sea Drilling Project* (Vol. 26, pp. 909–943). U.S. Government Printing Office. https://doi.org/10.2973/dsdp.proc.26.136.1974

MacLeod, K. G. (1994). Bioturbation, inoceramid extinction, and mid-Maastrichtian ecological change. *Geology*, *22*, 139–142. https://doi.org/10.1130/0091-7613(1994)022<0139:BIEAMM>2.3.CO;2

MacLeod, K. G., & Huber, B. T. (1996). Reorganization of deep ocean circulation accompanying a Late Cretaceous extinction event. *Nature*, *380*, 422–425. https://doi.org/10.1038/380422a0

MacLeod, K. G., & Huber, B. T. (2001). The Maastrichtian record at Blake Nose (western North Atlantic) and implications for global palaeoceanographic and biotic changes. In R. Kroon, R. D. Norris, & A. Klaus (Eds.), *Western North Atlantic Palaeogene and Cretaceous palaeoceanography* (Vol. 183, pp. 111–130). Geological Society, London, Special Publications. https://doi.org/10.1144/gsl.sp.2001.183.01.06

MacLeod, K. G., Huber, B. T., & Isaza-Londoño, C. (2005). North Atlantic warming during global cooling at the end of the Cretaceous. *Geology*, *33*, 437–440. https://doi.org/10.1130/G21466.1

MacLeod, K. G., Huber, B. T., Jiménez Berrocoso, Á., & Wendler, I. (2013). A stable and hot Turonian without glacial δ18O excursions is indicated by exquisitely preserved Tanzanian foraminifera. *Geology*, *41*(10), 1083–1086. https://doi.org/10.1130/G34510.1

MacLeod, K. G., Huber, B. T., & Le Ducharme, M. (2000). Paleontological and geochemical constraints on the deep ocean during the Cretaceous greenhouse interval. In B. T. Huber, K. G. MacLeod, & S. L. Wing (Eds.), *Warm climates in Earth history* (pp. 241–274). University of Cambridge.

MacLeod, K. G., Huber, B. T., Pletsch, T., Röhl, U., & Kucera, M. (2001). Maastrichtian foraminiferal and paleoceanographic changes on Milankovitch time scales. *Paleoceanography*, *16*, 133–154. https://doi.org/10.1029/2000pa000514

MacLeod, K. G., Londoño, C. I., Martin, E. E., Berrocoso, Á. J., & Basak, C. (2011). Changes in North Atlantic circulation at the end of the Cretaceous greenhouse interval. *Nature Geoscience*, *4*, 779–782. https://doi.org/10.1038/ngeo1284

Martin, E. E., MacLeod, K. G., Jiménez Berrocoso, Á., & Bourbon, E. (2012). Water mass circulation on Demerara Rise during the Late Cretaceous based on Nd isotopes. *Earth and Planetary Science Letters*, *327–328*, 111–120. https://doi.org/10.1016/j.epsl.2012.01.037

McKenzie, N. R., Horton, B. K., Loomis, S. E., Stockli, D. F., Planavsky, N. J., & Lee, C. T. A. (2016). Continental arc volcanism as the principal driver of icehouse-greenhouse variability. *Science*, *352*(6284), 444–447. https://doi.org/10.1126/science.aad5787

Melinte, M. C., & Lamolda, M. A. (2007). Calcareous nannofossil biostratigraphy of the Coniacian/Santonian boundary interval in Romania and comparison with other European regions. *Cretaceous Research*, *28*, 119–127. https://doi.org/10.1016/j.cretres.2006.05.021

Miller, K. G., Kominz, M. A., Browning, J. V., Wright, J. D., Mountain, G. S., Katz, M. E., et al. (2005). The Phanerozoic record of global sea-level change. *Science*, *310*, 1293–1298. https://doi.org/10.1126/science.1116412

Miniati, F., Petrizzo, M. R., Falzoni, F., & Erba, E. (2020). Calcareous plankton biostratigraphy of the Santonian-Campanian boundary interval in the Bottaccione section (Umbria-Marche basin, central Italy). *Rivista Italiana di Paleontologia e Stratigrafia*, *126*(3), 783–801. https://doi.org/10.13130/2039-4942/14399

Moiroud, M., Pucéat, E., Donnadieu, Y., Bayon, G., Guiraud, M., Voigt, S., et al. (2016). Evolution of neodymium isotopic signature of seawater during the Late Cretaceous: Implications for intermediate and deep circulation. *Gondwana Research*, *36*, 503–522. https://doi.org/10.1016/j.gr.2015.08.005

Moriya, K. (2011). Development of the Cretaceous greenhouse climate and the oceanic thermal structure. *Paleontological Research*, *15*(2), 77–88. https://doi.org/10.2517/1342-8144-15.2.077

Mulitza, S., Dürkoop, A., Hale, W., Wefer, G., & Niebler, H. S. (1997). Planktonic foraminifera as recorders of past surface-water stratification. *Geology*, *25*(4), 335–338. https://doi.org/10.1130/0091-7613(1997)025<0335:pfarop>2.3.co;2

Murphy, D. P., & Thomas, D. J. (2012). Cretaceous deep-water formation in the Indian sector of the Southern Ocean. *Paleoceanography*, *27*, PA1211. https://doi.org/10.1029/2011pa002198

Murphy, D. P., & Thomas, D. J. (2013). The evolution of Late Cretaceous deep – ocean circulation in the Atlantic basins: Neodymium isotope evidence from South Atlantic drill sites for tectonic controls. *Geochemistry, Geophysics, Geosystems*, *14*, 5323–5340. https://doi.org/10.1002/2013gc004889

Murray, J. W. (2006). *Ecology and Applications of Benthic Foraminifera* (p. 426). Cambridge University Press.

Müller, R. D., Seton, M., Zahirovic, S., Williams, S. E., Matthews, K. J., Wright, N. M., et al. (2016). Ocean basin evolution and global-scale plate reorganization events since Pangea breakup. *Annual Review of Earth and Planetary Sciences*, *44*(1), 107–138

Norris, R. D., & Wilson, P. A. (1998). Low-latitude sea-surface temperatures for the mid-Cretaceous and the evolution of planktonic foraminifera. *Geology*, *26*, 823–826. https://doi.org/10.1130/0091-7613(1998)026<0823:LLSSTF>2.3.CO;2

O'Brien, C. L., Robinson, S. A., Pancost, R. D., Sinninghe Damsté, J. S., Schoulten, S., Lunt, D. J., et al. (2017). Cretaceous sea-surface temperature evolution: Constraints from TEX86 and planktonic foraminiferal oxygen isotopes. *Earth-Science Reviews*, *172*, 224–247. https://doi.org/10.1016/j.earscirev.2017.07.012

Otto-Bliesner, B. L., Brady, E. C., & Shields, C. (2002). Late Cretaceous ocean: Coupled simulations with the National Center for Atmospheric Research Climate System Model. *Journal of Geophysical Research*, *107*. ACL–11. https://doi.org/10.1029/2001jd000821

Paul, C. R. C., Lamolda, M. A., Mitchell, S. F., Vaziri, M. R., Gorostidi, A., & Marshall, J. D. (1999). The Cenomanian–Turonian boundary at Eastbourne (Sussex, UK): A proposed European reference section. *Palaeogeography, Palaeoclimatology, Palaeoecology*, *150*(1–2), 83–121. https://doi.org/10.1016/s0031-0182(99)00009-7

Pearson, P. N. (1998). Stable isotopes and the study of evolution in planktonic foraminifera. *Paleontological Society Papers*, *4*, 138–178. https://doi.org/10.1017/s1089332600000425

Pearson, P. N., Ditchfield, P. W., Singano, J., Harcourt-Brown, K. G., Nicholas, C. J., Olsson, R. K., et al. (2001). Warm tropical sea surface temperatures in the Late Cretaceous and Eocene epochs. *Nature*, *413*(6855), 481–487. https://doi.org/10.1038/35097000

Perch-Nielsen, K. (1985). Mesozoic calcareous nannofossils. In H. M. Bolli, J. B. Saunders, & K. Perch-Nielsen (Eds.), *Plankton stratigraphy* (pp. 329–426). Cambridge Universitry Press.

Petrizzo, M. R. (2000). Upper Turonian-lower Campanian planktonic foraminifera from southern mid high latitudes (Exmouth Plateau, NW Australia): Biostratigraphy and taxonomic notes. *Cretaceous Research*, *21*, 479–505. https://doi.org/10.1006/cres.2000.0218

Petrizzo, M. R. (2001). Late Cretaceous planktonic foraminifera from Kerguelen Plateau (ODP Leg 183): New data to improve the Southern Ocean biozonation. *Cretaceous Research*, *22*, 829–855. https://doi.org/10.1006/cres.2001.0290

Petrizzo, M. R. (2002). Palaeoceanographic and palaeoclimatic inferences from Late Cretaceous planktonic foraminiferal assemblages from the Exmouth Plateau (ODP Sites 762 and 763, eastern Indian Ocean). *Marine Micropaleontology*, *45*, 117–150. https://doi.org/10.1016/S0377-8398(02)00020-8

Petrizzo, M. R. (2003). Late Cretaceous planktonic foraminiferal bioevents in the Tethys and in the Southern Ocean record: An overview. *Journal of Foraminiferal Research*, *33*, 330–337. https://doi.org/10.2113/0330330

Petrizzo, M. R. (2019). A critical evaluation of planktonic foraminiferal biostratigraphy across the Coniacian-Santonian boundary interval in Spain, Texas, and Tanzania. In R. A. Denne & A. Kahn (Eds.), *Geologic Problem Solving with microfossils IV* (Vol. 111, pp. 186–198). SEPM Special Publication. https://doi.org/10.2110/sepmsp.111.04

Petrizzo, M. R., Falzoni, F., & Premoli Silva, I. (2011). Identification of the base of the lower-to-middle Campanian *Globotruncana ventricosa* Zone: Comments on reliability and global correlations. *Cretaceous Research*, *32*, 387–405. https://doi.org/10.1016/j.cretres.2011.01.010

Petrizzo, M. R., Huber, B. T., Falzoni, F., & MacLeod, K. G. (2020). Changes in biogeographic distribution patterns of southern mid-to high latitude planktonic foraminifera during the Late Cretaceous hot to cool greenhouse climate transition. *Cretaceous Research*, *115*, 104547. https://doi.org/10.1016/j.cretres.2020.104547

Petrizzo, M. R., Huber, B. T., Wilson, P. A., & MacLeod, K. G. (2008). Late Albian paleoceanography of the western subtropical North Atlantic. *Paleoceanography*, *23*. https://doi.org/10.1029/2007PA001517

Petrizzo, M. R., Jiménez Berrocoso, Á., Falzoni, F., Huber, B. T., & MacLeod, K. G. (2017). The Coniacian–Santonian sedimentary record in southern Tanzania (Ruvuma Basin, East Africa): Planktonic foraminiferal evolutionary, geochemical and palaeoceanographic patterns. *Sedimentology*, *64*(1), 252–285. https://doi.org/10.1111/sed.12331

Petrizzo, M. R., Watkins, D. K., MacLeod, K. G., Hasegawa, T., Huber, B. T., Batenburg, S. J., & Kato, T. (2021). Exploring the paleoceanographic changes registered by planktonic foraminifera across the Cenomanian-Turonian boundary interval and Oceanic Anoxic Event 2 at southern high latitudes in the Mentelle Basin (SE Indian Ocean). *Global and Planetary Change*, *206*, 103595. https://doi.org/10.1016/j.gloplacha.2021.103595

Poulsen, C. J., Barron, E. J., Arthur, M. A., & Peterson, W. H. (2001). Response of the mid-Cretaceous global oceanic circulation to tectonic and $CO_2$ forcings. *Paleoceanography*, *16*, 576–592. https://doi.org/10.1029/2000PA000579

Poulsen, C. J., Gendaszek, A. S., & Jacob, R. L. (2003). Did the rifting of the Atlantic Ocean cause the Cretaceous thermal maximum? *Geology*, *31*, 115–118. https://doi.org/10.1130/0091-7613(2003)031<0115:DTROTA>2.0.CO;2

Premoli Silva, I., & Sliter, W. V. (1995). Cretaceous planktonic foraminiferal biostratigraphy and evolutionary trends from the Bottaccione section, Gubbio, Italy. *Palaeontographia Italica*, *81*, 2–90.

Premoli Silva, I., & Sliter, W. V. (1999). Cretaceous paleoceanography: Evidence from planktonic foraminiferal evolution. In E. Barrera & C. C. Johnson (Eds.), *The evolution of the cretaceous ocean-climate system* (Vol. 332, pp. 301–328). Special Papers of the Geological Society of America. https://doi.org/10.1130/0-8137-2332-9.301

Price, G. D. (1999). The evidence and implications of polar ice during the Mesozoic. *Earth-Science Reviews*, *48*, 183–210. https://doi.org/10.1016/s0012-8252(99)00048-3

Price, G. D., & Nunn, E. V. (2010). Valanginian isotope variation in glendonites and belemnites from Arctic Svalbard: Transient glacial temperatures during the Cretaceous greenhouse. *Geology*, *38*, 251–254. https://doi.org/10.1130/g30593.1

Pucéat, E., Lécuyer, C., Donnadieu, Y., Naveau, P., Cappetta, H., Ramstein, G., et al. (2007). Fish tooth $\delta^{18}O$ revising Late Cretaceous meridional upper ocean water temperature gradients. *Geology*, *35*, 107–110. https://doi.org/10.1130/G23103A.1

Pucéat, E., Lécuyer, C., & Reisberg, L. (2005). Neodymium isotope evolution of NW Tethyan upper ocean waters throughout the Cretaceous. *Earth and Planetary Science Letters*, *236*, 705–720.

Pucéat, E., Lécuyer, C., Sheppard, S. M. F., Dromart, G., Reboulet, S., & Grandjean, P. (2003). Thermal evolution of Cretaceous Tethyan marine waters inferred from oxygen isotope composition of fish tooth enamels. *Paleoceanography*, *18*, 1029. https://doi.org/10.1029/2002pa000823

R Core Team. (2021). *R: A language and environment for statistical computing*. R Foundation for Statistical Computing. Retrieved from https://www.R-project.org/

Robaszynski, F., & Caron, M. (1995). Foraminiféres planctoniques du Crétacé: Commentaire de la zonation Europe-Méditerranée. *Bulletin de la Societe Geologique de France*, *166*, 681–692.

Robaszynski, F., Caron, M., Amédro, F., Dupuis, C., & Hardenbol, J. (1993). Le Cénomanien de la région de Kalaat Senan (Tunisie centrale): Litho-biostratigraphie et interprétation séquentielle. *Revue de Paléobiologie*, *12*(2), 351–505.

Robinson, S. A., Murphy, D. P., Vance, D., & Thomas, D. J. (2010). Formation of "Southern Component Water" in the Late Cretaceous: Evidence from Nd-isotopes. *Geology*, *38*, 871–874. https://doi.org/10.1130/g31165.1

Robinson, S. A., & Vance, D. (2012). Widespread and synchronous change in deep-ocean circulation in the North and South Atlantic during the Late Cretaceous. *Paleoceanography*, *27*. https://doi.org/10.1029/2011pa002240

Rohling, E. J., Sprovieri, M., Cane, T., Casford, J. S., Cooke, S., Bouloubassi, I., et al. (2004). Reconstructing past planktic foraminiferal habitats using stable isotope data: A case history for Mediterranean sapropel S5. *Marine Micropaleontology*, *50*(1–2), 89–123. https://doi.org/10.1016/s0377-8398(03)00068-9

Royer, D. L., Berner, R. A., & Park, J. (2007). Climate sensitivity constrained by $CO_2$ concentrations over the past 420 million years. *Nature*, *446*, 530–532. https://doi.org/10.1038/nature05699

Ryan, W. B. F., & Cita, M. B. (1977). Ignorance concerning episodes of ocean-wide stagnation. *Marine Geology*, *23*, 197–215. https://doi.org/10.1016/0025-3227(77)90089-5

Sager, W. W., Evans, H. F., & Channell, J. E. T. (2005). Paleomagnetism of Early Cretaceous (Berriasian) sedimentary rocks, Hole 1213B, Shatsky Rise. In T. J. Bralower, I. Premoli Silva, & M. J. Malone (Eds.), *Proceedings of the Ocean Drilling Program, Scientific Results* (Vol. 198, pp. 1–14). Ocean Drilling Program. Retrieved from http://www-odp.tamu.edu/publications/198_SR/VOLUME/CHAPTERS/117.PDF

Savin, S. M. (1977). The history of Earth's surface temperature during the past 100 million years. *Annual Review of Earth and Planetary Sciences*, *5*, 319–355. https://doi.org/10.1146/annurev.ea.05.050177.001535

Schouten, S. O., Hopmans, E. C., Forster, A., van Breugel, Y., Kuypers, M. M. M., & Sinninghe Damsté, J. S. (2003). Extremely high sea-surface temperatures at low latitudes during the middle Cretaceous as revealed by archaeal membrane lipids. *Geology*, *31*(12), 1069–1072. https://doi.org/10.1130/g19876.1

Schlanger, S. O., & Jenkyns, H. C. (1976). Cretaceous oceanic anoxic events: Causes and consequences. *Geologie en Mijnbouw*, *55*, 179–184.

Scotese, C. R. (2016). *PALEOMAP PaleoAtlas for GPlates and the PaleoData plotter Program*. PALEOMAP Project. Retrieved from http://www.earthbyte.org/paleomap-paleoatlas-for-gplates/

Scotese, C. R., Song, H., Mills, B. J., & van der Meer, D. G. (2021). Phanerozoic paleotemperatures: The earth's changing climate during the last 540 million years. *Earth-Science Reviews*, *215*, 103503. https://doi.org/10.1016/j.earscirev.2021.103503

Sewall, J. O., van de Wal, R. S. W., van der Zwan, K., van Oosterhout, C., Dijkstra, H. A., & Scotese, C. R. (2007). Climate model boundary conditions for four Cretaceous time slices. *Climate of the Past*, *3*, 647–657. https://doi.org/10.5194/cp-3-647-2007

Sikora, P. J., Howe, R. W., Gale, A. S., & Stein, J. A. (2004). Chronostratigraphy of proposed Turonian–Coniacian (Upper Cretaceous) stage boundary stratotypes: Salzgitter-Salder, Germany, and Wagon Mound, New Mexico, USA. In A. B. Beaudoin & M. J. Head (Eds.), *The Palynology and Micropalaeontology of boundaries* (Vol. 230, pp. 207–242). Geological Society, London, Special Publications. https://doi.org/10.1144/gsl.sp.2004.230.01.11

Sinninghe Damsté, J. S., Kuypers, M. M., Pancost, R. D., & Schouten, S. (2008). The carbon isotopic response of algae, (cyano)bacteria, archaea and higher plants to the late Cenomanian perturbation of the global carbon cycle: Insights from biomarkers in black shales from the Cape Verde Basin (DSDP Site 367). *Organic Geochemistry*, *39*, 1703–1718.

Sprovieri, M., Sabatino, N., Pelosi, N., Batenburg, S. J., Coccioni, R., Iavarone, M., & Mazzola, S. (2013). Late Cretaceous orbitally-paced carbon isotope stratigraphy from the Bottaccione Gorge (Italy). *Palaeogeography, Palaeoclimatology, Palaeoecology*, *379*, 81–94. https://doi.org/10.1016/j.palaeo.2013.04.006

Steuber, T., Rauch, M., Masse, J. P., Graaf, J., & Malkoč, M. (2005). Low-latitude seasonality of Cretaceous temperatures in warm and cold episodes. *Nature*, *437*(7063), 1341–1344. https://doi.org/10.1038/nature04096

Stoll, H. M., & Schrag, D. P. (2000). High-resolution stable isotope records from the Upper Cretaceous rocks of Italy and Spain: Glacial episodes in a greenhouse planet? *Geological Society of America Bulletin*, *112*, 308–319. https://doi.org/10.1130/0016-7606(2000)112<308:hsirft>2.0.co;2

Suganuma, Y., & Ogg, J. G. (2006). Campanian through Eocene magnetostratigraphy of Sites 1257-1261, ODP Leg 207, Demerara Rise (western equatorial Atlantic). *Proceedings of the Ocean Drilling Program, Scientific Results* (Vol. 207, pp. 1–48). Retrieved from http://www-odp.tamu.edu/publications/207_SR/102/102.htm

Tabor, C. R., Poulsen, C. J., Lunt, D. J., Rosenbloom, N. A., Otto-Bliesner, B. L., Markwick, P. J., et al. (2016). The cause of Late Cretaceous cooling: A multimodel-proxy comparison. *Geology*, 44, 963–966. https://doi.org/10.1130/g38363.1

Takashima, R., Nishi, H., Huber, B. T., & Leckie, R. M. (2006). Greenhouse world and the Mesozoic Ocean. *Oceanography*, 19, 82–92. https://doi.org/10.5670/oceanog.2006.07

Takashima, R., Nishi, H., Yamanaka, T., Hayashi, K., Waseda, A., Obuse, A., et al. (2010). High-resolution terrestrial carbon isotope and planktic foraminiferal records of the upper Cenomanian to the lower Campanian in the northwest Pacific. *Earth and Planetary Science Letters*, 289(3–4), 570–582. https://doi.org/10.1016/j.epsl.2009.11.058

Takashima, R., Nishi, H., Yamanaka, T., Orihashi, Y., Tsujino, Y., Quidelleur, X., et al. (2019). Establishment of Upper Cretaceous bio-and carbon isotope stratigraphy in the northwest Pacific Ocean and radiometric ages around the Albian/Cenomanian, Coniacian/Santonian and Santonian/Campanian boundaries. *Newsletters on Stratigraphy*, 52(3), 341–376. https://doi.org/10.1127/nos/2019/0472

Thibault, N., Jarvis, I., Voigt, S., Gale, A. S., Attree, K., & Jenkyns, H. C. (2016). Astronomical calibration and global correlation of the Santonian (Cretaceous) based on the marine carbon isotope record. *Paleoceanography*, 31(6), 847–865. https://doi.org/10.1002/2016pa002941

Tsikos, H., Jenkyns, H. C., Walsworth-Bell, B., Petrizzo, M. R., Forster, A., Kolonic, S., et al. (2004). Carbon-isotope stratigraphy recorded by the Cenomanian–Turonian Oceanic Anoxic Event: Correlation and implications based on three localities. *Journal of the Geological Society*, 161, 711–719. https://doi.org/10.1144/0016-764903-077

van der Meer, D. G., Zeebe, R. E., van Hinsbergen, D. J., Sluijs, A., Spakman, W., & Torsvik, T. H. (2014). Plate tectonic controls on atmospheric CO$_2$ levels since the Triassic. *Proceedings of the National Academy of Sciences*, 111(12), 4380–4385. https://doi.org/10.1073/pnas.1315657111

van Helmond, N. A. G. M., Sluijs, A., Reichart, G.-J., Sinninghe Damsté, J. S., Slomp, C. P., & Brinkhuis, H. (2014). A perturbed hydrological cycle during Oceanic Anoxic Event 2. *Geology*, 42, 123–126. https://doi.org/10.1130/g34929.1

van Hinsbergen, D. J., De Groot, L. V., van Schaik, S. J., Spakman, W., Bijl, P. K., Sluijs, A., et al. (2015). A paleolatitude calculator for paleoclimate studies. *PLoS One*, 10(6), e0126946. https://doi.org/10.1371/journal.pone.0126946

Voigt, S., Friedrich, O., Norris, R. D., & Schönfeld, J. (2010). Campanian-Maastrichtian carbon isotope stratigraphy: Shelf-ocean correlation between the European shelf sea and the tropical Pacific Ocean. *Newsletters on Stratigraphy*, 44(1), 57. https://doi.org/10.1127/0078-0421/2010/0004

Voigt, S., Gale, A. S., & Flögel, S. (2004). Midlatitude shelf seas in the Cenomanian-Turonian greenhouse world: Temperature evolution and North Atlantic circulation. *Paleoceanography*, 19. https://doi.org/10.1029/2004PA001015

Voigt, S., & Hilbrecht, H. (1997). Late Cretaceous carbon isotope stratigraphy in Europe: Correlation and relations with sea level and sediment stability. *Palaeogeography, Palaeoclimatology, Palaeoecology*, 134(1–4), 39–59. https://doi.org/10.1016/s0031-0182(96)00156-3

Voigt, S., Püttmann, T., Mutterlose, J., Bornemann, A., Jarvis, I., Pearce, M., & Walaszczyk, I. (2021). Reassessment of the Salzgitter-Salder section as a potential stratotype for the Turonian–Coniacian boundary: Stable carbon isotopes and cyclostratigraphy constrained by calcareous nannofossils and palynology. *Newsletters on Stratigraphy*, 54(2), 209–228. https://doi.org/10.1127/nos/2020/0615

von Salis, K. (1998). Calcareous nannofossils column for Triassic and Cretaceous charts, Mesozoic and Cenozoic sequence chronostratigraphic framework of European basins. In P.-C. de Graciansky, J. Hardenbol, T. Jacquin, & P. R. Vail (Eds.), *Mesozoic-Cenozoic Sequence Stratigraphy of European basins* (Vol. 60, p. 779). SEPM Special Publication.

Wagner, T., & Pletsch, T. (1999). Tectono-sedimentary controls on Cretaceous black shale deposition along the opening Equatorial Atlantic Gateway (ODP Leg 159). In N. R. Cameron, R. H. Bate, & V. S. Clure (Eds.), *The oil and gas habitats of the south Atlantic* (Vol. 153, pp. 241–265). Geological Society, London, Special Publications. https://doi.org/10.1144/gsl.sp.1999.153.01.15

Wagreich, M. (2009). Coniacian-Santonian oceanic red beds and their link to Oceanic Anoxic Event 3. In X. Hu, C. Wang, R. W. Scott, M. Wagreich, & L. Jansa (Eds.), *Cretaceous oceanic red beds: Stratigraphy, composition, origins, and paleoceanographic and Paleoclimatic significance* (Vol. 91, pp. 235–242). SEPM Special Publications. https://doi.org/10.2110/sepmsp.091.225

Wagreich, M. (2012). "OAE 3" – Regional Atlantic organic carbon burial during the Coniacian-Santonian. *Climate of the Past*, 8, 1447–1455. https://doi.org/10.5194/cp-8-1447-2012

Walaszczyk, I., Čech, S., Crampton, J., Dubicka, Z., Ifrim, C., Jarvis, I., et al. (2021). The global boundary stratotype section and point (GSSP) for the base of the Coniacian stage (Salzgitter-Salder, Germany) and its auxiliary sections (Słupia Nadbrzezna, central Poland; Střeleč, Czech Republic; and El Rosario, NE Mexico). *Episodes*. https://doi.org/10.18814/epiiugs/2021/021022

Wang, Y., Huang, C., Sun, B., Quan, C., Wu, J., & Lin, Z. (2014). Paleo-CO$_2$ variation trends and the Cretaceous greenhouse climate. *Earth-Science Reviews*, 129, 136–147. https://doi.org/10.1016/j.earscirev.2013.11.001

Watkins, D. K. (1992). Upper Cretaceous nannofossils from ODP Leg 120, Kerguelen Plateau, Southern Ocean. *Proceedings of the Ocean Drilling Program, Scientific Results* (Vol. 120, pp. 343–370). Ocean Drilling Program.

Watkins, D. K., & Bergen, J. A. (2003). Late Albian adaptive radiation in the calcareous nannofossil genus *Eiffellithus*. *Micropaleontology*, 49, 231–252. https://doi.org/10.1661/0026-2803(2003)049[0231:laarit]2.0.co;2

Watkins, D. K., & Guerra, R. M. (2020). Calcareous nannofossils from the Great Australian Bight (IODP Site U1512) as a record of the peak and early decline of the mid-Cretaceous super greenhouse. *Marine Micropaleontology*, 158, 101893. https://doi.org/10.1016/j.marmicro.2020.101893

Watkins, D. K., Wise, S. W., Jr., Pospichal, J. J., & Crux, J. (1996). Upper Cretaceous calcareous nannofossil biostratigraphy and paleoceanography of the Southern Ocean. *Microfossils and oceanic environments* (pp. 355–381). British Micropalaeontological Society, University of Wales, Aberystwyth Press.

Wendler, I. (2013). A critical evaluation of carbon isotope stratigraphy and biostratigraphic implications for Late Cretaceous global correlation. *Earth-Science Reviews*, 126, 116–146. https://doi.org/10.1016/j.earscirev.2013.08.003

Wendler, I., Huber, B. T., MacLeod, K. G., & Wendler, J. E. (2011). Early evolutionary history of *Tubulogenerina* and *Colomia*, with new species from the Turonian of East Africa. *Journal of Foraminiferal Research*, 41(4), 384–400. https://doi.org/10.2113/gsjfr.41.4.384

Wendler, I., Huber, B. T., MacLeod, K. G., & Wendler, J. E. (2013). Stable oxygen and carbon isotope systematics of exquisitely preserved Turonian foraminifera from Tanzania-Understanding isotopic signatures in fossils. *Marine Micropaleontology*, 102, 1–33. https://doi.org/10.1016/j.marmicro.2013.04.003

Wise, S. W., Jr. (1983). Mesozoic and Cenozoic calcareous nannofossils recovered by DSDP Leg 71 in the Falkland Plateau region, SW Atlantic Ocean. *Initial Reports of the Deep Sea Drilling Project*, 71, 481–551.

Wise, S. W., Jr. (1988). Mesozoic-Cenozoic history of calcareous nannofossils in the region of the Southern Ocean. *Palaeogeography, Palaeoclimatology, Palaeoecology*, 67, 157–179. https://doi.org/10.1016/0031-0182(88)90127-7

Wonders, A. A. H. (1980). Middle and Late Cretaceous planktonic foraminifera of the western Mediterranean area. *Utrecht Micropaleontological Bulletins*, *24*, 1–158.

## References From the Supporting Information

Barr, F. T. (1962). Upper Cretaceous planktonic foraminifera from the Isle of Wight, England. *Palaeontology*, *4*(4), 552–580.

Basov, I. A., & Krasheninnikov, V. A. (1983). Benthic foraminifers in Mesozoic and Cenozoic sediments of the southerwestern Atlantic as an indicator of paleoenvironment, Deep Sea Drilling Project Leg 71. In W. J. Ludwig, V. A. Krasheninnikov, I. A. Basov, U. Bayer, J. Bloemendal, B. Bornhold, et al. (Eds.), *Initial Reports of the Deep Sea Drilling Project* (Vol. *71*, pp. 739–787). U.S. Government Printing Office.

Belford, D. J. (1958). The genera *Nuttallides* Finlay, 1939, and *Nuttallina*, n. gen. *Contributions from the Cushman Foundation for Foraminiferal Research*, *9*, 93–98.

Belford, D. J. (1959). *Nuttallinella*, new name for *Nuttallina* Belford, 1958 (non Nuttallina Dall, 1871). *Contributions from the Cushman Foundation for Foraminiferal Research*, *10*, 20.

Belford, D. J. (1960). Upper Cretaceous foraminifera from the Toolonga Calcilutite and Gingin Chalk, Western Australia. *Australia Bureau of Mineral Resources, Geology and Geophysics Bulletin*, *57*, 1–198.

Berthelin, G. (1880). Mémoire sur les Foraminifères fossiles de l'Etage Albien de Moncley (Doubs). *Memoires de la Societe Geologique de France*, ser. 3 31(3), 1–84.

Bolli, H. M. (1945). Zur Stratigraphie der oberen Kreide in den höheren helvetischen Decken. *Eclogae Geologicae Helvetiae*, *37*, 217–328.

Bolli, H. M. (1959). Planktonic foraminifera from the Cretaceous of Trinidad, B. W. I. *Bulletins of American Paleontology*, *39*(179), 253–277.

Brady, H. B. (1879). Notes on some of the Reticularian Rhizopoda of the "Challenger" Expedition. II. Additions to the knowledge of porcellanous and hyaline types. *Quarterly Journal of Microscopical Science*, *19*(75), 261–299.

Brady, H. B. (1881). Notes on some of the Reticularian Rhizopoda of the "Challenger" Expedition. Part III. *Quarterly Journal of Microscopical Science*, *21*(81), 31–71.

Brady, H. B. (1884). Report on the Foraminifera dredged by H.M.S. Challenger during the Years 1873–1876. Report on the Scientific Results of the Voyage of H.M.S. Challenger during the years 1873–76. *Zoology 9* (part 22), i–xxi, 1–814, 1–115.

Brotzen, F. (1936). Foraminiferen aus dem schwedischen untersten Senon von Eriksdal in Schonen. *Arsbok Sveriges Geologiska Undersökning Series C*, *30*(3), 1–206.

Brotzen, F. (1940). Flintrännans och Trindelrännans geologi (Öresund). *Arsbok. Sveriges Geologiska Undersokning*, *34*(5), 1–33.

Brotzen, F. (1942). Die Foraminiferengattung *Gavelinella* nov. gen. und die Systematik der Rotaliiformes. *Sveriges Geologiska Undersökning*, *36*(8), C (451), 1–60.

Bukalova, G. V. (1960). Булиминиды и эллипсоидиниды альбских отложений междуречья Белой и Кубани (Северное Предкавказье) – Buliminids and ellipsoidinids of the Albian deposits of the Belaya and Kuban interfluve (Northern Ciscaucasia). Тр. ВНИГНИ, Палеонт. сб. -. *Trudy VNIGNI, Pal. Sbornik*, *16*(3), 225–234.

Carpenter, W. B. (1869). On the Rhizopodal Fauna of the Deep Sea. *Proceedings of the Royal Society of London*, *18*(114–122), 59–62.

Casey, D. O. (1926). *Foraminifera of the Cretaceous of Central Texas* (Vol. 2612, pp. 1–56). University of Texas Bulletin.

Cole, W. S. (1938). Stratigraphy and micropaleontology of two deep wells in Florida. *Florida State Geological Survey, Geological Bulletin*, *16*, 1–73.

Cushman, J. A. (1925). Some new Foraminifera from the Velasco Shale of Mexico. *Contributions from the Cushman Laboratory for Foraminiferal Research*, *1*, 18–23.

Cushman, J. A. (1926a). The foraminifera of the Velasco Shale of the Tampico Embayment. *Bulletin of the American Association of Petroleum Geologists*, *10*(6), 581–612.

Cushman, J. A. (1926b). Some foraminifera from the Mendez shale of Eastern Mexico. *Contributions from the Cushman Laboratory for Foraminiferal Research*, *2*(1), 16–24.

Cushman, J. A. (1927). Some new genera of the foraminifera. *Contributions from the Cushman Laboratory for Foraminiferal Research*, *2*(4), 77–81.

Cushman, J. A. (1933). New American Cretaceous foraminifera. *Contributions from the Cushman Laboratory for Foraminiferal Research*, *9*(3), 49–64.

Cushman, J. A. (1936). Part IV. Cretaceous and Late Tertiary foraminifera. *Bulletin of the Geological Society of America*, *47*(3), 413–440. https://doi.org/10.1130/gsab-47-413

Cushman, J. A. (1937). Some notes on Cretaceous species of *Marginulina*. *Contributions from the Cushman Laboratory for Foraminiferal Research*, *13*(4), 91–99.

Cushman, J. A. (1938). Some new species of rotaliform Foraminifera from the American Cretaceous. *Contributions from the Cushman Laboratory for Foraminiferal Research*, *14*(3), 66–71.

Cushman, J. A. (1940). Midway foraminifera from Alabama. *Contributions from the Cushman Laboratory for Foraminiferal Research*, *16*(3), 51–73.

Cushman, J. A., & Church, M. A. (1929). Some upper Cretaceous foraminifera from near Coalinga, California. *Proceedings of the California Academy of Sciences*, *18*(16), 497–530.

Cushman, J. A., & Bermúdez, P. J. (1948). *Colomia*, a new genus from the Upper Cretaceous of Cuba. *Contributions from the Cushman Laboratory for Foraminiferal Research*, *24*(12), 13.

Defrance, J. L. M. in Blainville. (1826). *Dictionnaire des Sciences Naturelles* (Vol. 41). F.G. Levrault.

Defrance, J. L. M. in Blainville. (1824). *Dictionnaire des Sciences Naturelles* (Vol. 32). F.G. Levrault.

d'Orbigny, A. (1839). *Foraminifères* (pp. 1–224). Arthus Bertrand Editeur.

d'Orbigny, A. (1840). Mémoire sur les foraminifères de la craie blanche du bassin de Paris. *Memoires de la Societe Geologique de France*, *4*(1), 1–51.

Douglas, R. G., & Rankin, C. (1969). Cretaceous planktonic foraminifera from Bornholm and their zoogeographic significance. *Lethaia*, *2*, 185–217.

Earland, A. (1933). Foraminifera, Part II, South Georgia. *Discovery Reports*, *7*, 27–138.

Ehrenberg, C. G. (1840). *Uber die Bildung der Kreidenfelsen und des Kreidemergels durch unsichtbare Organismen* (pp. 59–147). Physik. Abh. 1838, pls. 1–4.

Ehrenberg, C. G. (1854). *Mikrogeologie: Das Erden und Felsen schaffende Wirken des unsichtbar kleinen selbständigen Lebens auf der Erde* (pp. 1–374). Leopold Voss.

Eternod Olvera, Y. (1959). Foraminíferos del Cretácico Superior de la cuenca de Tampico-Tuxpan, Mexico. *Boletin de la Asociacion Mexicana de Geologos Petroleros*, *11*, 61–134.

Fichtel, L. v., & Moll, J. P. C. (1798). *Testacea microscopia, aliaque minuta ex generibus Argonauta et Nautilus, ad naturam delineata et descripta*. A. Pichler. xii + 123 pp., 24 pl., p. 103, pl. 19 b, c.

Finlay, H. J. (1939). New Zealand foraminifera: Key species in stratigraphy – No. 3. *Transactions of the Royal Society of New Zealand*, *69*, 309–329.

Fisher, M. J. (1969). Benthonic foraminifera from the Maestrichtian chalk of the Galicia Bank, west of Spain. *Palaeontology*, *12*, 189–200.

Gawor-Biedowa, E. (1992). New foraminifera of the Campanian and Maastrichtian in the Lublin Region (Eastern Poland). *Kwartalnik Geologiczny*, *36*(1), 75–96.

Georgescu, M. D. (2008). A new planktonic foraminifer (Family Hedbergellidae Loeblich and Tappan, 1961) from the lower Campanian sediments of the Falkland Plateau, South Atlantic Ocean (DSDP Site 511). *Journal of Foraminiferal Research*, *38*, 157–161.

Georgescu, M. D. (2010). *Liuenella*, new name for *Liuella* Georgescu, 2008. *Journal of Foraminiferal Research*, *40*, 206.

Grzybowski, J. (1896). *Otwornice czerwonych ilow z Wadowic. Rozprawy, Akademia Umiejetnosci w Krakowie*. Wydzial Matematyczno-Przyrodniczy.

Heron-Allen, E., & Earland, A. (1910). On the recent and fossil Foraminifera of the shore-sands of Selsey Bill, Sussex – V. The Cretaceous Foraminifera. *Journal of the Royal Microscopical Society*, 401–426.

Herrmann, A. (1917). Vierter Beitrag zur Kenntnis des Vorkommens von Foraminiferen im Tertiär des Unterelsass. *Mitteilungen der Geologischen Landesanstalt von Elsass-Lothringen*, *10*, 1–286.

Hofker, J. (1953). Types of genera described in part III of the "Siboga Foraminifera". *The Micropaleontologist*, *7*(1), 26–28.

Kaiho, K. (1998). Phylogeny of deep-sea calcareous trochospiral benthic foraminifera: Evolution and diversification. *Micropaleontology*, *44*(3), 291.

Kanmacher, F. (1798). *Essays on the microscope*. The Second Edition, with considerable additions and improvements. Dillon & Keating, xvii + [7 unnumbered] + 724 pp., 32 pl.

Lamarck, J. B. P. A. de (1804). Suite des mémoires sur les fossiles des environs de Paris. *Annales du Muséum d'Histoire Naturelle 5*, 28–36; 91–98; 179–188; 237–245; pl. 59–62 [plates published 1806 in vol. 8].

Lamarck, J. B. P. A. de M. de (1816). *Tableau encyclopédique et méthodique des trois règnes de la nature* (pp. 432–488). Mollusques et polypes divers. Part 23 [Livraison 84, 14 December 1816], Tome 3, pp. 1–16, pls. 391–431, 431 bis, 431 bis*.

Loeblich, A. R., & Tappan, H. (1961). Cretaceous planktonic foraminifera: Part I-Cenomanian. *Micropaleontology*, *7*, 257–304.

Loeblich, A. R., & Tappan, H. (1986). Some new and revised genera and families of hyaline calcareous foraminiferida (Protozoa). *Transactions of the American Microscopical Society*, *105*(3), 239–265.

Malumián, N., & Masiuk, V. (1976). Foraminiferos de la formacion Cabeza de Leon (Cretacio Superior, Tierra del Fuego, República Argentinia). *Revista Asocoación Geológica Argentinia*, *31*(3), 180–202.

Montfort, P. (1808–1810). *Conchyliologie systématique et classification méthodique des coquilles* (Vol. 2, p. 676). Schoell. Vol. 1: pp. lxxxvii + 409 [1808].

Morrow, A. L. (1934). Foraminifera and ostracoda from the Upper Cretaceous of Kansas. *Journal of Paleontology*, *8*, 186–205.

Neagu, T. (2012). *"Rosalina" marginata* Reuss 1845 (Foraminifera) and its taxonomic position. *Studia UBB Geologia*, *57*, 35–38.

Orbigny, A. D. d'. (1826). Tableau méthodique de la classe des Céphalopodes. *Annales des Sciences Naturelles*, *7*(96–169), 245–314.

Orbigny, A. D. d'. (1839). *Foraminifères, in de la Sagra R., Histoire physique, politique et naturelle de l'ile de Cuba* (pp. 1–224). A. Bertrand.

Orbigny, A. D. d'. (1840). *Mémoire sur les foraminifères de la craie blanche du bassin de Paris*. Mémoires de la Société géologique de France. 1ère série, tome IV, mémoire no 1.

Pessagno, E. A. (1960). Stratigraphy and micropaleontology of the Cretaceous and lower tertiary of Puerto Rico. *Micropaleontology*, *6*(1), 87–110.

Pessagno, E. A. (1967). Upper Cretaceous planktonic foraminifera from the western Gulf Coastal Plain. *Palaeontographica Americana*, *5*, 245–445.

Quilty, P. G. (1992). Upper Cretaceous planktonic foraminifera and biostratigraphy, & (Eds.), Upper Cretaceous planktonic foraminifera and biostratigraphy. *Proceedings of the Ocean Drilling Program, Scientific Results* (Vol. 120, pp. 371–392). Ocean Drilling Program.

Reichel, M. (1946). Sur quelques foraminifères nouveaux du Permien méditerranéen. *Eclogae Geologicae Helvetiae*, *38*(2), 524–560. [1945].

Reuss, A. E. (1845). *Die Versteinerungen der böhmischen Kreideformation*. E. Schweizerbart'sche Verlagsbuchhandlung und Druckerei.

Reuss, A. E. (1851). Über die fossilen Foraminiferen und Entomostraceen der Septarienthone der Umgegend von Berlin. *Zeitschrift der Deutschen Geologischen Gesellschaft*, *3*(1), 49–92.

Reuss, A. E. (1860). Die Foraminiferen der westphälischen Kreideformation. *Sitzungsberichte der mathematisch-naturwissenschaflichen Classe der kaiserlichen Akademie der Wissenschaften*, *40*(8), 147–238.

Reuss, A. E. (1863). *Die Foraminiferen – Familie der Lagenideen* (Vol. 46, pp. 308–342). Sitzungsberichte der Akademie der Wissenschaften. Mathematisch-naturwissenschaftliche Klasse.

Rhumbler, L. (1895). *Entwurf eines natürlichen Systems der Thalamophoren* (pp. 51–98). Nachrichten der Gesellschaft der Wissenschaften zu Göttingen, Mathematisch-Physikalische Klasse.

Risso, A. (1826–1827). Histoire naturelle des principales productions de l'Europe Méridionale et particulièrement de celles des environs de Nice et des Alpes Maritimes. *Paris, F.G. Levrault*, *3*(XVI), 1–480. 14 pls.

Roemer, F. A. (1839). *Die Versteinerungen des norddeutschen Oolithengebirges, ein Nachtrag* (pp. 1–59). Hahn.

Römer, F. A. (1841). *Die Versteinerungen des Norddeutschen Kreidegebirges* (pp. 8–20). Mit sechszehn lithographirten Tafeln. Hahn'schen, Hofbuch-handlung. [1840] iv + 49–145, pls.

Sars, G. O. (1872). Undersøgelser over Hardangerfjordens fauna I. *Förhadlingar i Videnskabsselskabet i Christiania*, *1871*, 246–286.

Scheibnerová, V. (1962). Stratigrafia strednej a vrchnej kriedy tetydní oblasti na zaklade globotruncanid – Stratigraphy of the Middle and Upper Cretaceous of the Tethyan region on the basis of the Globotruncanids. *Geologiscky Zbornik -Geologica Carpathica*, *13*(2), 219–226.

Sigal, J. (1952). Apercu stratigraphique sur la micropaleontologie du Cretace. *XIX International Geological Congress, Algiers, Monographies Regionales*, *1*(26), 3–43.

Silvestri, A. (1900). Sur genere *Ellipsoglandulina*. Atti e Rendiconti R. Accademia di Scienze, Lettere ed Arte degli Zelanti, Acireale, Cl. Sci. *Mem.*, *10*, 1–9.

Silvestri, A. (1901). Sulla struttura di certe Polimorfine dei dintorni di Caltagirone. *Bollettino Accademia Gioenia di Scienze Naturali, Catania n. ser.*, *69*, 14–18.

Silvestri, A. (1903). Alcune osservazioni sui Protozoi fossili piemontesi. *Atti Reale Accademia delle Scienze di Torino*, *38*(6), 206–217.

Silvestri, A. (1904). Ricerche strutturali su alcune forme dei Trubi dei Bonfornello (Palermo). *Memorie dell'Accademia Pontificia dei Nuovi Lincei*, *22*, 235–276.

Silvestri, A. (1924). Fauna Paleogenica di Vasciano presso Todi. *Bollettino della Societa Geologica Italiana*, *42*, 7–29.

Sliter, W. V. (1968). Upper Cretaceous foraminifera from southern California and northwestern Baja California. *University of Kansas Paleontological Contributions*, *49*, 1–141.

Storm, H. (1929). Zur Kennthis der Foraminiferenfauna im Oberturon und Emscher der Böhmischen Kreideformation. *Lotos, Prag, Tschechoslowakei*, *77*, 39–62.

Subbotina, N. N. (1949). Микрофауна меловых отложений южного склона Кавказа [Microfauna from the cretaceous of the southern slope of the Caucasus]. *VNIGRI, Microfauna of the oil fields of the USSR, 2*(34), 5–36.

Tappan, H. (1940). Foraminifera from the Grayson formation of Northern Texas. *Journal of Paleontology*, *14*(2), 93–126.

Thalmann, H. E. (1939). Bibliography and index to new genera, species and varieties of foraminifera for the year 1936. *Journal of Paleontology*, *13*, 425–465.

Vasilenko, V. P. (1961). Upper Cretaceous foraminifera of the Mangyshlak Peninsula. *Trudy Vsesoyuznego Neftyanogo Nauchno-Issledovatel'skogo Geologo-Razvedochnogo Instituta (VNIGRI)*, *171*, 160–161.

Vogler, J. (1941). Ober-Jura und Kreide von Misol. In G. Boehm & J. Wanner (Eds.), *Beitrage zur Geologie von Niederlandisch-Indian* (pp. 243–293).

von Hagenow, K. F. (1842). Monographie der Rügen'schen Kreide-Versteinerungen. III Abtheilung: Mollusken. *Neues Jahrbuch für Mineralogie, Geognosie, Geologie und Petrefaktenkunde*, *528–575*, pl. 9.

White, M. P. (1928). Some index foraminifera of the Tampico Embayment area of Mexico. Parts 1, 2. *Journal of Paleontology*, *2*(3–4), 280–317. 177–215.